Author:
Ryk, Aleksandra

Title:
The impact of insulin exposure on colorectal cancer metabolism

The impact of insulin exposure on colorectal cancer metabolism

Aleksandra Ryk

A thesis submitted to the University of Bristol in accordance with the requirements for award of the degree of Master of Science by Research in the Faculty of Life Sciences, School of Cellular and Molecular Medicine.

September 2019

Word Count: 18 968

Abstract

According to epidemiological data people with type 2 diabetes have a 50% increased risk of developing colorectal cancer. Hyperinsulinemia, which occurs in type 2 diabetes, is considered to be a factor linking these two diseases. One mechanism by which exposure to higher and more sustained levels of insulin might encourage tumourigenesis is by driving metabolic reprogramming in colorectal cells. As such, the aim of this investigation is to examine the impact of insulin exposure on metabolic reprogramming in colorectal tumour cells.

In order to address this aim, assays were performed to assess the effect of insulin on tumour cell proliferation across the progressive stages of carcinogenesis. Early adenoma cells were found to be the most sensitive to insulin exposure in comparison to cell line models of the later stages of carcinogenesis. In the next part of this study, stable isotope tracer analysis (SITA), western blotting and quantitative real time PCR were performed to examine the changes in metabolic pathways upon insulin stimulation in early and late stage cells. Data obtained from SITA showed that insulin increases the levels of glycolysis in both cell lines tested. The results of western blotting and quantitative real time PCR suggest that insulin may promote aerobic glycolysis in tumour cells by increasing PDK1 expression via HIF1α. In addition, SITA showed that insulin increased glutamine anaplerosis and amino acid uptake in the early stage cells exclusively. This result may explain how insulin induces an increase in proliferation in early but not late stage cells.

Together, the results of this investigation suggest that insulin exposure may encourage tumour progression by promoting metabolic reprogramming in colorectal tumour cells. However, further research is needed to confirm these findings.

Acknowledgements

I am extremely grateful to my supervisor Dr Emma Vincent for her expertise, generous advice and encouragement throughout the course of my work. I would like to also thank Tracey Collard and Caroline Bull for their kind, endless help and support.

I would like to express deep gratitude to my parents for their unconditional support and giving me the opportunity to study and develop my interests in science.

I would like to give special thanks to Mila and Kamil, whose support enabled me to complete this thesis.

Author's declaration

I declare that the work in this dissertation was carried out in accordance with the requirements of the University's *Regulations and Code of Practice for Research Degree Programmes* and that it has not been submitted for any other academic award. Except where indicated by specific reference in the text, the work is the candidate's own work. Work done in collaboration with, or with the assistance of, others, is indicated as such. Any views expressed in the dissertation are those of the author.

SIGNED: [redacted] DATE: 08/09/19

Abbreviations

APC - Adenomatous Polyposis Coli

ASCT2 - Alanine, Serine, Cysteine Transporter 2

ATP - adenosine triphosphate

BAD – BCL2-associated agonist of cell death

CK1 - casein kinase 1

C1- AA/C1 cell line

CI – mitochondrial electron transport chain complex 1

CII – mitochondrial electron transport chain complex 2

CIII – mitochondrial electron transport chain complex 3

CIV – mitochondrial electron transport chain complex 4

Dvl – dishevelled

EGFR – epidermal growth factor receptor

ETC – electron transport chain

$FADH_2$ - flavin adenine dinucleotide

FOXO – forkhead box protein O

GLUT1 – glucose transporter 1

GLUT4 – glucose transporter 4

Grb2 - Growth factor receptor-bound protein 2

GSK3 – glycogen synthase kinase-3

IR – insulin receptor

IRS – insulin receptor substrate

LDH – lactate dehydrogenase

LDHA – lactate dehydrogenase A

M – AA/C1/SB/10C/M cell line

MPC – mitochondrial pyruvate carrier

mTORC1 – mammalian target of rapamycin complex 1

NADH - nicotinamide adenine dinucleotide – hydrogen

OAA – Oxaloacetate

PDK1 – pyruvate dehydrogenase kinase

PIP2 - phosphatidylinositol-2-phosphate

PIP3 - phosphatidylinositol-3-phosphate

PKM1 - pyruvate kinase isozymes M1

PKM2 - pyruvate kinase isozymes M2

PI3K - phosphatidylinositol-3-kinase

PTEN - Phosphatase and tensin homolog

qPCR – quantitative real time polymerase chain reaction

SB – AA/C1/SB cell line

SERBP – sterol regulatory element-binding protein 1

SITA – stable isotope tracer analysis

SOS - son of sevenless

S6 – ribosomal S6 kinase

TCA cycle - tricarboxylic Acid Cycle

TP53 – tumour protein 53

T2DM – type 2 diabetes mellitus

4EBP – eukaryotic translation initiation factor 4E-binding protein

10C – AA/C1/SB/10C cell line

α-KG - α-ketoglutarate

β-TrCP - beta-transducin repeat containing E3 ubiquitin protein

Contents

List of Tables and Figures

Chapter 1: Introduction

1.1. Colorectal Cancer Incidence

Colorectal cancer is the third most common cancer worldwide (1) with 1.2 million people diagnosed every year (2). It accounts for approximately 10% of cancer associated death in industrialized countries. Incidence of colorectal cancer varies geographically with around 50% of cases in developed parts of the world. Higher prevalence of colorectal cancer in higher income countries has been linked to western lifestyle including unhealthy diet, smoking, low physical activity and high obesity rates (2).

According to the National Cancer Registration and Analysis Service (NCRAS), 50.7% of colorectal cancer patients in England will be alive five years after diagnosis (3). However, the survival rate depends on the stage of disease at diagnosis. The five year survival rate for people diagnosed with the first stage of disease (Dukes A) is 93.2%, whereas for people diagnosed with advanced disease (Dukes D) it drops to 6.6% (3). Therefore, early diagnosis of colorectal cancer is crucial to improve outcomes. In England, bowel cancer screening is offered every two years to people from 60 to 74 years old (4). People above this age can request a screening kit every two years (4). In addition, a one-off test is offered to people at the age of 55 (4). A statistical analysis performed by the Cancer Research UK showed that colorectal cancer incidence in people aged 60-74 has decreased by 5% since early 1990s (5).

Although the incidence of colorectal cancer in older people is decreasing, because of large scale screening programs (6), the number of young adults suffering with colorectal cancer is getting higher (7). A statistical analysis performed on 143.7 million people from 20 European countries has shown that incidence of colorectal cancer increased with 7.9% per year among people aged 20-29 years old between 2004 and 2014 (7). In the UK, colorectal cancer incidence in people aged 25-49 has increased by 39% since early 1990s (5).

The rise in colorectal cancer incidence in young people may be caused by lack of screening programs as well as lifestyle factors such as poor eating habits and lack of exercise (8). For example, unhealthy diet and sedentary lifestyle often lead to obesity and diabetes, which has been associated with increased risk of developing colorectal cancer by numerous studies (9–12). It is important to understand the molecular mechanisms underlying colorectal cancer in young patients in order to develop appropriate therapies and screening programs.

1.2. Hereditary Colorectal Cancer Syndromes

Colorectal cancers are usually sporadic, however, around 5% of cases occur as a result of inherited mutations (13). The most common hereditary syndromes giving predisposition to colorectal cancer are Lynch syndrome and Familial Adenomatous Polyposis (FAP) (13).

1.2.1. Lynch Syndrome

Lynch syndrome, also known as hereditary non-polyposis colorectal cancer (HNPCC), is caused by a germ line mutation in DNA mismatch repair genes (MMR). In 90% of cases mutations occur in *MSH1* and *MSH2* genes. Less commonly mutations may be found in other MMR genes such as: *MSH6, PMS2*, and *EPCAM*. As a consequence of impaired DNA MMR machinery, any secondary mutations remain unrepaired and increase the risk of developing cancers (14). Lynch syndrome patients have about 80% lifetime risk of developing colorectal cancer (15). They are diagnosed with colorectal cancer at the age of 45 on average (15), which is about two decades earlier than for sporadic colorectal cancer (16). Besides colorectal cancer, Lynch syndrome has been shown to increase the risk of developing other cancers such as endometrial, ovarian, stomach and urinary tract (17).

1.2.2. Familial Adenomatous Polyposis

FAP is characterized by the development of numerous benign polyps in the colon and rectum in early life. Those polyps are usually asymptomatic, but some of them will eventually progress and give rise to colorectal cancer (18). The median age when FAP patients develop colorectal cancer is 40 (7). FAP is an autosomal dominant disorder caused by a mutation in Adenomatous Polyposis Coli (*APC*) gene (18). APC mutation is one of the most important triggers of colorectal cancer, not only in FAP, but also in sporadic cases. It occurs in 90% of all colorectal cancer cases in the early stages of tumorigenesis (19).

1.3. Spontaneous Colorectal Cancer - Mutations

Colorectal cancer is a multistage process, following an adenoma to carcinoma sequence. Tumorigenesis begins in the crypts of the colonic epithelium and subsequently gives rise to benign adenomas, which gradually advance into invasive carcinomas. This step-wise tumour progression is accompanied by an ordered sequence of genetic mutations and epigenetic alterations (20) (Figure 1).

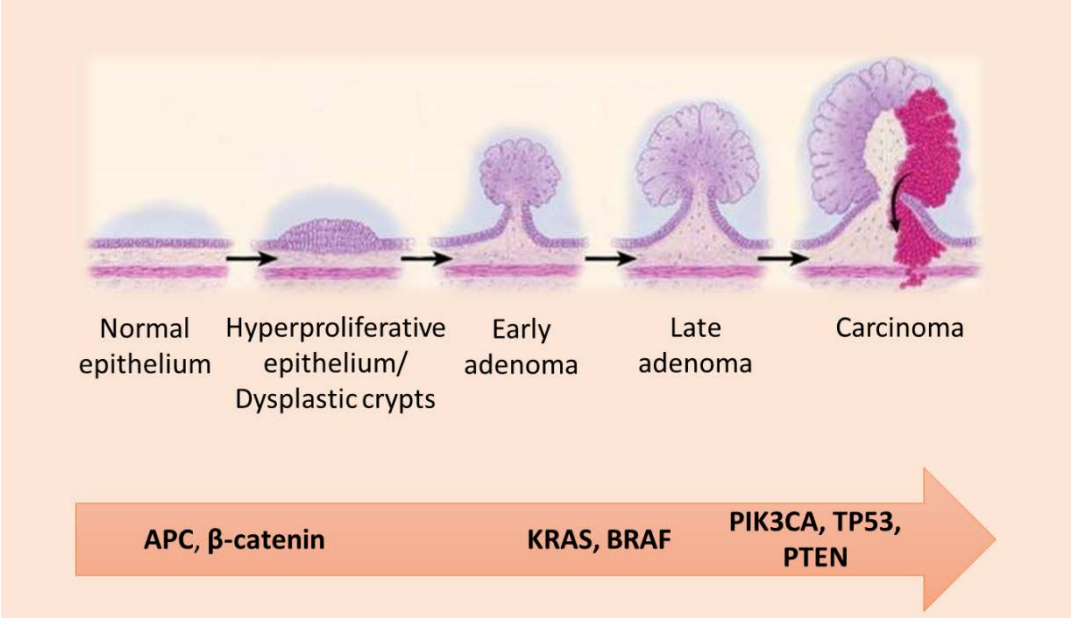

Figure 1. Colorectal tumour progression. Diagram represents stages of colorectal tumour development and mutations associated with particular stages. Mutations in APC and β-catenin appear early in tumourigenesis. At the stage of adenoma, mutations in Ras or Raf proteins are often visible. Mutations in PI3K, p53, PTEN occur later on during tumour progression. Diagram adapted from (21,22).

1.3.1. APC and Wnt signalling pathway

Inactivation of the *APC* tumour suppressor gene is the most common initiating event in the majority of colorectal cancers (23). APC mutation leads to constitutive activation of the Wnt signalling pathway, which is thought to be a key driver of colorectal cancer (23). Under normal conditions, the role of Wnt signalling is to maintain epithelial stem cell populations, which reside at the bottom of the colonic crypts (23). Constitutive Wnt signalling, which occurs in cancer, leads to the retention of the stem cell phenotype, as a result undifferentiated cells accumulate and start forming benign polyps (23). Two models of Wnt signalling have been proposed: the canonical and non-canonical model (24).

1.3.1.1. Canonical model of Wnt signalling

According to the canonical model, in the absence of the Wnt ligand binding to the Frizzled receptor, a destruction complex composed of APC, glycogen synthase kinase 3 (GSK3), the scaffolding protein Axin, casein kinase (CK1), and Dishevelled (Dvl) binds and phosphorylates β-catenin in the cytosol (24). Phosphorylated β-catenin is targeted for ubiquitination by E3-ubiquitin ligase β-TrCP and degradation via proteasome. In the presence of Wnt ligands, Axin

binds to the phosphorylated low density lipoprotein receptor related protein 5/6 (LRP5/6). As a result, destruction complex disassembles and β-catenin is stabilized. β-catenin accumulates in the cytoplasm and translocates to the nucleus, where it activates T-cell factor (TCF) and the lymphoid enhancer factor (LEF) family of transcription factors and up-regulates Wnt signalling target genes expression (24) (Figure 2).

1.3.1.2. Non-canonical model of Wnt signalling

An alternative model of Wnt signalling was proposed after investigating the endogenous destruction complex components (25). According to this model, in the absence of Wnt ligand binding, the destruction complex binds, phosphorylates and ubiquitinates β-catenin by β-TrCP (24). Subsequently, the proteasome degrades β-catenin and as a result recycles the destruction complex. In contrast to the canonical model, a non-canonical model shows that upon Wnt ligand binding, the whole, intact destruction complex is recruited by the LRP receptor where it binds and phosphorylates β-catenin. However, the ubiquitination of β-catenin by β-TrCP is blocked, therefore newly synthesized β-catenin accumulates in the cytosol (24) (Figure 2).

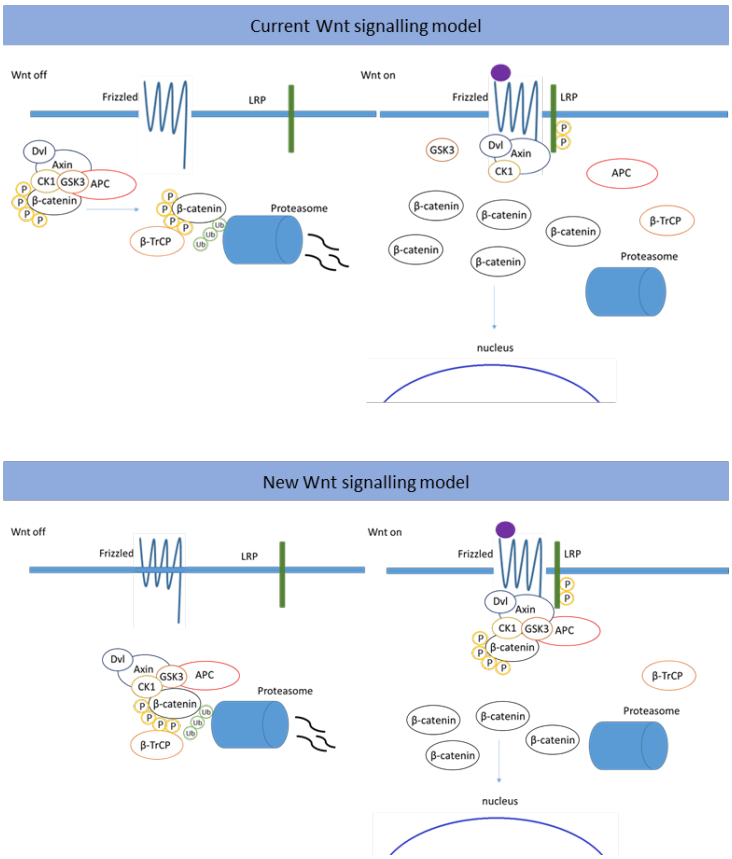

Figure 2. Canonical and non-canonical models of Wnt signalling. A. Canonical model of Wnt signalling: In the absence of Wnt ligand binding to the Frizzled receptor, the destruction complex binds β-catenin and targets it for ubiquitination by βTrCP. Ubiquitinated β-catenin is targeted for degradation via the proteasome. Wnt ligand binding to the Frizzled receptor leads

to Axin recruitment to the LRP receptor, disassembly of the destruction complex and accumulation of β-catenin in the cytoplasm. B. Non-canonical model of Wnt signalling: In the absence of Wnt ligand binding to Frizzled receptor, destruction complex binds β-catenin and ubiquitinates it by β-TrCP. Ubiquitinated β-catenin is targeted for degradation via proteasome. When Wnt ligand binds to the receptor destruction complex is recruited to LRP receptor. B-catenin is bound by destruction complex, howeve, ubiquitination of β-catenin is blocked, therefore it accumulates in the cytoplasm. Figure adapted from (24).

98% of mutations in the *APC* gene are loss of function mutations (frameshifts or nonsense mutations) leading to formation of truncated APC protein (26). As a result the destruction complex cannot be fully formed (26). That leads to accumulation of β-catenin and sustained upregulation of Wnt target genes such as c-myc, LEF-1, matrix metalloproteinase MMP-7(27). In sporadic colorectal cancers with a wild type APC, there is often a mutation directly in the β-catenin gene which leads to sustained Wnt signalling (26).

1.3.2. MAPK signalling pathway

Another important pathway which is often mutated in colorectal tumours is the MAPK signalling pathway. This pathway starts with a growth factor binding to a trans-membrane receptor called Epidermal Growth Factor Receptor (EGFR). This leads to the recruitment and activation of the GRB2/SOS complex, which subsequently activates Ras. RAS is a small GTPase protein which induces activation of a kinase cascade starting with RAF and followed by MEK and Erk (28) (Figure 3) . Around 30-50% and 5-10% of colorectal tumours harbour a mutation in KRAS and BRAF oncogenes respectively (29). Mutations in this pathway result in constitutive up-regulation of growth promoting genes (30).

1.3.3. PI3K/Akt signalling pathway

EGFR stimulation also leads to activation of the *PIK3CA* oncogene, which encodes the p110α subunit of phosphatidylinositol 3-kinase (PI3K) (30). Activated PI3K converts phosphatidylinositol-2-phosphate (PIP_2) to phosphatidylinositol-3-phosphate (PIP_3) and results in phosphorylation and activation of Akt. Akt activation triggers numerous molecular pathways resulting in proliferation, migration, cell survival and angiogenesis (30). Akt can be switched off by the PTEN tumour suppressor protein which dephosphorylates and converts PIP_3 back to PIP_2. PI3K and PTEN are often mutated in colorectal cancer resulting in constitutive activation of the Akt signalling pathway (30). PI3K/Akt pathway is able to influence cellular metabolism is via activation of its downstream target – mTORC1 (31). In non-transformed cells, mTORC1 senses the energy status of a cell and in the presence of nutrients responds by driving anabolic processes such as protein synthesis, nucleic acid synthesis and lipogenesis (32). The outcome of these reactions is production of building blocks necessary for cell growth (32). In cancer cells with deregulated activation of the PI3K/Akt pathway, there is a constitutive

stimulation of mTORC1. This results in high levels of biomass production which is used to support uncontrolled proliferation (31) (Figure 3).

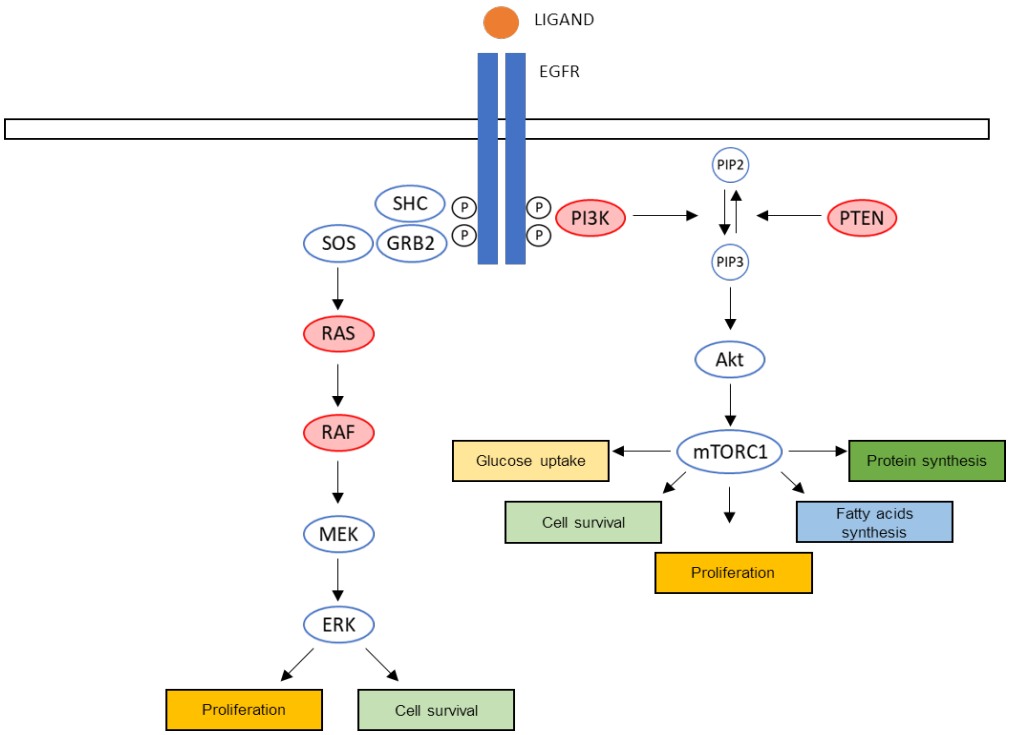

Figure 3. Signalling pathways involved in colorectal cancer development. Ligand binding to the EGFR receptor activates PI3K, which drives conversion of PIP2 to PIP3. PIP3 activates Akt, which triggers activation of mTORC1. Activation of EGFR also recruits Shc and Grb2. Grb2 activates SOS, which drives a kinase cascade leading to activation of Erk. Proteins commonly mutated in colorectal cancer are indicated in red.

1.3.4. TP53 tumour suppressor gene

Another common mutation occurs in the *TP53* tumour suppressor gene. *TP53* is responsible for the induction of G1 cell cycle arrest and DNA repair before allowing cells to enter S phase (26). Upon failure to repair DNA, p53 is responsible for inducing apoptosis (26). It is thought that the mutation in *TP53* occurs at the stage of adenoma to carcinoma transition (26).

1.4. Metabolic reprogramming in cancer

During the multistep colorectal tumour progression, mutations discussed above drive the hallmarks of cancer (Figure 4). For example, a constitutive activation of MAPK and Akt signalling pathways leads to sustained growth promoting signals and uncontrolled proliferation (33). Activation of Wnt signalling results in expression of such genes as MMP-7(27), which promote tissue invasion and metastasis (34) and inactivating mutations in *TP53*, a tumour suppressor gene, lead to evasion of apoptosis (33).

This study is focused on one hallmark of cancer in particular, that is metabolic reprogramming. Metabolic reprogramming was classified as a hallmark of cancer by Hanahan and Weinberg in 2011 (35). The alterations in cellular metabolism are necessary to provide energy and building blocks to support chronic proliferation (35). Multiple oncogenic pathways involved in colorectal cancer initiation and progression have been found to directly influence metabolic reprogramming.

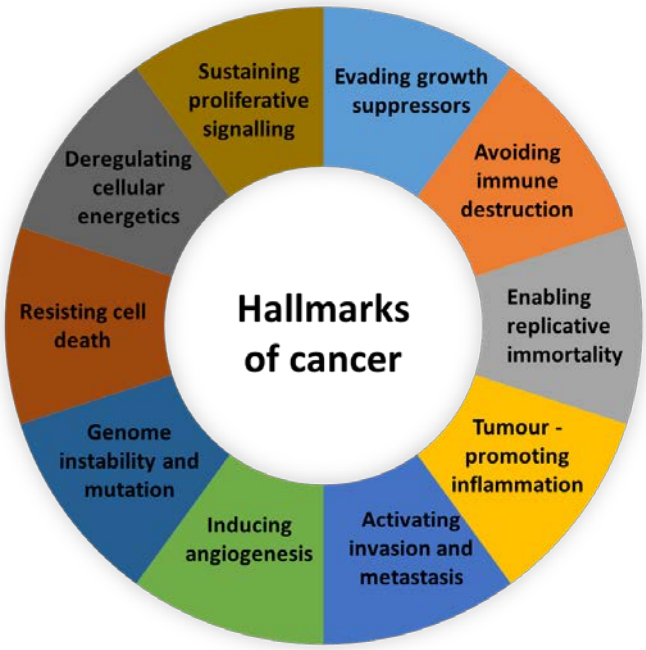

Figure 4. The hallmarks of cancer cells. Figure presents ten hallmark characteristics of cancer cells. Cancer cells develop these capabilities as a result of acquired mutations. Adapted from (36).

1.4.1. The key metabolic pathways used by cancer cells

Metabolism is defined as a collection of all the chemical reactions within a cell, which produce and release energy in order to sustain life. Metabolic reactions can be divided into three categories: catabolic, by which cells produce energy, anabolic, used for biosynthesis, and waste disposal necessary to get rid of toxic by-products (37). The main metabolic pathways used by cells to produce energy are glycolysis, the TCA cycle and oxidative phosphorylation (37). As mentioned above, metabolic reprogramming has been defined as a hallmark of cancer cells (35). This is where cancer cells up- or down-regulate certain metabolic pathways in order to maximize energy production and biomass synthesis to support chronic proliferation (38).

1.4.2. The Warburg effect

One of the most common characteristics of cancer cell metabolism is elevated levels of glycolysis regardless of oxygen availability, this is known as the Warburg effect (39). In the 1920s, Otto Warburg observed that tumour cells consume large amounts of glucose compared to surrounding tissue (39). In addition, he noticed that glucose taken up by tumour cells was converted into lactate in the presence of oxygen (39). Nowadays, the Warburg effect is considered to be one of a key differences between quiescent and tumour cells (40). In quiescent cells, glycolysis occurs at a basal level and most energy is produced via oxidative phosphorylation (40). Glycolysis is not an efficient form of metabolism as it only allows for the production of two ATP molecules per cycle (40). By contrast, 36 molecules of ATP are produced via the TCA cycle (Figure 5) (40). Regardless of the energy inefficiency tumour cells increase their levels of glycolysis and predominantly convert the resulting pyruvate into lactate rather than oxidize it in the TCA cycle (40). Warburg hypothesized that this behaviour of tumour cells is caused by damaged mitochondria (41). Today, we know that mitochondrial activity is intact in most cancer cells (42). Currently, the most popular theory states that the Warburg effect is used to produce metabolic intermediates necessary for biosynthetic processes (41). Glycolytic intermediates supply such biosynthetic pathways as the hexosamine pathway, the pentose phosphate pathway and one carbon metabolism (43). As a result there is increased synthesis of amino acids, nucleotides and lipids, which are essential building blocks needed for cell growth (43).

The principle of the Warburg effect has been used to develop a method of tumour detection called fluorodeoxyglucose positron emission tomography (FDG-PET) (44). FDG-PET is a non-invasive method of tumour detection, staging and monitoring (45). Fluorine-18 fluorodeoxyglucose (FDG) is a glucose analogue used as a tracer, this allows clinicians to detect excessive glucose uptake in tissues to indicate the presence of a tumour (45).

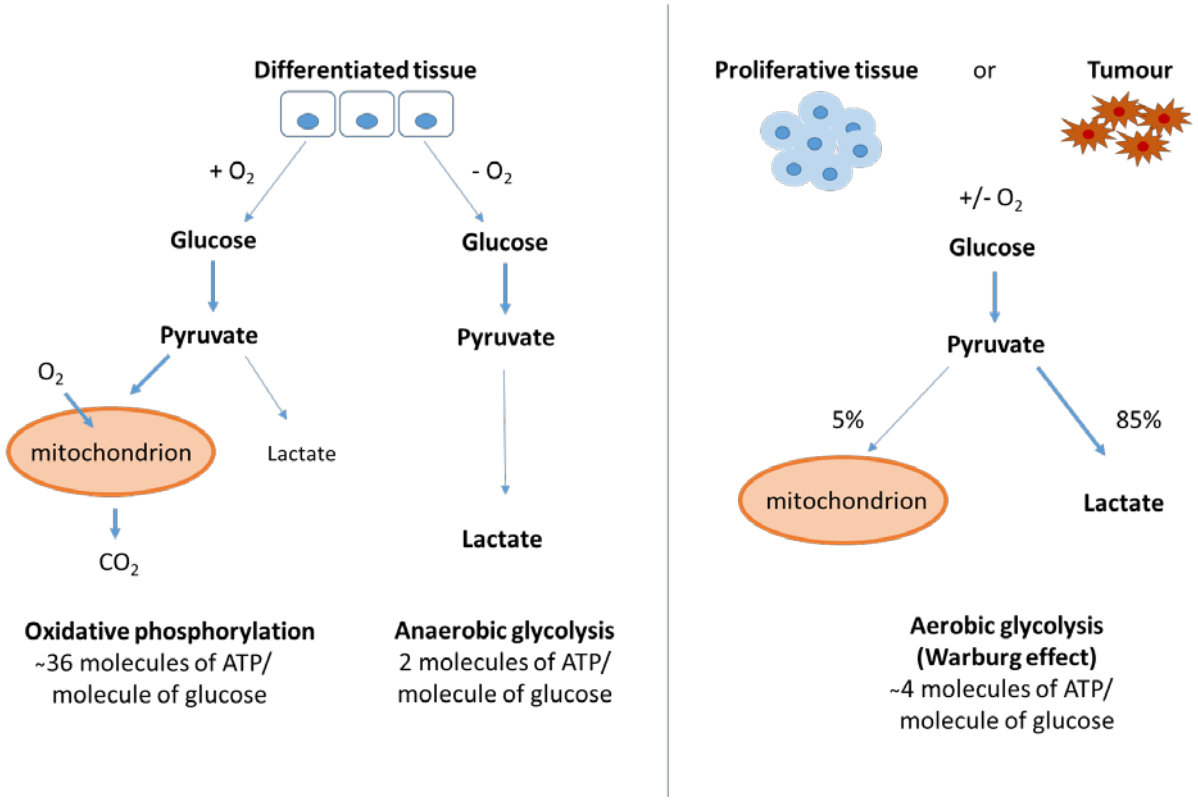

Figure 5. Diagram representing differences in cellular metabolism in quiescent and tumour cells. In quiescent cells, when there is oxygen available, pyruvate, produced as a result of glycolysis, enters the TCA cycle. Most of the energy is produced via oxidative phosphorylation. When there is no oxygen available, pyruvate is converted into lactate and anaerobic glycolysis occurs. In proliferative tissue or tumour cells, pyruvate is converted into lactate regardless of oxygen availability. That is known as aerobic glycolysis or the Warburg effect. Figure adapted from (40).

Below I describe how different mutations drive metabolic reprogramming in tumour cells, these are summarised in Figure 6:

1.4.2.1. Changes in PKM2 expression

One of the mechanisms that promotes the Warburg effect in cells is the expression of a specific isoform of pyruvate kinase (PK) – PKM2. PK is a glycolytic enzyme responsible for the conversion of phosphoenolpyruvate (PEP) to pyruvate (44) (Figure 6). There are two splice variants of PK; PKM1 and PKM2 (46). Splice variant M2 is less efficient at converting PEP to pyruvate. As a result pyruvate is produced at a lower rate so more of the glycolytic intermediates upstream of PEP build up and can be used for biosynthetic pathways (44). PKM2 expression is often increased in colorectal cancers. Moreover, high expression of PKM2 has

been associated with poor prognosis in colorectal cancer patients. It has also been shown in *in vitro* models that PKM2 knockdown in colorectal cancer cells increases the efficacy of the chemotherapeutic, 5-flurouracil (5-FU).

1.4.2.2. Changes in LDHA expression

Another glycolytic enzyme which has been reported to be overexpressed in numerous cancers is lactate dehydrogenase A (LDHA). LDHA facilitates the conversion of pyruvate to lactate and converts NADH to NAD^+ in the process (47). It has been found that high expression of LDHA promotes many characteristics of the tumour cell phenotype. It has been observed that tumour cells with down-regulated LDHA activity are not able to maintain high ATP levels. This resulted in decreased proliferation of tumour cells in normoxic and hypoxic conditions (48). In addition, LDHA overexpression promotes invasion and migration. It has been found that there is a positive correlation between LDHA expression and distant metastasis of colorectal cancer (49).

1.4.2.3. Changes in GLUT1 expression

Glucose transporter 1 (GLUT1) is another protein that when elevated may facilitate the Warburg effect. GLUT1 is encoded by the *SLC2A1* gene and it functions to transport glucose molecules across the plasma membrane into cells. It has been reported to be overexpressed in many types of cancer, for example in colorectal cancer (50). Moreover, it has been shown by Shen *et al.* that the expression of GLUT1 is increased in colorectal tumours with mutated *KRAS*. In addition, overexpression of GLUT1 has been associated with poor prognosis in most solid tumours (50) including colorectal cancer (51).

1.4.2.4. Changes in MPC expression

Loss of mitochondrial pyruvate carrier (MPC) expression is another way tumour cells shift metabolism towards increased glycolysis. The role of the MPC is to transfer pyruvate from the cytosol across the mitochondrial membrane. The MPC protein consists of two subunits; MPC1 and MPC2 that are encoded by the *MPC1* and *MPC2* genes (52). As a results of decreased expression of one or both MPC subunits less pyruvate enters mitochondria. That promotes pyruvate conversion into lactate and the Warburg effect. Reduced expression of *MPC1* positively correlates with poorer prognosis in colorectal cancer (53).

1.4.2.5. Changes in PDK1 expression

Increased expression of pyruvate dehydrogenase kinase 1 (PDK1) can also promote the Warburg effect. PDK1 inhibits pyruvate dehydrogenase (PDH), an enzyme which converts pyruvate into acetyl-CoA; one of the major TCA cycle carbon sources. As a result of PDH inhibition, pyruvate is diverted to lactate instead and the levels of glycolysis are increased,

contributing to the Warburg effect (54)**.** PDK1 overexpression has been shown to promote a malignant phenotype in many cancer types. For example, Liu *et al.* has reported that elevated expression of PDK1 increases cell proliferation and mobility as well as inhibiting apoptosis in non-small cell lung cancer (NSCLC) (55). In addition, Nam *et al.* has shown that PDK1 levels are increased in the HT29 colorectal cancer cell line and that it is one of the proteins involved in driving aerobic glycolysis in this colorectal cancer cell line (56). Moreover, Wnt signalling has been found to affect PDK1 expression levels in colorectal tumour cells. In 2014, Pate *et al.* showed that dysregulation of Wnt signalling in cells increases the level of glycolysis. In addition, they identified that PDK1 is a direct target of Wnt signalling (57). Due to the fact that the role of PDK1 is to inhibit carbon entry into the TCA cycle, the levels of glycolysis in cells harbouring this mutation are increased, contributing to the Warburg effect (54).

1.4.2.6. Changes in HIF1α expression

Hypoxia inducible factor 1α (HIF1α) is an important regulator of many metabolic proteins and enzymes involved in facilitating the Warburg effect. It is known to play a role in supporting tumour cell proliferation during hypoxia. However, in normoxic conditions HIF1α has been recognized to support metabolic reprogramming by positively regulating expression of numerous proteins including PKM2, LDHA, GLUT1 and PDK1. Overexpression of HIF1α has been reported to be positively correlated with poorer prognosis in colorectal cancer patients (58).

1.4.3. Oxidative metabolism

Although glycolysis is upregulated in cancer cells, this is often not at the expense of oxidative metabolism. TCA cycle metabolism and ATP production in the mitochondria remain important for tumour cells. The TCA cycle not only produces energy, but also provides intermediates for fatty acid and amino acid synthesis (59). These molecules serve as building blocks for rapidly dividing cells (60). For example, fatty acids are the most important component of the cell membrane. In addition, fatty acid derivatives are used in cell signalling (60). Amino acids serve as building blocks for proteins, messengers for intercellular communication as well as energy generating metabolites (61). In addition, the TCA cycle provides precursors for nicotinamide adenine dinucleotide (NADH) synthesis, which is then used for energy production in the electron transport chain (ETC) (59).

1.4.3.1. Mutations in TCA cycle metabolic enzymes

The TCA cycle consists of eight steps, which are catalysed by different enzymes (59). Mutations in TCA cycle enzymes such as citrate synthase, succinate dehydrogenase (SDH), aconitase, isocitrate dehydrogenase (IDH) and fumarate hydratase (FH) have been reported

in numerous cancers (62). These mutations result in aberrant production of TCA cycle intermediates, so called oncometabolites (62). For example, IDH is an enzyme, which catalyses the conversion of isocitrate to α-ketoglutarate (α-KG) (59). IDH is encoded by two genes: *IDH1* and *IDH2* (59). Mutations can occur in either of these genes, however, they are more prevalent at *IDH1*. Mutated IDH is able to convert α-KG to 2-hydroxyglutarate (2-HG) (59). 2-HG has been found to promote development and progression of some cancers, such as gliomas, and is considered an oncometabolite (59). Another example of a TCA cycle enzyme found to be mutated in cancers is SDH (59). SDH catalyses conversion of succinate to fumarate (59) Reduced activity of SDH results in decreased production of fumarate and an accumulation of succinate (59). Mutations in an enzyme catalysing conversion of fumarate into malate – FH, are also common in some cancers (59). Mutations in FH lead to an accumulation of fumarate in cells (59). Fumarate is also considered an oncometabolite (63). Generation of oncometabolites such as fumarate, succinate and 2-HG lead to the stabilization of HIF1α (64). In normal cells, when oxygen is available HIF1α is hydroxylated by prolyl hydroxylase (PHD) and then ubiquitinated by pVHL (the von Hippel-Lindau tumour suppressor protein) and degraded (64). Accumulation of oncometabolites inhibits PHD activity. As a result, HIF1α cannot be ubiquitinated by pVHL and degraded (64). Activation of HIF1α has multiple effects on cellular metabolism as described in section 1.4.2.6. In this way reprogrammed TCA cycle metabolism can drive tumour cell growth and survival (62).

1.4.3.2. Glutamine anaplerosis

Another important aspect of metabolic reprogramming in cancer is increased uptake of glutamine. Glutamine is not only an important source of nitrogen but also a source of energy for rapidly proliferating cells. As a result of decreased amounts of glucose entering the TCA cycle due to the Warburg effect, carbon from glutamine can fuel the TCA cycle, entering as α-ketoglutarate (α-KG) and be used to produce ATP (65). This is known as TCA cycle anaplerosis. Increased glutaminolysis has been reported in many cancers (66)**.** Glutaminase (GLS – the enzyme converting glutamine to glutamine, the first step in glutaminolysis) expression and ASCT2 (a glutamine transporter) expression in increased in many cancers including colorectal cancer. In addition, mutations in Wnt signalling has been found to promote glutamine anaplerosis. This occurs via activation of one of its target genes – c-myc. Myc has been shown to increase mitochondrial gene expression and as a result promote mitochondrial biogenesis (31). Moreover, it has been demonstrated that overexpression of myc increases usage of glutamine by the mitochondria. It does so by enhancing the expression of the metabolic enzyme GLS, which deaminates glutamine to produce glutamate. Glutamate can be converted into α-ketoglutarate, which serves as a TCA cycle intermediate (31).

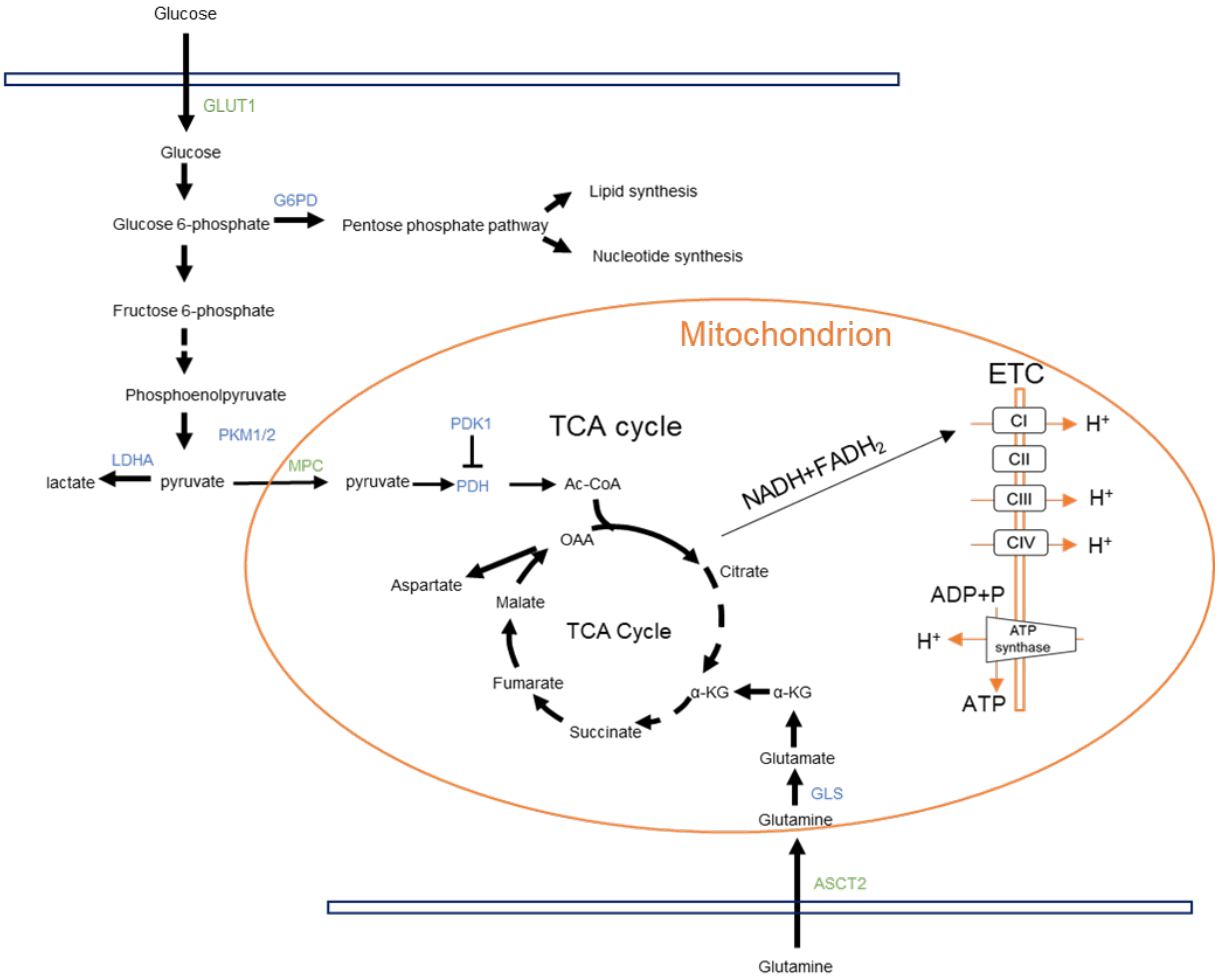

Figure 6. The main metabolic pathways in tumour cells. GLUT1 transports glucose into the cells for usage in glycolysis. The pentose phosphate pathway (PPP) branches off glycolysis and results in lipid and nucleotide synthesis. The end product of glycolysis – pyruvate is transported into the mitochondria where it is converted in acetyl-CoA, which enters TCA cycle. NADH and $FADH_2$ produced by TCA cycle are used as electron donors for the electron transport chain, which occurs at the mitochondrial membrane.

1.5. Diabetes Mellitus

Diabetes Mellitus is emerging as one of the major global health problems in recent years. According to the International Diabetes Federation (IDF), it affects around 425 million adults worldwide and its incidence is steadily increasing (67). IDF estimates that the number of individuals with diabetes will rise to 629 million by 2045 (67). Currently, diabetes is placed 9th as a major cause of reduced life expectancy (68). Diabetes can be divided into two types. Type 1 diabetes is an autoimmune disease most commonly of juvenile-onset, whereas type 2 diabetes is a non-insulin dependent metabolic disorder most commonly occurring in adults, however earlier and earlier onset is being recorded (69).

1.5.1. Type 2 Diabetes Mellitus

Type 2 Diabetes Mellitus (T2DM) accounts for 90% of all cases of diabetes (70). Although some genetic factors can influence the predisposition to this disease (71), the key drivers are environmental (72). The main risk factors for developing diabetes include: obesity, unhealthy diet and sedentary lifestyle (72). T2DM is characterized by insulin resistance in insulin responsive tissues: liver, skeletal muscle and adipose tissue (73). Insulin resistance leads to elevated hepatic glucose production, which results in systemic hyperglycaemia (74). As a consequence, pancreatic β cells produce excessive amounts of insulin in order to overcome insulin resistance and this leads to hyperinsulinemia (74).

The pathophysiological disturbances occurring in T2DM lead to abnormal levels of circulating metabolites. As a result people with T2DM have an increased risk of developing other health issues including cardiovascular disease, blindness, kidney failure (44) and cancer (75).

1.5.2. Type 2 Diabetes Mellitus and Cancer

Epidemiological data shows that T2DM increases the risk of developing cancer at various sites such as breast, bladder, endometrium, pancreas, colon and rectum. Moreover, several cohort studies have indicated that T2DM also increases the risk of cancer related mortality from several cancers including endometrial, breast and colorectal (76,77). For example, a retrospective cohort study performed by Lipscombe *et al.* has shown that women with T2DM have around 40% greater mortality within first five years after developing breast cancer compared to women without diabetes (77). A meta-analysis of observational studies carried out by Mills *et al.* has indicated that people with diabetes and colorectal cancer have a 17% increased risk of all-cause mortality and a 12% increased risk cancer-specific mortality (78).

Cancer and T2DM share common risk factors such as obesity, which may be partially responsible for the associations between these two diseases. However, there is accumulating evidence that T2DM is an independent risk factor for developing cancer and increased cancer

related mortality. Several studies have reported that the association between T2DM and cancer is independent of BMI (79–81). Biological associations between diabetes and cancer are still poorly understood. However, it is thought that T2DM may create a favourable environment for cancer initiation and progression (42). The best investigated potential mechanisms explaining a link between the two diseases include: hyperglycaemia, chronic inflammation and hyperinsulinemia.

1.5.3. Hyperglyceamia

Hyperglycaemia is a key feature of T2DM (75). High levels of circulating glucose, which occurs as a result of hyperglycaemia, may facilitate tumour cell energetics and promote chronic proliferation (75). Tumour cells use glucose as a preferential source of energy, therefore, a glucose abundant environment may create advantageous conditions for tumour growth (75). Moreover, high glucose levels benefit tumour cell resistance to chemotherapy and reduce chemotherapy survival rates (82). Hyperglycaemia has been shown to increase the toxicity of chemotherapeutic drugs such as carboplatin and 5-fluorouracil by *in vitro* studies (82). In addition, according to a systematic review and meta-analysis performed by Alenzi *et al.* hyperinsulinemia increases the risk of chemotherapy induced neutropenia (CIN) by 32% (83). CIN is a condition which results in the reduction in neutrophil numbers leading to increased risk of developing infections by cancer patients undergoing chemotherapy (84). This may also contribute to the increased cancer specific mortality rates occurring in people with T2DM.

1.5.4. Chronic inflammation

Another factor which may benefit neoplastic processes in people with T2DM is fat induced chronic inflammation (85). T2DM and related obesity results in adipocytes producing abnormal levels of various inflammatory factors such as tumour necrosis factor-α (TNFα), interleukin-6 (IL-6), plasminogen activator inhibitor-1 (PAI-1), monocyte chemoattractant protein, as well as adiponectin and leptin (85). Some of these changes in the levels of inflammatory factors are known to promote cancer development. For example, elevated expression of serine protease inhibitor PAL-1 has been shown to promote progression of several cancers including: breast, colorectal, endometrial, renal and thyroid cancers (85). Increased expression of the pro-inflammatory cytokine TNF-α activates nuclear factor κβ (NFκβ), which upregulates expression of anti-apoptotic proteins and results in increased cell survival (86). Elevated serum levels of TNF-α have been reported to correspond with increased cancer-related death (85).

1.5.5. Hyperinsulinemia

Hyperinsulinemia is a term used to describe abnormally high insulin levels in the blood (87). Insulin is a hormone which regulates blood sugar levels by inducing glucose uptake into the cells and acts as a growth factor signalling to cells to proliferate (88). Insulin stimulation activates numerous biological pathways with many functions including growth, proliferation and

cell survival (88). Therefore, it is thought that chronic exposure to high levels of insulin may promote tumour growth (85). The stimulating effect of insulin on tumour cell proliferation was first reported in animal studies (89). In 1972, Heuson *et.al* showed that insulin promotes growth of mammary tumours induced by carcinogen (7,12-dimethylbenz(a)anthracene) treatment in artificially insulin deficient rats (89).

Epidemiological data shows that hyperinsulinemia increases the risk of colorectal (90) and endometrial (91) cancers. Moreover, it has been shown that it is an independent risk factor for breast cancer development in post-menopausal women (92). Hyperinsulinemia is very likely to explain the association between T2DM and cancer. It is a very early symptom of the disorder, usually developing before diagnosis (75). Therefore, it may be linked to the fact that the increase in incidence of cancers like colorectal, endometrium or breast occur within months after T2DM onset (93).

In addition, high levels of insulin enhance hepatic production of insulin growth factor (IGF-1) (85). High concentrations of IGF-1 has been also associated with increased risk of cancer development (85). Some studies reported that IGF-1 has stronger mitogenic and anti-apoptotic effects on cells than insulin itself (85).

The importance of hyperinsulinemia as a factor increasing risk of cancer in people with T2DM is supported by studies on metformin (94). Metformin is a drug used to treat T2DM, which increases tissue sensitivity to insulin and in this way reduces hyperinsulinemia (95). There is increasing evidence that people treated with metformin have lower risk of developing cancers than people treated with insulin or insulin analogues (94).

1.6. Diabetes and colorectal cancer

According to epidemiological data, people with T2DM have a 50% increased risk of developing colorectal cancer. In addition, T2DM increases the risk of dying from colorectal cancer by ~12% compared to people without diabetes (96). The connection between T2DM and colorectal cancer has been acknowledged by the American Diabetes Association (ADA) (97). According to the guidelines of the association, people with T2DM should be advised to change unhealthy lifestyle habits which increase cancer risk as well as undergo cancer screening befitting their age and sex (97).

An association between T2DM and more aggressive colorectal tumours has been reported by some studies (98). The results of a retrospective analysis performed by Sharma *et.al* show that people with diabetes and colorectal cancer exhibit deeper tumour invasion and greater lymphovascular invasion than people without diabetes (98). In addition, the same study has

also indicated that people with diabetes have higher TNM (tumour node metastasis) staging and are more likely to develop transverse tumours (98).

1.6.1. Hyperinsulinemia and colorectal cancer

The impact of insulin on colorectal cancer has been examined by many *in vitro* and *in vivo* studies. For example, research performed by Tran *el al.* investigated the effect of various markers of insulin resistance on colorectal cancer in rats (99). The factors they examined included: hyperinsulinemia, elevated blood levels of glucose, fatty acids and triglycerides (99). The results of this study showed that hyperinsulinemia alone is able to increase proliferation of colorectal epithelial cells (99). The infusion of insulin in rats for 10 hours increased growth of colorectal epithelial cells in dose dependent manner (99). Similar results were obtained in an animal study performed by Corpet *et al.*, where experimental rats were given either saline injections or ultralente bovine insulin injections (100). Data obtained from their investigation indicated that insulin promotes growth of aberrant crypt foci in the colon in rat models (100). Another example of a study investigating effects on insulin exposure on colorectal cancer phenotype was performed by Lu *et.al.* (101) The results of this investigation show that insulin stimulation promotes proliferation and migration of human colon cancer cell line - HCT-116 (101). They showed that insulin promotes cancer development by increasing activity of the PI3K/Akt and MAPK signalling pathways. Furthermore, a study carried out by *Liu et al.* showed that hyperinsulinaemia may be a factor promoting angiogenesis in colorectal cancer (102).

A study performed by Keku *et al.* also indicated an important role of hyperinsulinemia in colorectal tumour development (103). In their investigation, tissue samples from colonoscopy patients were collected in order to assess the relationship between plasma insulin, physiologic apoptosis and adenoma risk (103). The results of this study showed that high levels of circulating insulin positively correlate with increased adenoma risk. In addition, they found that elevated levels of circulating insulin may promote early adenoma progression by inhibiting apoptosis in normal colonic mucosa (103). Decreased levels of apoptosis caused by insulin stimulation may lead to accumulation of mutated cells, which may promote colorectal tumour development (103). Another study involving human subjects was carried out by Ortiz *et al.* In this study blood samples were collected from colonoscopy participants (104). In this study, researchers concluded that insulin resistance is a risk factor for the development of early stage colorectal tumours (104).

1.7. Insulin signalling in insulin responsive tissues

In the insulin responsive tissues, insulin signalling starts with the hormone binding to the insulin receptor (IR) on the cell surface. Upon insulin binding, the IR undergoes autophosphorylation on tyrosine residues, what leads to the recruitment of insulin receptor substrates (IRS) (88). The IR binds and phosphorylates IRS on tyrosine residues present within SH2 and PTB

domains. Phosphorylated IRS are able to bind and activate effector proteins including PI3K. Activated PI3K triggers conversion of membrane phospholipid - phosphatidylinositol (4,5)-bisphosphate (PIP_2) to phosphatidylinositol (3,4,5)-trisphosphate (PIP_3) (29). PIP_3 recruits PH domain containing proteins such as Akt (88). Akt mediates the metabolic and mitogenic effects of insulin through downstream signalling (105).

To exert a proliferative effect on cells, the PI3K/Akt pathway activates mTORC1 (105). mTORC1 induces cell growth by increasing the level of anabolic processes within the cell (32). For instance, it activates SREBP1, which mediates lipid synthesis and regulates mRNA translation via S6 kinase and 4EBPs (105). Furthermore, in order to release cells from cell cycle arrest, Akt mediates deactivation of the transcription factor FOXO, which subsequently gets degraded via the proteasome (105). In addition, Akt inhibits apoptosis by deactivating the pro-apoptotic protein – BAD (105). In order to push cells into S phase of the cell cycle, Akt phosphorylates GSK3, what results in the increase of cyclin D levels (105).

With regards to the metabolic response to insulin stimulation, in muscle and adipose tissue, Akt drives the translocation of GLUT4 to the plasma membrane in order to facilitate glucose uptake (106). Moreover, Akt downregulates GSK3, which is an inhibitor of glycogen synthesis and lipogenesis (107). As a result, there is an increase in glucose uptake into cells, and any excess glucose is converted into glycogen (106).

Besides activating the PI3K/Akt pathway, insulin binding to the IR also triggers the MAPK pathway. Activated IR and IRS recruit SH2 binding proteins such as Grb2 and Shc. Grb2 binds to proline rich-regions of son-of-sevenless (SOS) protein. SOS acts as a guanine nucleotide exchange factor for Ras. SOS activates Ras by catalysing a switch from GDP-bound Ras to GTP-bound Ras. Activated Ras triggers a downstream kinase cascade resulting in cellular proliferation.

In addition, insulin has been shown to upregulate the pentose phosphate pathway as well as an uptake of glutamine and fatty acids into the cell (42). Increase in these anabolic pathways provides the energy and biomass necessary for proliferation (42).

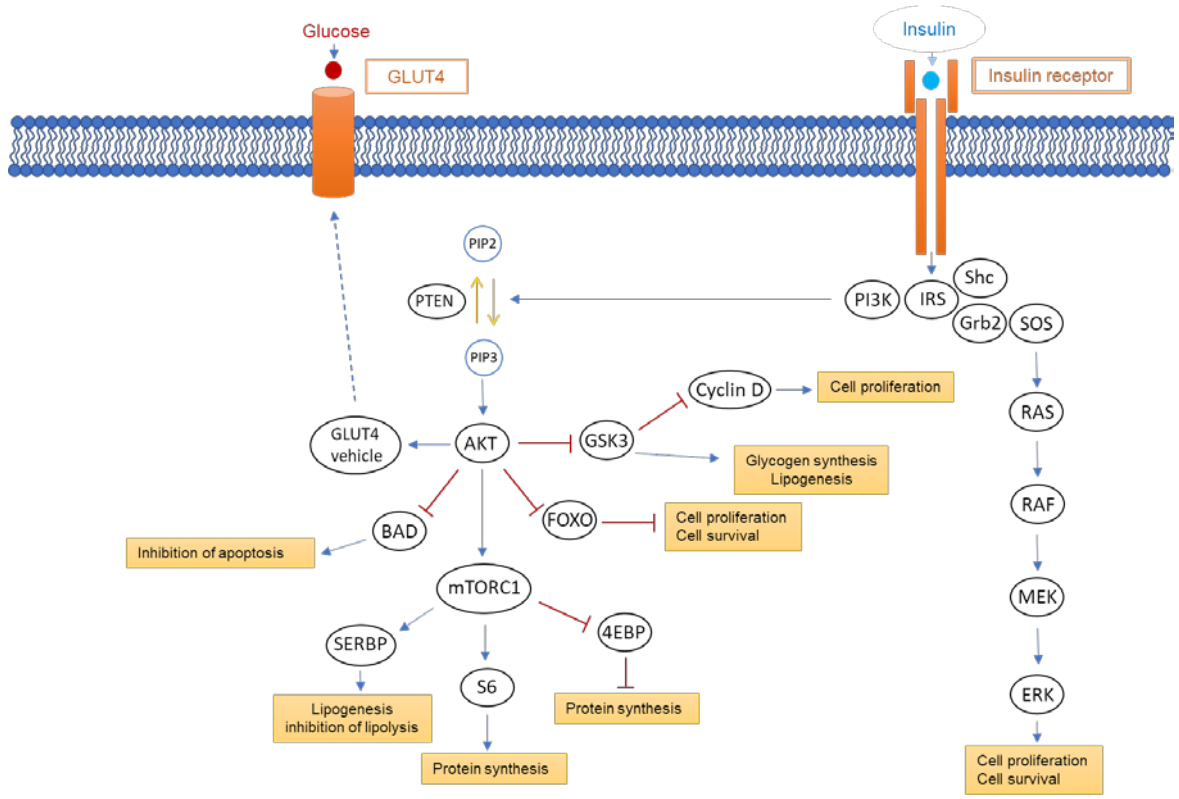

Figure 7. Insulin signalling pathways. Insulin binds to the insulin receptor (IR), which phosphorylates insulin receptor substrates (IRS). IRS recruit Shc and Grb, which activate SOS and drives MAPK signalling pathway. IRS also recruits PI3K, which triggers PIP2 conversion to PIP3 and Akt activation follows. Akt inhibits GSK3, FOXO and BAD and activates mTORC1. In addition, Akt triggers translocation of GLUT4 to the plasma membrane.

1.8. Insulin and cancer metabolism

The impact of insulin on cancer cell proliferation through its effects on cellular signalling has been extensively studied (as described earlier in this chapter). However, the effect of insulin on cancer cell metabolism has not been extensively explored. Some studies, which investigated the impact of insulin on cancer metabolism are discussed below:

1.8.1.1. Insulin and HIF1α

It has been shown that hyperinsulinemia induces HIF1α expression during normoxia in several cancers (108–110). As discussed above, HIF1α expression promotes the Warburg effect. Hlf1α acts as a positive regulator of PDK1 (111) and LDH (112). Moreover, HIF1α also increases transcription of glucose transporters such as GLUT1 and in this way increases the

uptake of glucose to cells (113). In addition, HIF1α up-regulates transcription of PKM2, which also contributes to increased levels of glycolysis in cancer cells (114). In this way insulin may promote the Warburg effect in tumour cells.

1.8.1.2. Insulin and PKM2

In 2013, Iqbal *et al.* demonstrated that insulin stimulation up-regulates expression of the glycolytic enzyme PKM2 via the PI3K/mTOR pathway and concomitantly reduces it's activity through an independent pathway in hepatocellular carcinoma cells. This rise in PKM2 expression has been demonstrated to increase levels of glycolysis in cancer cells (114). Insulin induces the production of ROS which disrupt the tetrameric (most active) form of PKM2 and causes accumulation of its dimeric and monomeric structures (114). As a result, there is an increase in glucose uptake and a decrease in glycolytic flux, what leads to the accumulation of glycolytic intermediates and NADPH. The net outcome is upregulation of biosynthetic pathways in cancer cells (114).

1.8.1.3. Insulin and G6PD

There are also other ways by which hyperinsulinemia may stimulate biosynthetic pathways besides inducing aerobic glycolysis. Insulin is a known regulator of glucose-6-phosphate dehydrogenase (G6PD) expression (115). G6PD is an enzyme involved in initiating the pentose phosphate pathway. It is possible that chronic insulin exposure may upregulate the pentose phosphate pathway (PPP) in cancer cells (42). PPP results in lipid and nucleotide synthesis (116). Therefore, increased levels of PPP is beneficial for cancer cells as it provides building blocks necessary for chronic proliferation (116).

1.8.1.4. Insulin and ASCT2

Another aspect of cellular metabolism that insulin has been shown to influence is glutamine uptake (117). According to the protein atlas database, there is an increase in expression of the glutamine transporter - ASCT2 in colorectal cancer cells (118). Glutamine may be used by cells as a carbon source for the TCA cycle (119).

1.9. Aims and Objectives

The aim of this project was to examine the impact of insulin exposure on colorectal tumour cell metabolism. Understanding the impact and mechanism of insulin action on colorectal tumour cell phenotype will help us to understand how T2DM promotes colorectal cancer development. In addition, better understanding of the specific molecular mechanisms by which insulin reprogrammes colorectal tumour cell metabolism may contribute to the development of new targets for cancer therapy. The specific aims of this study are:

- To determine what stages of colorectal tumour development are the most sensitive to insulin stimulation.
- To examine what signalling pathways are affected in sensitive cells lines.
- To examine the effect of insulin on tumour cell metabolism.

Chapter 2: Methods & Materials

2.1. Tissue culture

2.1.1. Cell lines

In this study various human colorectal adenoma and carcinoma cells were used as *in vitro* models:

2.1.1.1. HT29

HT29 cell line was isolated from a sporadic colorectal adenocarcinoma (120). This cell line has mutations in *APC* (121), *BRAF* and *TP53* (122) genes.

2.1.1.2. SW480

SW480 cell line was derived from a patient with colorectal adenocarcinoma (123). SW480 harbour mutations in *APC* (121), *KRAS* and *TP53* (122) genes.

2.1.1.3. S/RG

S/RG is a clonogenic cell line derived from a human tubular adenoma. This cell line has mutations in *TP53*. In addition, most of S/RG cells have one normal copy of chromosomes number 6, 7, 14, 17, 18, and 22 (124).

2.1.1.4. AA cell line series

The AA cell line series was established by progressive transformation of an adenoma cell line to a malignant carcinoma cell line using carcinogens (125). This cell line series was isolated and developed by the Williams' group before I started my work in the laboratory (125). It was derived from a single large adenoma of 3-4cm in diameter from a patient with Familial Adenomatous Polyposis (FAP). The first cell line isolated (AA) was diploid, fibroblast feeder dependent and non-tumourigenic. Four cell lines were subsequently and sequentially generated from AA: AA/C1, AA/C1/SB, AA/C1/SB/10C, AA/C1/SB/10C/M (125). It is these four cell lines that I used in this project.

Cells were transformed in a following order:

AA/C1 represents the earliest stage of tumourigenesis. AA/C1 cells were isolated from AA after 50 passages. AA/C1 was aneuploid, clonogenic and fibroblast feeder independent with some evidence of tumour progression *in vitro*. AA/C1 were treated with sodium butyrate for 14 days and this gave rise to AA/C1/SB. AA/C1/SB cells had 6.13% increased colony forming efficiency but remained anchorage dependent and non-tumouigenic. Next, AA/C1/SB cells were exposed to *N*-methyl-*N*'-nitro-*N*-nitrosoguanidine and this gave rise to AA/C1/SB/10C, which had 17.3% increased colony forming efficiency. They were also anchorage independent and became

tumourigenic in nude mice. AA/C1/SB/10C/M was derived from a tumour produced by inoculation of AA/C1/SB/10C in to nude mice (6).

All AA series cell lines are aneuploid. They all carry one or two copies of abnormal chromosome 1 as well as one or two copies of normal chromosome 1. Abnormal chromosome 1 is characterized by a pericentic inversion at bands p32 and q23 and loss of a fragment of short arm distal to band p32. In addition, they show monosomy of chromosome 18 and carry up to six copies of chromosome 6,9 and 13. The original paper by Paraskeva *et al.* stated that abnormalities in chromosome 1 and multiple copies of chromosome 13 present in those cells may be important in colorectal tumour development and progression (126).

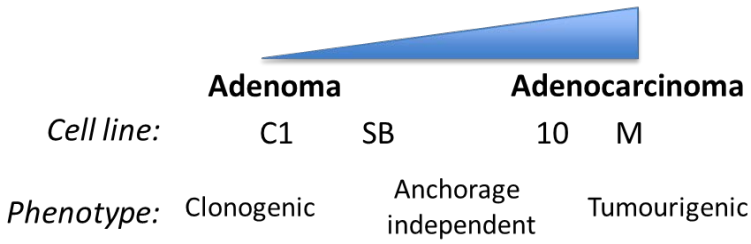

Figure 8. Progression of AA cell line series. AA/C1 represents the earliest stage of colorectal tumourigenesis. It is clonogenic and anchorage dependent, but not tumorigenic. AA/C1/SB is a subsequent stage, still anchorage dependent and non-tumorigenic. AA/C1/SB/10C is an anchorage independent cell line. AA/C1/SB/10C/M is anchorage independent and tumorigenic in nude mice.

2.1.2. Cell maintenance

Dulbecco's Modified Eagles Medium (DMEM, Sigma-Aldrich) cell growth media was used for all cell culture. HT29 and SW480 cell lines were cultured in DMEM supplemented with 10% (v/v) foetal bovine serum (FBS, Life technologies, Paisley, UK), 2mM L-glutamine, 100 units/ml penicillin (Life Technologies, Paisley, UK) and 100µg/ml streptomycin (Life Technologies, Paisley, UK). The AA cell line series and S/RG cell line were cultured in DMEM supplemented with 20% (v/v) FBS, 4mM L-glutamine, hydrocortisone (1µg/ml), 100 units/ml penicillin (Life Technologies, Paisley, UK), 100µg/ml streptomycin (Life Technologies, Paisley, UK) and 0.2 units/ml insulin (Sigma, Poole, UK). Cell lines were cultured in 25cm^3 (T25) flasks (Corning Incorporated, Corning, New York, USA) in a non-humidified incubator at 37˚C with 5% CO_2. Growth media was changed every 3-4 days.

2.1.3. Cell passaging

Cell lines were routinely passaged with the following frequency and split ratio: HT29 and SW480 – every 7 to 10 days with split ratio 1:10, S/RG – every 2 weeks with split ratio 1:4, AA/C1 – every 3 to 4 weeks with split ratio 1:4, AA/C1/SB – every 2 to 3 weeks with split ratio 1:6, AA/C1/SB/10C – every 2 to 3 weeks with split ratio 1:8-1:10, AA/C1/SB/10C/M – every 10 to 14 days with split ratio 1:8 – 1:10.

Cells were washed two times with 3ml of phosphate buffered saline (PBS, pH 7.4; Severn Biotech Ltd, Kidderminster, UK) and subsequently incubated with 1ml of 0.1% (w/v) trypsin solution (BD Bioscience, Oxford, UK) and 0.1% (w/v) ethylene-diamine-tetra-acetic acid (EDTA) (Sigma, Poole, UK). When cells detached from the plastic, media was added to the flasks to neutralize the trypsin. For HT29 and SW480 cell lines, the cell suspension was transferred into a universal and spun at 3000rpm for 3 minutes. Next, the liquid was aspirated off and the pellet was resuspended in 10ml of fresh media and used to seed new flasks. For the AA cell line series and S/RG cell line, cell suspension was mixed by pipetting up and down several times and directly transferred to new flasks.

2.1.4. Cell counting

Cells were counted using a 0.1mm Neubauer haemocytometer. Trypsinized cells were resuspended in media. 20ųl of cell suspension was mixed with 20µl of trypan blue dye (Gibco® Life Technologies, USA) in order to distinguish live and dead cells. Next, the mixture was loaded on haemocytometer and counted either manually or by using the Corning Cell Counter (CytoSMART, Netherlands).

2.1.5. Freezing down and recovery of cells

To freeze down, cells were trypsinized and resuspended in DMEM with 10% dimethylsulphoxide (DMSO). Next, 1ml of cell suspension was transferred into a 1.2ml Cryovial® (Simport, Saint-Mathieu-de-Beloeil, Canada). Cryovials were placed in a Mr Frosty™ Freezing Container (Life Technologies, Paisley, UK) and kept in a -80˚C freezer for four hours. Subsequently, cryovials with cells were transferred into a -174˚C liquid nitrogen container.

To bring up, 1ml of cell suspension from the cryovial was transferred into T25 flask and 3ml of DMEM was added to it.

2.2. Crystal violet cell viability assay

2.2.1. Seeding cells

Cells were seeded in 96 well plates with seeding density 6000 – 40 000 cells per well in 100µl, depending on the cell line. Cells were seeded in the 60 wells in the middle of the plate (excluding the outer wells). 200µl of PBS was added into the surrounding, outer wells in order to prevent evaporation of media. The growth media used for cell seeding was the same as that used for routine cell culture for each particular cell line. Plates were stored in a non-humidified incubator at 37˚C and 5% CO_2.

2.2.2. Treatment

24 hours after seeding, growth media was aspirated off the plates and replaced with treatment media (this varies depending on the experiment and cell line). For the AA series, DMEM with 10% FBS, 2mM glutamine, 100 units/ml penicillin and 100 µg/ml streptomycin was used for experiments. For HT29 and SW480, DMEM with 2mM glutamine, 100units/ml penicillin and 100 µg/ml streptomycin (supplemented with 4% FBS and with either 25mM or 3mM glucose (10% D-(+)-Glucose solution, Sigma Aldrich, UK) was used. In addition, treatment media contained various concentrations of a particular treatment agent. Plates were stored in a non-humidified incubator at 37˚C and 5% CO_2 until fixing. Treatment agents included: insulin or an AKT1/2 kinase inhibitor (Sigma, Poole, UK) prepared in DMSO (VWR International Ltd., Lutterworth, UK). For concentrations of treatments used see figure legends.

2.2.3. Fixing

Growth media was aspirated off the plates and 100µl of cold 4% paraformaldehyde (PFA) was added into each well with cells and five control wells containing just PBS. Plates were left for 30 minutes to allow fixing of cells. Next, PFA was removed and 200µl of PBS was added to each well. Plates were covered with cling film and stored at 4˚C until staining.

2.2.4. Staining

PBS was aspirated off the plates. 100µl of 0.5% crystal violet stain (Sigma) was added to each well with cells and the five control wells without cells. Plates were placed on the rocker for 30 minutes. Next, crystal violet stain was removed using a multichannel pipette and plates were rinsed with water. Plates were left to dry overnight.

2.2.5. Solubilisation and absorbance measurement

100µl of 2% SDS solution was added into each well. Plates were placed on a rocker for 1 hour. Next, the absorbance was measured at 595nm wavelength using the iMark™ Microplate Absorbance Reader (Bio-Rad, CA, USA).

2.3. Western Blotting

2.3.1. Cell lysis

Firstly, 1.5X cell lysis buffer (Cell Signalling Technology) was made. It was prepared out of 10X cell lysis buffer by mixing 20mM Tris-HCl pH 7.5, 1% v/v Triton-X100, 150mM NaCl, 1mM EDTA 1mM β-glycerophosphate, 2.5M sodium pyrophosphate and 1mM sodium orthovanadate and diluting in ddH_2O with Roche Complete Mini Protease Inhibitor tablet dissolved in 10ml. Growth media was aspirated off the flasks and cells were washed twice with 2ml of ice cold PBS. 100ul of 1.5X cell lysis buffer was added to the flasks. Flasks were placed on ice and incubated on a rocker for 10 minutes. Subsequently, cells were scraped and transferred into a chilled Eppendorf tube. Next, the lysates were spun in the centrifuge at 18500g at 1˚C for 10 minutes. After spinning supernatant was collected and transferred into an ice cold Eppendorf tube. Cell lysates were stored in -80˚C.

2.3.2. Protein assay and sample preparation

A blank (water) sample and the bovine serum albumin (BSA) protein standards with following concentrations: 6.25, 12.5, 25, 50, 100, 200, 400, 800 µg/ml were prepared.

31ul of each standard and water control was added in duplicate to 96 well plate. Next, 1ul of each lysate and 30ul of ddH_2O were added to a 96 well plate in triplicate. Subsequently, Bio-Rad Protein assay reagents (Bio-Rad, CA, USA) were added to protein standards and samples in quantities stated in the manufacturer's protocol in order to determine protein concentration in each sample. Absorbance was read at 750nm wavelength using the iMark™ Microplate Absorbance Reader (Bio-Rad, CA, USA).

Samples were prepared with concentrations of 15-30µg/ml per 15µl and 5µl of 5X Laemmli sample buffer per 25µl of sample was added. Samples were boiled for 5 minutes, spun and stored at -20˚C.

2.3.3. SDS-PAGE

Polyacrylamide gels were prepared using Mini-Protean 3 Electrophoresis equipment (Bio-Rad, Hemel Hempstead, UK). Compositions and concentrations of gels are presented in the tables. 15µl of each sample was loaded on a gel alongside 5µl the Precision Plus Protein™ Dual Colour Standard markers (Bio-Rad Laboratories Ltd., Watford, UK). The gel was run at 100V for 15 minutes and then at 180V for 60 minutes in running buffer (Table 1) until the samples reached the end of a gel.

2.3.4. Transfer

The glass cassette was disassembled, and the gel was pre-soaked in transfer buffer for 5 minutes. Immobilon® polyvinylidene difluoride (PVDF) membrane was pre-soaked in

methanol, washed with ddH_2O and soaked in transfer buffer. Next, a transfer cassette was assembled in a following order: sponge, two pieces of filter papers, acrylamide gel, Immunobilon membrane, two pieces of filter paper and sponge. The transfer was run using a Transblot Cell (Bio-Rad, Hemel Hampstead, UK) at 100V for 1.5 hour.

2.3.5. Blocking and protein detection

When the transfer was finished, the membrane was incubated in blocking buffer (5% milk in TBST) on a rocker for 1 hour. Next, the primary antibody was prepared and diluted in 0.5% milk in TBST. The membrane was placed in a plastic bag and incubated with a primary antibody overnight at 4˚C. On the next day, the membrane was washed in TBST for 15 minutes three times. The secondary antibody was prepared by diluting an appropriate volume of the antibody in 0.5% milk in TBST. Membrane was incubated in secondary antibodies for 1 hour at room temperature. Next, the membrane was washed three times in TBST. Each wash lasted 15 minutes. After the last wash, the membrane was rinsed in ddH_2O. Detection of proteins was performed using LumiGLO Peroxidase Chemiluminescence Substrate (KPL, Maryland, USA) according to manufacturer's protocol. Subsequently, the membrane was placed in a cassette on a stack of three x-ray films. Films were developed using a Compact X4 Film Processor and scanned using SilverFast® Ai Studio 9 software (Lasersoft Imaging AG).

Table 1. Compositions of buffers used for western blotting.

Buffer	Composition	Source
Running Buffer	192mM Glycine	National Diagnostics, Hessle, UK
	25mM Tris	National Diagnostics, Hessle, UK
	0.1% (w/v) SDS	Sigma, Gillingham, UK
Transfer Buffer	192mM Glycine	National Diagnostics, Hessle, UK
	25mM Tris	National Diagnostics, Hessle, UK
	20% (w/v) methanol	Sigma, Gillingham, UK
Tris-Buffered saline - Tween 20 (TBST)	50mM Tris, HCl pH 7.4	National Diagnostics, UK
	150mM sodium chloride	BDH, VWR, Poole, UK
	0.1% Tween 20	Sigma, Gillingham, UK

Table 2. Reagents used to prepare acrylamide gels and their source.

Reagent	Source	12.5%	10%	7.5%	Stack (4.5%)
30% Acrylamide/1%Bis	National Diagnostics, Hessle, UK	7.3ml	5.8ml	4.4ml	1.2ml
Resolving Buffer 1.5M Tris, pH 8.0 0.4% SDS	National Diagnostics, Hessle, UK	4.4ml	4.4ml	4.4ml	-
Stack buffer 0.5M Tris pH6.8/0.4% SDS	National Diagnostics, Hessle, UK	-	-	-	2.0ml
Distilled water		5.8ml	7.3ml	8.7ml	2.0ml
Ammonium Persulfate 0.5g/ml	Sigma, Gillingham, UK	110µl	110µl	110µl	58µl
TEMED	Sigma, Gillingham, UK	3.6µl	3.6µl	3.6µl	1.8µl

Table 3. List of antibodies used in western blotting.

Type of antibody	Target	Host species	Dilution	Source
Primary	Phospho-Akt (s473)	Rabbit	1:2000	Cell Signalling Technology #4060S
Primary	Akt	Rabbit	1:2000	Cell Signalling Technology #9272S
Primary	ASCT2	Rabbit	1:1000	Cell Signalling Technology #5345S
Primary	Insulin Receptor β	Rabbit	1:200	Santa Cruz Biotechnology #sc-711
Primary	IGFRβ	Rabbit	1:1000	Cell Signalling Technology #3027
Primary	GLS1	Rabbit	1:1000	Cell Signalling Technology #88964
Primary	MPC1	Rabbit	1:1000	Cell Signalling Technology #14462S
Primary	LAT1	Rabbit	1:1000	Cell Signalling Technology #5347
Primary	PCK2	Rabbit	1:1000	Cell Signalling Technology #6924
Primary	Pyruvate dehydrogenase kinase (PDK1)	Rabbit	1:1000	Cell Signalling Technology #3820
Primary	Phospho-PRAS40	Rabbit	1:2000	Cell Signalling Technology #2997
Primary	α-tubulin	Mouse	1:10 000	Sigma, Gillingham, UK T9026
Secondary	Anti-Mouse IgG Peroxidase	Goat	1:1000	Sigma, Gillingham, UK
Secondary	Anti-Rabbit IgG Peroxidase	Goat	1:1000	Sigma, Gillingham, UK

2.4. Stable isotope tracer analysis

Cells were seeded in 60mm/15mm plates (Corning®, USA) in 3ml of growth media. Seeding density used for AA/C1 was 4.5×10^6 cells per plate, whereas seeding density for AA/C1/SB/10C/M was 0.5×10^6 cells per plate. After 72h cells were treated with or without 50ng/ml insulin for a further 72h.

Next, media was prepared for stable isotope incubation. Glucose-free or glutamine free DMEM (Thermo Fisher Scientific, Paisley, UK) was supplemented with 10% dialysed foetal bovine serum (dFBS) and either 10mM uniformly labelled ^{13}C-glucose (U-[^{13}C]-glucose) or 2mM ^{13}C-glutamine (U-[^{13}C]-glutamine) respectively (Cambridge Isotope Laboratories Inc., USA). Before incubation, media was aspirated off and cells were washed with 2.5ml PBS. Media containing stable isotope tracers was added to plates with or without 50ng/ml insulin. Plates were incubated in tracer containing media for 2 hours.

After 2 hours of incubation, media was aspirated off the plates and cells were washed with 2ml of ice-cold 9g/L saline solution. 800µl of ice-cold 80% methanol was added onto the plates. Plates were immediately placed on dry ice to stop cellular metabolism. Cells were scraped and transferred to pre-cooled Eppendorf tubes. A parallel set of plates was trypsinized and the cells were counted in order to normalize the data to cell number after analysis.

Cellular debris were cleared from metabolomics samples by centrifugation at 21,000 x g at 4˚C for 10min and subsequently dried by vacuum centrifuge (Concentrator 5301, Eppendorf) (≤ 4˚C, 18-24h). At this stage samples were sent to the Metabolomics Core Facility at McGill University, Montreal for analysis. Members of the Metabolomics Core Facility at McGill University carried out further preparation of the samples and ran them on the mass spectrometer, the data was returned and my supervisor, Dr Emma Vincent carried out the analysis. The data was then returned to me for presentation.

Although I did not carry out the below, I have briefly described how the samples were prepared for mass spectrometry and analysed, this was adapted from (127) and further detail can be found in this reference:

Cell pellets were dried and then resuspended in 30µl of pyridine with 10mg/ml methoxyamine hydrochloride (Sigma). Next, cell pellets were vortexed and sonicated. That was done in order to ensure pellet dissolution. Subsequently, 1µl of internal standard, myristic acid-D27 was dissolved in 750ng/µl of pyridine and added to the samples. Then, samples were moved to sealed autoinjection vials. Vials were heated at 70˚C for 30 minutes. After heating, 70µl of N-tert-Butyldimethylsilyl-N-methyltrifluoroacetamide (MTBSTFA) (Sigma) was added into the samples. Samples were incubated at 70˚C for 1 hour.

GC/MS analysis was carried out by using an Agilent 5975C GC/MS, which was containing a DB-5MS+DG (30m x 250µm x 0.25µm) capillary column (Agilent J&W, Santa Clara, CA, USA). Electron impact set at 70 eV was used to collect the data. 1µl of the derivatized sample was added through injection in the GC in splitless mode. The inlet temperature was at 280˚C. Helium was used as a carrier gas. A flow rate of 1.5512ml per min was used. This is a rate at which myristic acid elutes at 17.94min. The quadrupole temperature was set to 150˚C, whereas the GC/MS interface was set to 285˚C. The oven was programmed to start with 60˚C for 1 min. Then, the temperature in the oven was increasing for 10˚C per min until achieving 320˚C. Samples were kept at 320˚C for 10 minutes. Metabolites used in this investigation were validated in the past using authentic standards (all standards from Sigma) in order to confirm the mass spectra as well as the retention times.

Agilent ChemStation software was used to integrate ion intensities. Stable isotope tracer analysis was acquired by mass isotopomer distribution analysis using an algorithm, which was created by the Metabolomics Core Facility at McGill adapted from (128). This algorithm was used in order to produce matrices correcting for natural abundance of ^{13}C isotopomer in every metabolite. These matrices were then subtracted from each metabolite. The integrated ion intensities for each metabolite were normalised. Normalization was done by dividing the values obtained from the algorithm by the integrated ion intensities of the internal standard (myristic acid D27). Finally, the obtained values were divided by the mean number of cells, which was determined from parallel culture plates grown at the same time as the plates used in the experiment.

2.5. Quantitative real time PCR (qPCR)

2.5.1. Insulin treatment

Cells were seeded in 60 mm/15 mm plates in 3ml of 20% DMEM and grown for 72 hours. Subsequently, media was aspirated off the plates and replaced with 10% DMEM either with or without 50ng/ml of insulin. Plates were stored in the incubator.

2.5.2. RNA extraction

After 72 hours, plates were washed two times with 2ml of PBS and 1ml of TRI reagent (Sigma, Gillingham, UK) was added onto the plates. Next, cells were extracted by scraping and transferring them into an Eppendorf tube. Subsequently 200µl of chloroform (BDH, VWR, Poole UK) was added into the Eppendorf tubes. After incubating for 5 minutes at room temperature, samples were centrifuged at 11 500rpm for 15 minutes at 4˚C. This resulted in samples separating into three layers. The top layer was collected and transferred into a clean Eppendorf tube. 500µl of isopropanol (BDH, VWR, Poole UK) was added, samples were

shaken and left for 10 minutes at room temperature. Subsequently, the samples were centrifuged at 11 500rpm for 10 minutes at 4˚C. The supernatant was disposed of and 1ml of 70% ethanol was added into the pellet. Samples were spun at 8 500rpm for 5 minutes at 4˚C. Again, the supernatant was disposed of and the pellet was left for 5 minutes to air-dry. 100µl of molecular grade water was added and extracts were stored at -70˚C until proceeding to the washing steps.

2.5.3. Washing

Qiagen RNeasy Mini kit (Qiagen, Manchester, UK) was used for RNA purification. 350µl of RLT buffer and 250µl of 100% ethanol was added to the Eppenforf tubes. Samples were mixed by pipetting and transferred into RNeasy mini spin column placed in a 2ml collection tube. Columns were centrifuged at 10 000 rpm for 1 minute. Next, a mix of 10µl of DNase and 70µl of RDD buffer was prepared and added to each column. Columns were left at room temperature for 15 minutes. Subsequently, 350µl of RW1 buffer was added to the columns and they were centrifuged again at 10 000rpm for 1 minute. Next, 500µl of RPE buffer was added and columns were centrifuged at 10 000 rpm for 1 minute. This step was repeated, however, the second time columns were centrifuged for 2 minutes. Column was placed in 1.5ml Eppendorf tube, 50µl of water was added to the columns. Columns were spun at 13 000rpm for 1 minute. After centrifuging samples were left at room temperature for 30 minutes. Next, the samples were kept on ice for 1 hour.

2.5.4. Nanodroping and cDNA preparation

A nanodrop spectrophotometer (Thermo Scientific, Karlsruhe, Germany) was used to determine RNA concentrations. 1.5µl of molecular grade water was used to calibrate the machine. Next, 1.5µl of each sample was loaded onto the machine and RNA concentration was measured.

2µg RNA was added to a pair of PCR tubes. Next, 0.5µg Oligo dT primer (Promega, Southampton, UK) was added to the RNA. The PCR tubes were heated at 70°C for 5 minutes in order to allow annealing of the primer. After heating, the PCR tubes were placed on ice to avoid degeneration of secondary structures. Next, 5µl of 5x M-MLV reaction buffer (Promega, Southampton, UK) was added to each tube along with 5µl DeoxyribonucleotideTriphosphate (dNTPs) (10mM stock) (Promega, Southampton, UK) and 25 units of Recombinant RNasin Ribonuclease Inhibitor (Promega, Southampton, UK). In addition, 200 units of M-MLV reverse transcriptase enzyme was added to one PCR tube of the pair. The second PCR tube of the pair was a negative control with no enzyme added, hence no cDNA should be produced. Molecular grade water was added to the samples, so their final volume is equal to 25µl each. The PCR tubes were heated at 40˚C for one hour to allow cDNA synthesis. Later on, 75µl of

molecular grade water was added to each PCR tube, so the final concentration of cDNA produced was 20 ng/µl. cDNA was stored at -20˚C.

2.5.5. Running a plate

2µl of each cDNA sample was added into 96 well PCR plate (Agilent Technologies, West Lothian, UK) in triplicate. In addition, the negative control was added to a single well for each cDNA sample. Next, a master mix was prepared containing: 0.37 µl of forward and reverse primer, 6.25µl SYBR Green PCR Mix (Qiagen, Manchester, UK) and 3.5µl of molecular grade water for each sample. Plates were covered with strip lids and spun at 1,000rpm for 2 minutes. After spinning plates were placed in an MxPro 3005P Real-time Thermal Cycler (Agilent Technologies, West Lothian, UK) and analysed. In all experiments, a housekeeping gene; TATA-binding protein (*TBP)* was used as a control.

Table 4. Sequences for primers used in quantitative real time PCR.

Gene name	Primer sequence	
	Forward	Reverse
HIF1α	TATGAGCCAGAAGAACTTTTAGGC	CACCTCTTTTGGCAAGCATCCTG
PDK1	CGGATCAGAACCGACACA	ACTGAACCATTCTGGCTGGTGA
PKM1	ACCGCAAGCTGTTTGAAGAA	TCCATGAGGTCTGTGGAGTG
PKM2	GAGGCCTCCTTCAAGTGCT	CCGACTTGGTGAGAGACGAT
MPC1	TGACCTTTGCTTTGTGTTGC	CACCTTGGATCAATTGTGCT
LDHA	TGGAGTGGAATGAATGTTGC	ATAGCCCAGGATGTGTAGCC

Chapter 3: Investigating the impact of insulin exposure on cell lines representing different stages of colorectal tumourigenesis

3.1. Introduction

As described in Chapter 1, hyperinsulinemia has been linked to increased risk of colorectal cancer development. However, it is unclear what stage of colorectal tumourigenesis is the most sensitive to insulin stimulation. Insulin has been shown to promote colorectal tumour cell proliferation by many *in vitro* studies (85,101,114,129,130). However, the majority of these studies use cell lines representing one stage of colorectal tumourigenesis (commonly adenocarcinoma). In this project I had the rare opportunity to test the effects of insulin on a cell line series modelling progressive transformation and representing the different stages of colorectal tumourigenesis. Therefore, I could observe the effects of insulin on colorectal cells at different stages of tumourigenesis. In addition, many of the studies to date have used supra-physiological concentrations of insulin. In this investigation I used lower doses of insulin compared to other studies. In this way I could observe the effect of insulin on colorectal cells in conditions more similar to the physiological environment. It is important to explore the impact of insulin on colorectal cancer development in order to better understand why people with T2DM have an increased risk of colorectal cancer.

The aim of this chapter was to assess what stages of colorectal tumourigenesis are most sensitive to insulin stimulation. Tumour cell proliferation in response to insulin was assessed by a crystal violet based cellular proliferation assay. This was performed on cell lines representing different stages of colorectal tumour progression. In addition, cellular responsiveness to insulin was examined by performing western blotting to assess the extent of Akt phosphorylation. Later in this Chapter, the impact of insulin on cellular signalling was further analysed by assessing the expression of various insulin signalling pathway components. To assess whether Akt signalling was responsible for mediating the impact of insulin on cell proliferation, the cell line most sensitive to insulin stimulation was treated with an Akt inhibitor. Finally, a different *in vitro* model was used to replicate my findings.

3.2. The impact of insulin on the proliferation of adenocarcinoma cells

3.2.1. Optimisation of the proliferation assay for adenocarcinoma cell lines

I first examined the effect of insulin treatment on the proliferation of two colorectal adenocarcinoma cell lines – HT29 and SW480. These cell lines represent the later stages of tumourigenesis. Before I attempted to assess the effect of insulin on the proliferative response of these cells, I performed an optimization experiment to determine which serum concentration to use in the assay. The aim of this experiment was to determine the minimum serum concentration that permits cell proliferation, which would also enable me to observe an effect of insulin above the normal level of proliferation. Previous experience in the laboratory has shown that these cell lines struggle to survive in serum free conditions for longer than 48 hours. HT29 cells were grown in 96 well plates with media containing various serum concentrations. Subsequently, the proliferative response of cells in each condition was measured (Figure 9). The results of this experiment indicate that the optimum serum concentration, which allows HT29 cells to proliferate is 4%. The result of this experiment is presented in Figure 9.

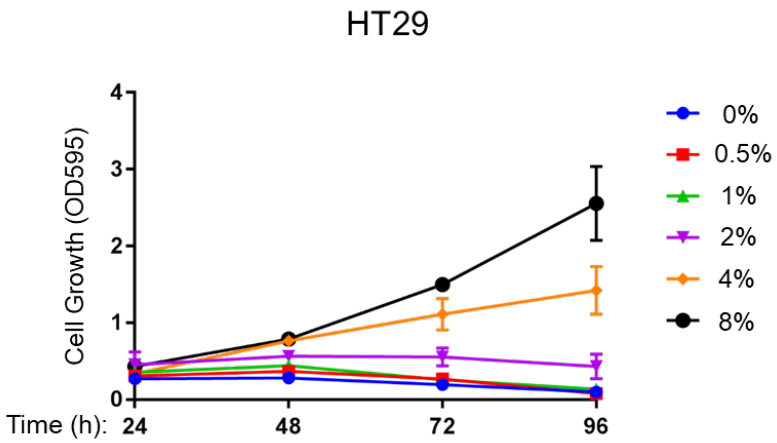

Figure 9. Proliferative response of HT29 when treated with media containing various concentrations of serum. Cells were seeded in 96 well plates (6000 cells per well) in growth media containing following concentrations of serum: 0%, 0.5%, 1%, 2%, 4%, 8%. Plates were fixed after 24, 48, 96 and 168 hours and stained using crystal violet. Error bars represent standard deviation from one experiment with 10 technical replicates (n=10).

3.2.2. The effect of insulin on the proliferation of HT29 and SW480 cell lines

After establishing the optimal conditions for the crystal violet assay for colorectal adenocarcinoma cell lines, the proliferative response of HT29 and SW480 was measured in response to insulin dosing. The results of this experiment show that insulin significantly increased proliferation of HT29 after 24 hours of treatment. All concentrations of insulin used in the experiment significantly increased proliferation of HT29 at this timepoint. Increase in the number of viable cells occurred in a dose dependent manner. At the later timepoints (48h, 72h and 96h) insulin did not have any positive effect on proliferation of HT29 cells. After 72h and 96h of insulin stimulation the number of treated cells decreased compared to control. In contrast to HT29, SW480 did not respond to insulin proliferatively after 24 hours. The only significant increase in proliferation of SW480 cells was observed when cells were treated with 50ng/ml insulin for 48 hours. After that timepoint, SW480 cells did not show increased or decreased proliferation in response to insulin treatment. Taken together these data suggest that proliferation of these adenocarcinoma cell lines is not sensitive to insulin.

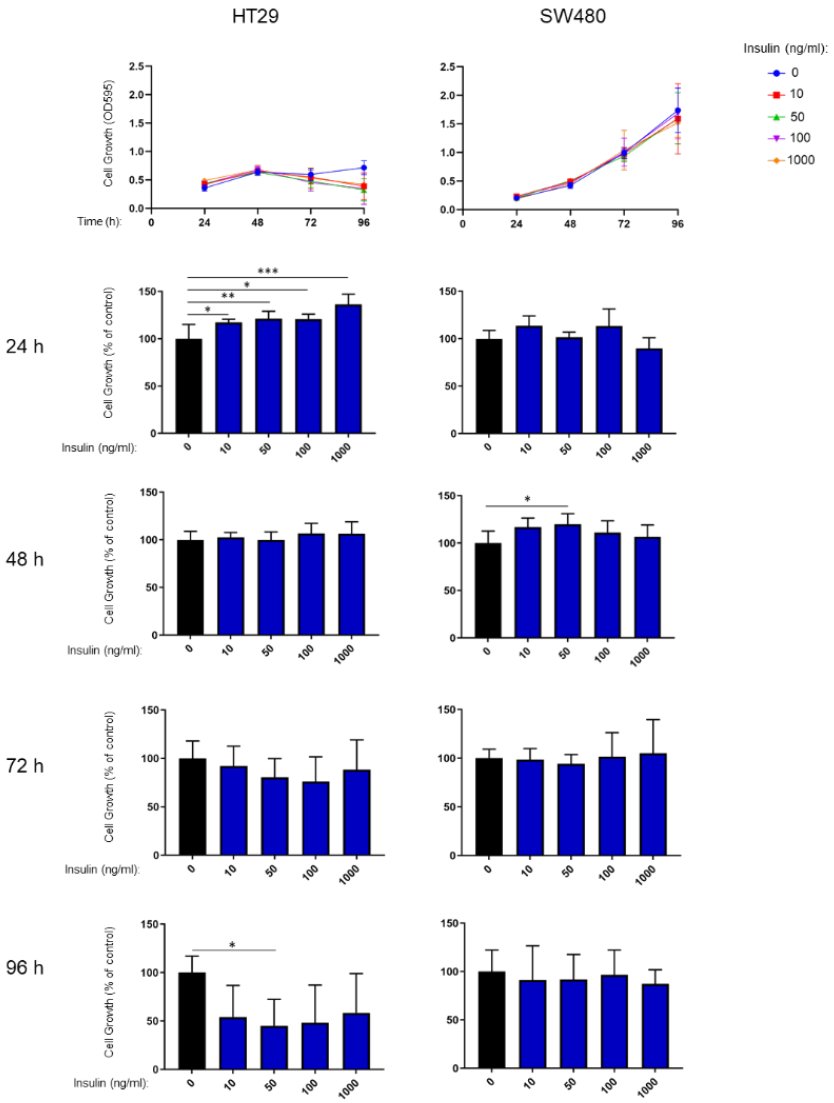

Figure 10. The effect of insulin adenocarcinoma cell proliferation. HT-29 and SW480 cells were seeded in 96 well plates in growth media. After 24 hours of incubation, media was changed to media with 4% FBS and cells were treated with various concentrations of insulin (0,10, 50, 100 and 1000 ng/ml). Plates were fixed after 0, 24, 48, and 96 hours and proliferation was analysed by crystal violet staining. The line graphs represent all the data from the experiment. The bar graphs indicate proliferation of cells at each time point: either 24, 48, 72 and 96 hours of insulin exposure. Error bars represent standard deviation from one experiment with 5 technical replicates (n=5). Data were analysed by one-way Anova and Dunnett's test of multiple comparisons. Statistically significant values are indicated (using a p value threshold of p = 0.05). Significance indicated in asterisk (*), where: * means $p \leq 0.05$, ** means $p \leq 0.01$, *** means $p \leq 0.001$.

3.2.3. The effect of insulin on cellular signalling in adenocarcinoma cells

Given that insulin did not increase proliferation of the adenocarcinoma cells, I next decided to examine whether insulin incubation stimulated cellular signalling in these cells. Western blotting analysis was performed to assess activation of Akt, as measured by phosphorylation at serine 473, upon insulin stimulation (Figure 11). The results of this experiment show that HT-29 cells respond to insulin exposure at lower timepoints (2h, 4h, 6h), however, this effect is not sustained at higher timepoints (24h, 48h). The level of phospho-Akt induction is greatest after 2 hours of treatment and decreases over time. In addition, the basal level of phospho-Akt rises after 48 hours in non-treated cells.

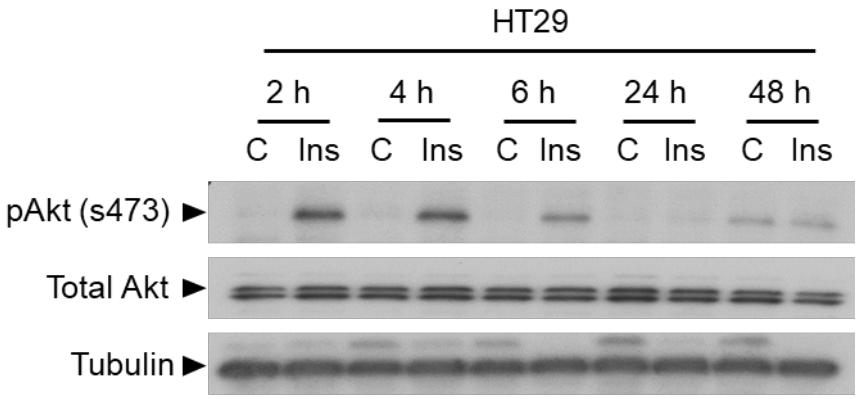

Figure 11. The effects of insulin treatment on Akt signalling in adenocarcinoma cells. HT-29 cells were treated with insulin (100ng/ml) for 2, 4, 6, 24 and 48 hours. Cell lysates were collected at each timepoint and immunoblotting analysis was performed for total and phospho-Akt (S473). Tubulin was used as a loading control.

3.3. The effect of insulin on the different stages of colorectal tumourigenesis

3.3.1. The effect of insulin on proliferation of the cell line series modelling adenoma to adenocarcinoma tumour progression.

As insulin treatment did not affect the proliferation of colorectal adenocarcinoma cells, representing late stage disease, I decided to test whether it influences the proliferative response of cells representing earlier stages of tumourigenesis. To do this I used a cell line series representing an *in vitro* model of tumour progression – an adenoma to carcinoma sequence of the same lineage. This model consists of four cell lines, which progress from early adenoma to carcinoma as follows: AA/C1 (anchorage dependent and nontumourigenic), AA/C1/SB, AA/C1/SB/10C and AA/C1/SB/10C/M (anchorage independent and tumourigenic).

The proliferation of each cell line was examined in both the presence and absence of insulin (Figure 12).

Data obtained from this experiment indicate that the cell line representing the earliest stage of adenoma progression – AA/C1, was the most sensitive to insulin treatment. All concentrations of insulin used in this assay, except of the lowest (1ng/ml), significantly increased proliferation of this cell line at the latest timepoint and did so in a dose dependent manner. The higher insulin concentrations – 50ng/ml, 100ng/ml and 1000ng/ml also significantly increased proliferation of AA/C1 cells after 72 hours. The proliferative effect of insulin on this cell line magnifies as time progresses. After 120 and 168 hours 10ng/ml insulin also significantly increased proliferation of AA/C1. Although there is no significant effect detected when these cells are stimulated with 1ng/ml of insulin, the p value obtained from one way Anova is equal to 0.7.

The proliferative response to insulin on the successive AA series cell lines decreases as the series progresses. There was no significant change observed in the proliferation of AA/C1/SB, AA/C1/SB/10C or AA/C1/SB/10C/M when treated with insulin.

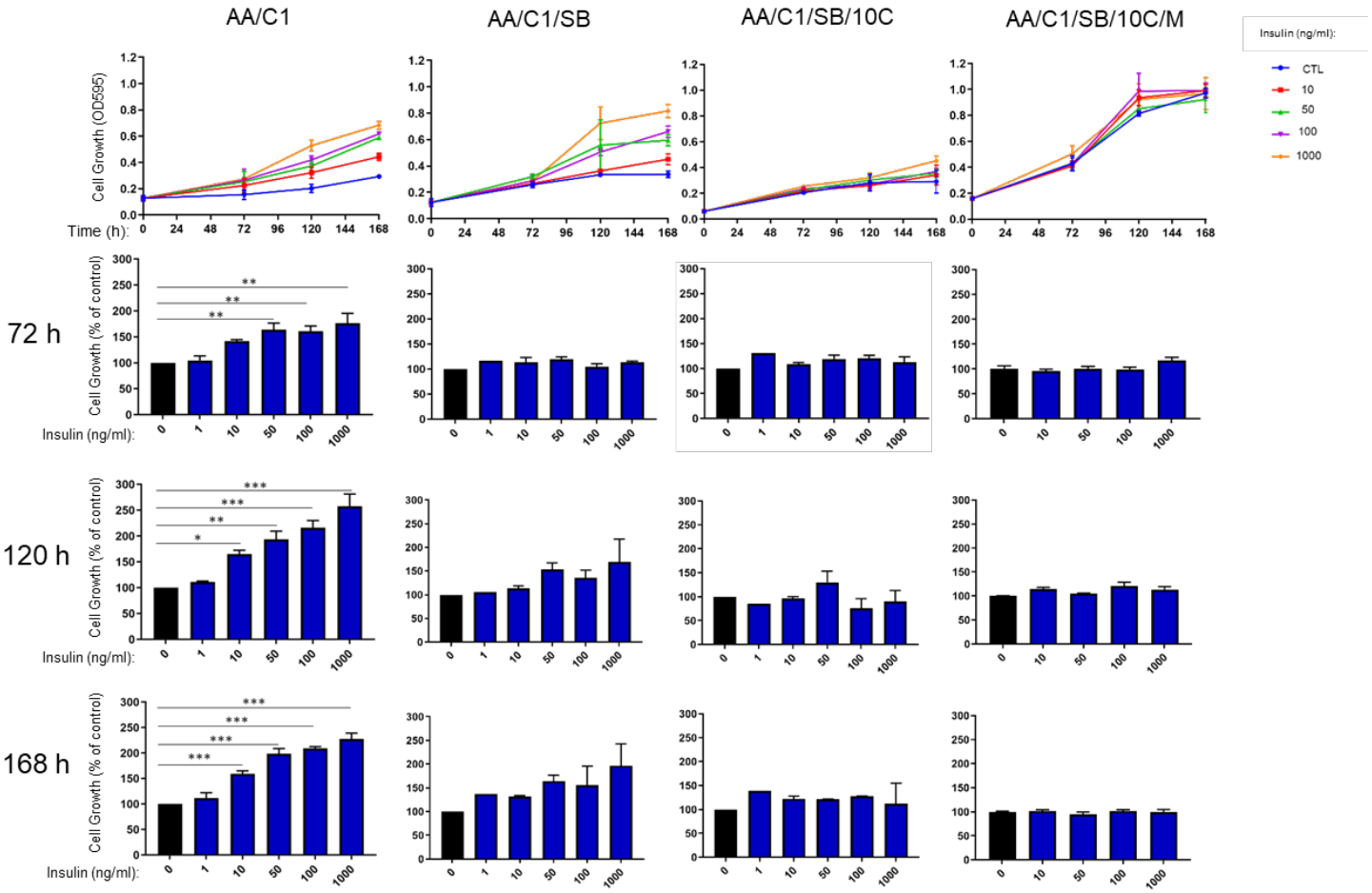

Figure 12. Proliferative response of an adenoma derived cell line series following incubation with insulin. Cells were seeded in 96 well plates in growth media. After 72 hours of incubation, media was changed to experiment media with various concentrations of insulin (0, 10, 50, 100 and 1000 ng/ml). Plates were fixed after 0, 72, 120 and 168 hours and proliferation was analysed by crystal violet staining. Line graphs on the top row are representative data from one experimental repeat (the graphs for the other experiments performed are in the appendix). The bar graphs in the rows below represent averaged data across experimental repeats for each individual time point; 72, 120 and 168 hours of insulin exposure respectively. Error bars represent SEM for three separate experiments for AA/C1, two experiments for AA/C1/SB and AA/C1/SB/10C and one experiment for AA/C1/SB/10C/M. All individual experiments have 5 technical replicates (n=5). Data were analysed by one-way Anova and Dunnett's test of multiple comparisons. Statistically significant values are indicated (using a p value threshold of p = 0.05). Significance indicated by asterisk (*), where: * means $p \leq 0.05$, ** means $p \leq 0.01$, *** means $p \leq 0.001$.

3.3.2. The effect of insulin on the proliferation of the adenoma to adenocarcinoma cell line series following long term insulin withdrawal.

Insulin is used in the routine cell culture of the AA series cells. This may affect the cellular sensitivity to insulin that we observe in the assay (Figure 12). It may also mean that rather than testing cellular response to insulin I was more likely testing cellular response to insulin withdrawal. Therefore, I decided to repeat the proliferation assays for the AA cell line series following long term insulin withdrawal (1 month for all cell lines with the exception of AA/C1 which was withdrawn from insulin for 5 days). Crystal violet proliferation assays were performed to assess whether there were any changes in proliferation of cells after they were re-stimulated with insulin following long term withdrawal. Data obtained from this experiment show that insulin treatment increases proliferation of AA/C1 and AA/C1/SB the most significantly. The change in AA/C1/SB/10C proliferation is only significant when cells are treated with the highest concentration of insulin. The results also show a decrease in proliferation of AA/C1/SB/10C/M when treated with insulin. Although AA/C1/SB and AA/C1/SB/10C cell lines became more sensitive to insulin treatment after long term insulin withdrawal, the overall pattern of insulin sensitivity of this cell line series remains similar. Insulin increases proliferation of cell lines representing the early stages of colorectal tumour progression, but does not stimulate proliferation in cellular models of the later stages of tumour progression (Figure 13).

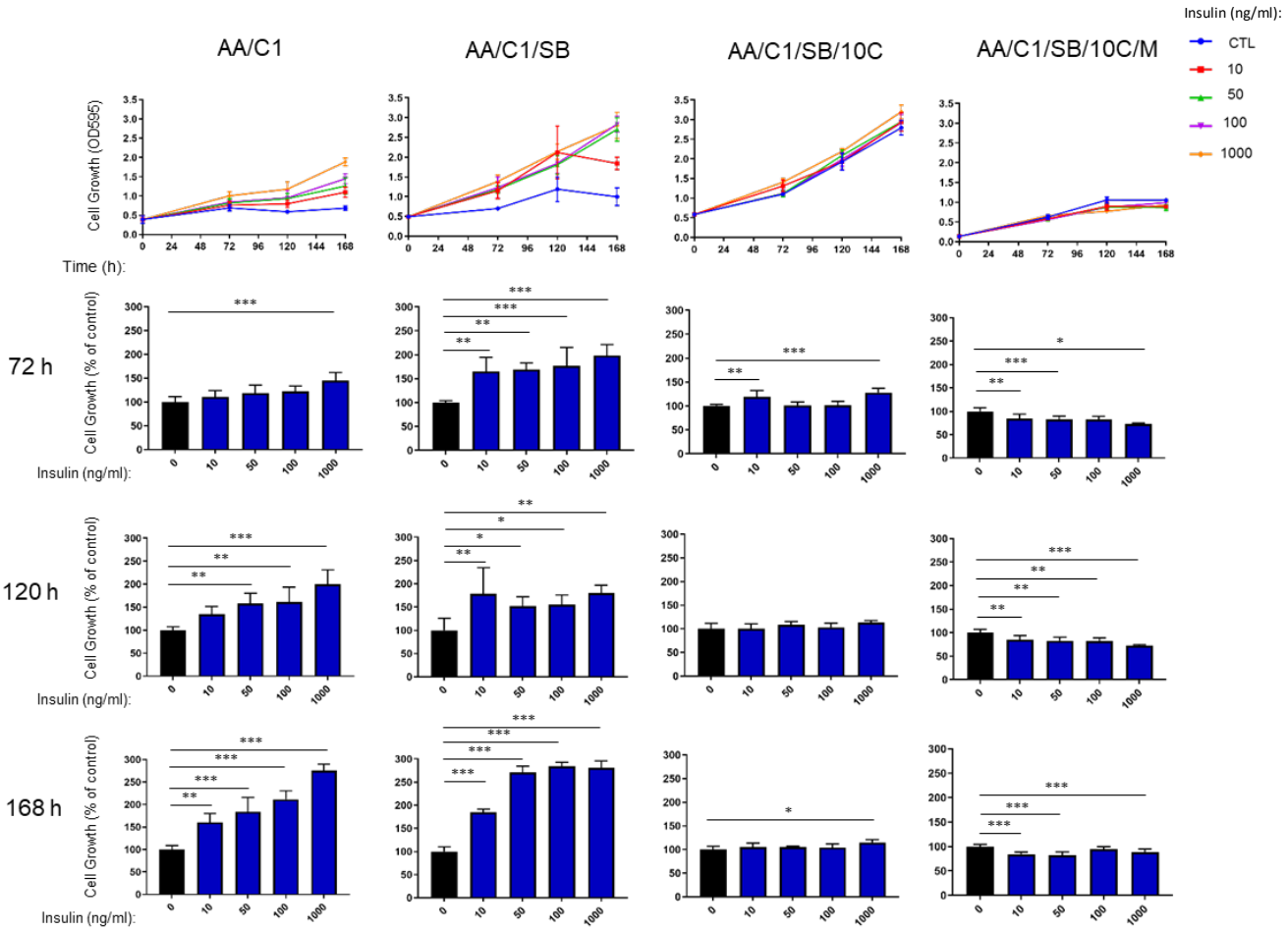

Figure 13. Proliferative response of the adenoma cell line series following insulin withdrawal and re-stimulation. Cells were grown in insulin free conditions for one month (AA/C1/SB, AA/C1/SB/10C, AA/C1/SB/10C/M) or 5 days (AA/C1). Next, cells were seeded in 96 well plates in growth media. After 72 hours of incubation, media was changed to experiment media with various concentrations of insulin (0,10, 50, 100 and 1000 ng/ml). Plates were fixed after 0, 72, 120 and 168 hours. The line graphs represent all the data from the experiment. The bar graphs indicate proliferation of cells at each time point: either 72, 120 and 168 hours of insulin exposure. Error bars represent SD from one experiment with 5 technical replicates (n=5). Data were analysed by one-way Anova and Dunnett's test of multiple comparisons. Statistically significant values are indicated (using a p value threshold of p = 0.05). Significance indicated in asterisk (*), where: * means $p \leq 0.05$, ** means $p \leq 0.01$, *** means $p \leq 0.001$.

3.3.3. The effect of insulin on cellular signalling in adenoma cells.

Next, to determine the effect of insulin on cellular signalling, induction of Akt activity was determined for each cell line. The results of western blotting analysis indicate that the cell line representing the earliest stage of tumour progression was the most responsive to insulin stimulation. There is a visible increase in phosphorylation of Akt at S473 after 2 h of insulin stimulation in AA/C1. Moreover, this level of phospho-Akt expression is sustained after 24 hours of treatment in this cell line. Although insulin appears to trigger the greatest induction of phospho-Akt expression in AA/C1, it also exerts an effect on the other cell lines. There is a visible increase in phospho-Akt induction in AA/C1/SB and AA/C1/SB/10C/M after 10 minutes, 2 hours and 24 hours of treatment. The induction of phospho-Akt in AA/C1/SB/10C is the least affected by insulin stimulation. The level of phospho-Akt slightly increases in this cell line after 10 minutes and 2 hours of treatment, however, it falls after 24 hours. It is worth mentioning that the basal level of phospho-Akt expression is noticeably higher in all three cell lines, when compared to AA/C1. Overall, the results of western blotting analysis indicate that all of the examined cell lines are responsive to insulin, however, AA/C1 appears to be the most sensitive (Figure 14).

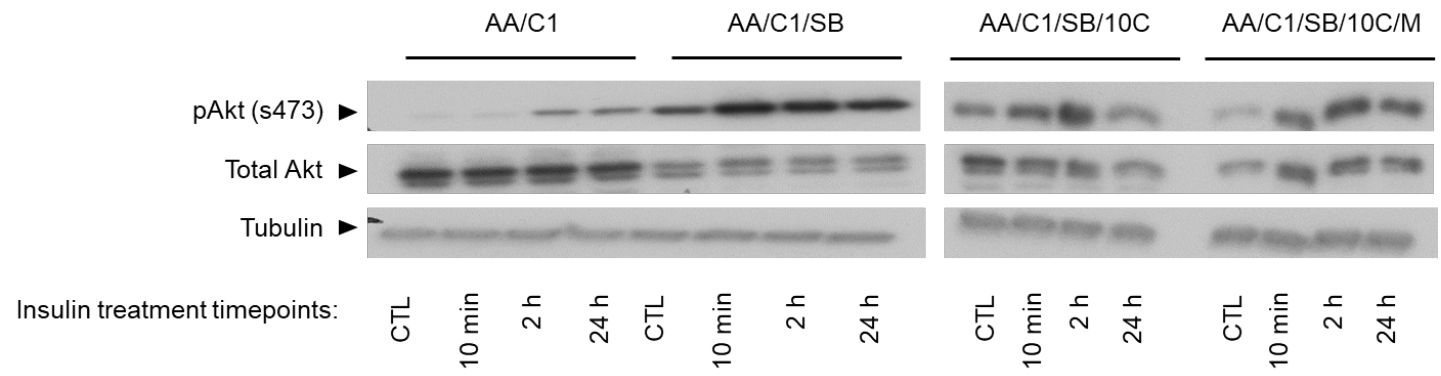

Figure 14. The effects of insulin treatment on Akt signalling in colorectal adenoma cell lines. Cells were treated with insulin (100ng/ml) for 10 minutes, 2 hours and 24 hours. Cell lysates were collected at each timepoint and immunoblotting analysis for total and phospho-Akt (s473) was performed. Tubulin was used as a loading control. A replicate of this experiment can be found in the appendix.

Subsequently, I decided to further explore the ways cellular signalling induced by insulin differed between the four cell lines. I performed western blotting analysis to detect any changes in expression levels of phospho-Akt, insulin growth factor receptor β, insulin receptor and the Akt substrate phospho-PRAS40 (131). This analysis was performed to compare expression levels of the above proteins in cells treated with and without insulin (100ng/ml) for 72 hours.

Consistent with Figure 15 the results of this experiment showed that after 72 hours of treatment, insulin has the greatest effect on phospho-Akt induction in the AA/C1 cell line. In addition, insulin stimulation increased induction of phospho-Akt in AA/C1/SB and AA/C1/SB/10C cell lines. Interestingly, there is no phospho-Akt induction upon insulin treatment in the AA/C1/SB/10C/M cell line. This is consistent with the failure of this cell line to respond to insulin in the proliferation assay. We can observe a similar pattern of expression in the Akt target protein – phospho-PRAS40 (131). Insulin increases induction of phospho-PRAS40 in AA/C1/SB and AA/C1/SB/10C cell lines, but it does not trigger any phospho-PRAS40 induction in AA/C1/SB/10C/M cell line. However, insulin induces only a very small increase in expression of phospho-PRAS40 in the AA/C1 cell line, this is inconsistent with the phospho-Akt result. Furthermore, AA/C1 is the only cell line which shows decreased expression levels of the insulin receptor and IGFRβ upon insulin stimulation.

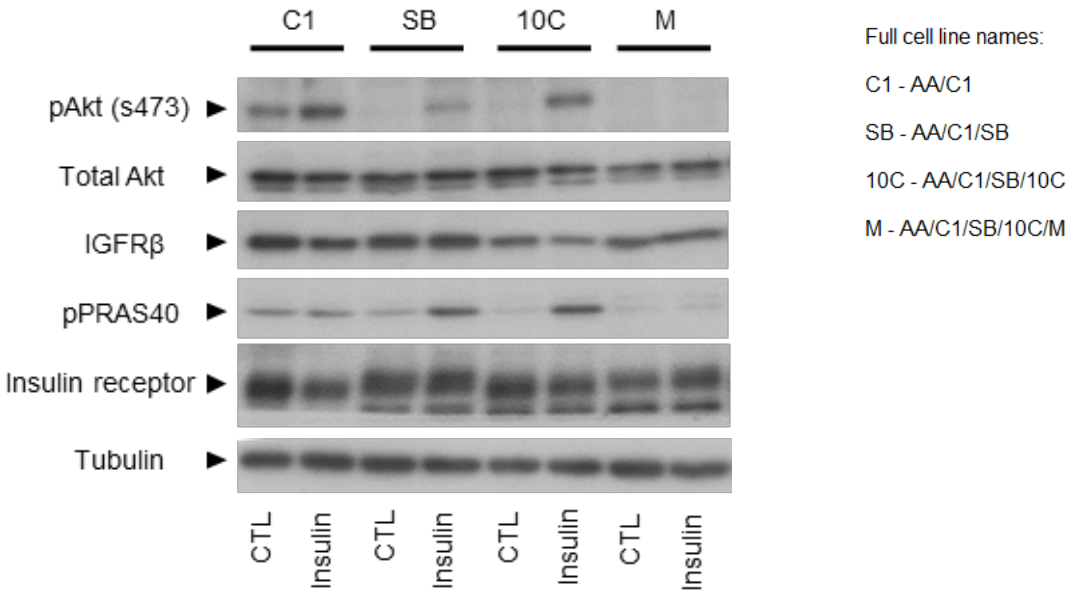

Figure 15. The effects of insulin treatment on insulin signalling in colorectal adenoma cell lines. Cell were treated with insulin (100ng/ml) for 72 hours. Cell lysates were collected and immunoblotting analysis for total and phospho-Akt (s473), IGFRβ, phospho-PRAS40 and the insulin receptor was performed. Tubulin was used as a loading control.

After observing that insulin was able to sustain activation of the Akt signalling pathway for 72 hours in cell lines representing early, but not late stages of colorectal tumourigenesis I decided to examine the proliferative response of the AA/C1 cell line when treated with insulin and incubated with an Akt inhibitor. That was done in order to test whether the proliferative response to insulin was dependent on Akt activation. In this experiment I performed the crystal violet proliferation assay to compare the proliferation of cells when treated with different concentrations of an Akt inhibitor with or without insulin. I performed two experiments, first with a lower range of Akt inhibitor concentrations (Experiment 1: 0-10μM) then with a higher range (Experiment 2: 0-20μM). The results of both experiments (Figure 16) show that the proliferative effect of insulin on the AA/C1 cell line is inhibited to a large extend when cells are treated with 10, 15 and 20μM of Akt inhibitor. However, the Akt inhibitor also inhibits proliferation of cells when they are untreated with insulin. Despite this, the fold decrease in proliferation when comparing Akt inhibitor treated cells to control is greater for insulin treated cells than for the non-insulin treated cells. For example, in Experiment 1 at 168h the average fold decrease in proliferation with 20μM of Akt inhibitor in 2.54 fold in non-insulin treated cells vs 3.75 fold in insulin treated cells. There was no difference in cell proliferation when cells where treated with 15μM or 20μM of Akt inhibitor, suggesting 15μM of the Akt inhibitor is the maximal dose.

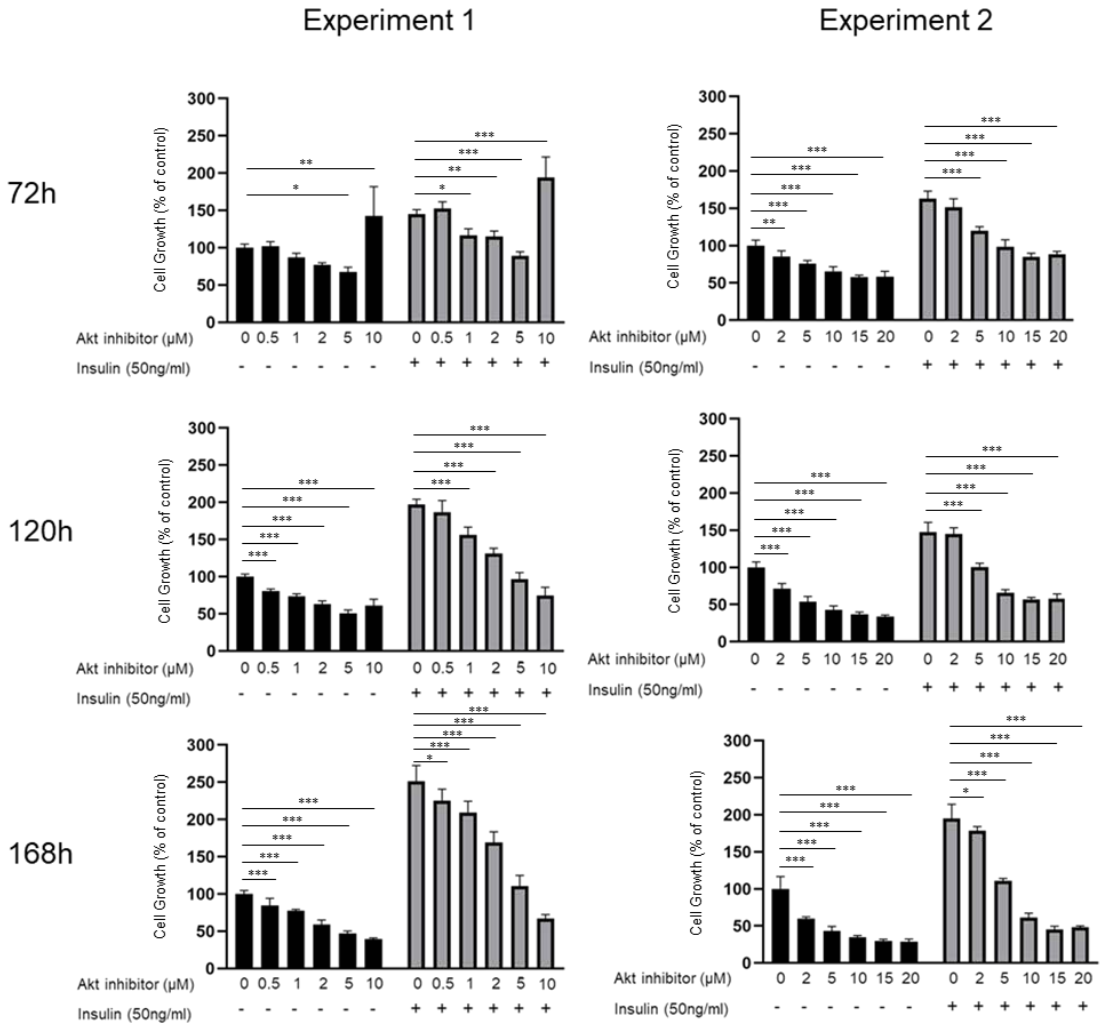

Figure 16. Proliferative response of AA/C1 to insulin following treatment with an Akt inhibitor. Cells were seeded in 96 well plates in growth media. After 72 hours of incubation, media was changed to experiment media and cells were treated with various concentrations of Akt inhibitor. Concentrations used in Experiment 1 were to 0, 0.5, 1, 2, 5 and 10μM, whereas concentrations used in Experiment 2 were to 0, 2, 5, 10, 15 and 20μM. Each condition was repeated with the addition of 50ng/ml of insulin. Plates were fixed after 0, 72, 120 and 168 hours. Crystal violet staining was performed to measure proliferation. Data were normalized to control without insulin or Akt inhibitor. Multiple t-tests were performed between control and cells treated with Akt inhibitor and between control and cell treated with Akt inhibitor plus insulin. Statistically significant values are indicated (using a p value threshold of $p = 0.05$). Significance indicated in asterisk (*), where: * means $p \leq 0.05$, ** means $p \leq 0.01$, *** means $p \leq 0.001$.

Next, I performed western blotting analysis to assess the level of phospho-Akt induction in AA/C1 cells treated with 50ng/ml of insulin and various concentrations of Akt inhibitor. The Akt inhibitor doses used in this experiment were in the same range as used for the proliferation assay (Figure 17). The results of this analysis show that cells stimulated with insulin express phospho-Akt and this is ablated by the addition of any concentration of Akt inhibitor used.

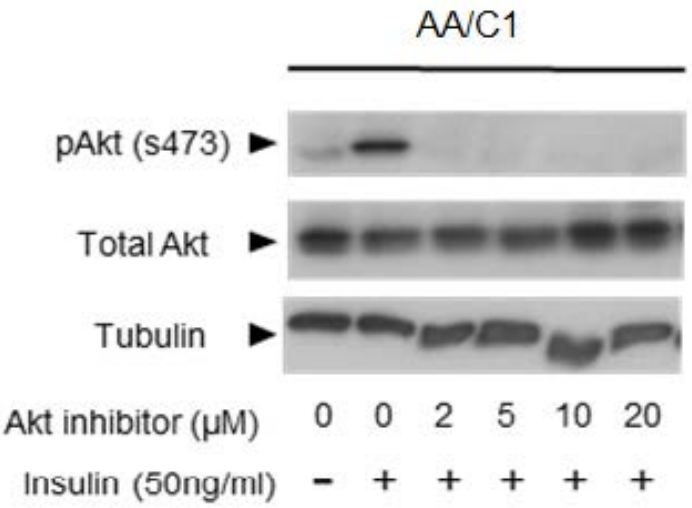

Figure 17. The effects of insulin treatment on levels Akt signalling in the AA/C1 cell line. Cell were treated with various concentrations of Akt inhibitor (0, 2, 5, 10, 20 μM), with or without 50ng/ml of insulin for 72 hours. Cell lysates were collected and immunoblotting analysis for total and phospho-Akt (s473) was performed. Tubulin was used as a loading control.

In my next experiment I examined the effect of insulin on proliferation of another cell line representing early stage of colorectal tumour progression – S/RG (Figure 17). I did this with the aim to replicate my findings in the AA/C1 cell line. I carried out the crystal violet proliferation assay using the same conditions as for the AA/C1 cell line, to determine whether insulin promotes proliferation of early adenoma cells in different models. The results of this experiment show that insulin increases proliferation of the S/RG cell line. Insulin dosed at 50 ng/ml, 100 ng/ml and 1000 ng/ml significantly increases proliferation of S/RG cell line after 72h of treatment. After 120h, the highest concentration of insulin still significantly increases proliferation of this cell line. After 168h, insulin dosed at each concentration, except of 1ng/ml, significantly increases proliferation of S/RG cell line. The effects of insulin are similar to those observed in AA/C1 cell line. However, the S/RG cells seem to be more sensitive to higher

concentrations of insulin. There is a large increase in proliferation of this cell line upon stimulation with 1000ng/ml compared to 100ng/ml. This effect was not observed in AA/C1 cell line.

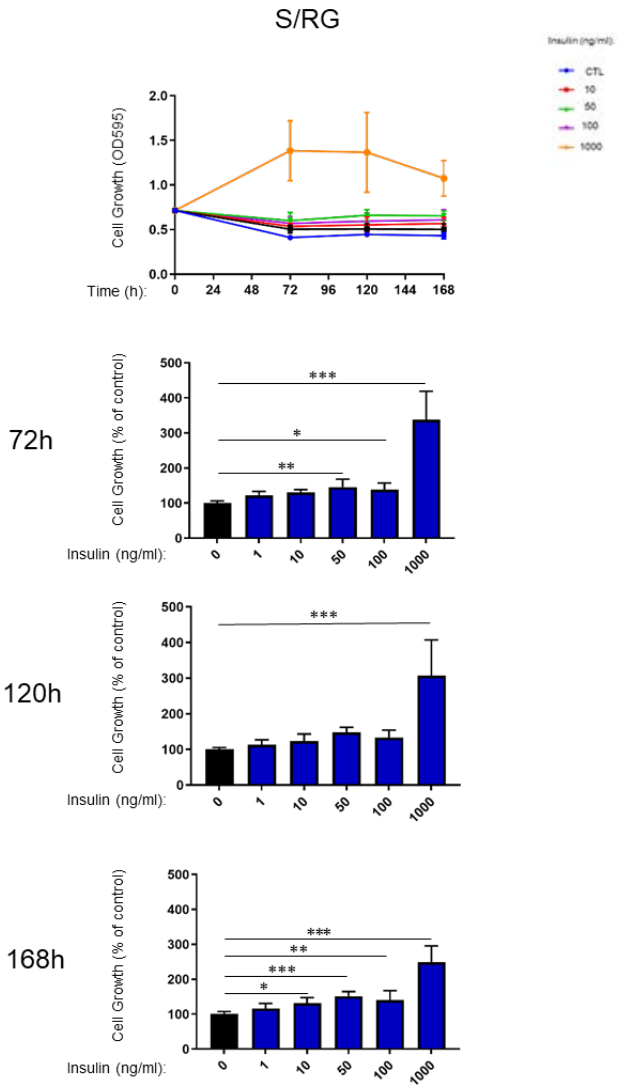

Figure 18. Proliferative response of the S/RG cell line following incubation with insulin. Cells were seeded (seeding density 20 000 cells/well) in 96 well plates in growth media. After 72 hours of incubation, media was changed to experiment media and cells were treated with various concentrations of insulin (0,10, 50, 100 and 1000 ng/ml). Plates were fixed after 0, 72, 120 and 168 hours and proliferation was analysed by crystal violet staining. The line graph displays all the data from this experiment. The bar graphs indicate proliferation of cells at the individual time points: 72, 120 and 168 hours of insulin exposure. Error bars represent SEM from one experiment with 5 technical replicates (n=5). Data were analysed by one-way Anova and Dunnett's test of multiple comparisons. Statistically significant values are indicated (using

a p value threshold of p = 0.05). Significance indicated in asterisk (*), where: * means p ≤ 0.05, ** means p ≤ 0.01, *** means p ≤ 0.001.

3.4. Discussion

In this part of my investigation, I examined the impact of insulin exposure on colorectal adenoma and carcinoma cell proliferation. Proliferation assays were performed to assess which stage of colorectal tumour progression was the most sensitive to insulin. Data obtained from these experiments indicate that insulin increases proliferation of early adenoma cells – AA/C1 the most significantly. The proliferative effect of insulin was absent in subsequent adenoma stages AA/C1/SB, AA/C1/SB/10C and AA/C1/SB/10C/M. In order to confirm my finding that early adenoma cells are the most sensitive to insulin treatment, the proliferation assay was repeated using a different adenoma cell line - S/RG. This cell line also represents the early adenoma stage of colorectal tumourigenesis.

After long term insulin withdrawal, all cell lines became more sensitive to insulin treatment. There was a significant increase in proliferation of AA/C1/SB and also AA/C1/SB/10C. However, sensitivity of the cell line series to insulin was still most apparent in the models of the early stages of colorectal tumorigenesis. In addition, there was no increase in proliferation of adenocarcinoma cell lines – HT29 and SW480 upon insulin stimulation. Hence, I determined that the early stages of colorectal tumour progression are the most sensitive to the effects of insulin.

The lack of a proliferative effect of insulin on cell line models representing the later stages of colorectal tumourigenesis may be connected to an increase in the number of oncogenic mutations carried by these cells. Progressive accumulation of mutations observed in cancer cells may make them less reliant on exogenous growth factors such as insulin. The results of western blotting analysis for phospho-Akt showed that the greatest level of phospho-Akt induction is apparent in the cell line model of an early adenoma (AA/C1) upon insulin treatment in comparison to models representing the later stages of colorectal tumourigenesis. Moreover, phospho-Akt induction was sustained in AA/C1 after 72 hours. In contrast, there was no phospho-Akt induction visible in cell line models representing the later stages of colorectal tumourigenesis after 72 hours. These results may be explained by the presence of additional mutations downstream of Akt in cell lines representing the later stages of colorectal tumourigenesis. Another explanation of this phenomena could be that late stage colorectal tumour cells decrease their dependency on the Akt pathway for tumorigenicity. It has been found by Vasudevan *et.al* that some cancer cells with a mutation in *PIK3CA* and low pAkt induction become dependent on SGK3 for viability (132). The kinase domain of SGK3 shares

a high level of homology with the Akt kinase domain, therefore it can be activated in *PIK3CA* mutant cancer cells via PDK1 dependent phosphorylation. They showed that mutations in PI3K may affect PDK1 positioning on the cell membrane and hence the affinity for Akt/SGK3 proteins (132).

Differences in phospho-Akt activation between cell lines may also be a result of increased expression of AMPK in later stages of colorectal tumour. It has been shown in other cancers that as cells become more metastatic the levels of AMPK expression increases (133). Saha *et. al* has found that in breast cancer cells AMPK is able to upregulate protein phosphatase 2A (PP2A), which dephosphorylates and inactivates Akt. In this way AMPK drives cellular adaptation to matrix detachment (133).

The results from my western blotting and proliferation assay experiments suggest a critical role for Akt signalling in the proliferative response to insulin in the early adenoma cell line, AA/C1. Using an Akt inhibitor in the proliferation assay demonstrated that phospho-Akt induction in AA/C1 in response to insulin is a potential reason for the increased proliferation observed in this cell line.

Western blotting analysis in the adenocarcinoma cell line – HT29 indicated an increase in phospho-Akt induction at lower timepoints – 10 minutes and 2 hours, however, this was not sustained after 24 and 48 hours of treatment. Taking into consideration that the cell cycle takes around 24 hours to complete, this may explain why there was no effect on proliferation in these cells after insulin treatment. In addition, lack of phospho-Akt induction at later timepoints in the HT29 cell line may suggest that later stages of colorectal tumourigenesis do not rely on growth factors to activate Akt signalling pathway target proteins.

According to my results, insulin treatment did not exert any effect on proliferation of colorectal adenocarcinoma cells. This contradicts the evidence in the literature, in which several studies state that insulin increases the proliferation of colorectal carcinoma cell (129,134,135). For example, Ayiomamitis *et al.* shows that insulin treatment induces proliferation of CaCo2 and HT29 cell lines (135). However, these studies use assays that measure reducing equivalent such as MTT and CCK8 as a way to measure cellular proliferation (135). Reducing equivalent assays measure the metabolic activity of cells and make the assumption that this correlates to the number of viable cells (136). In MTT assays, tetrazolium salt is reduced by mitochondrial and extra-mitochondrial dehydrogenases, this results in the formation of insoluble blue formazan crystals, which when solubilised indicate the number of viable cells (136). In contrast to the MTT assay, in the CCK8 assay a highly water soluble tetrazolium salt - WST-8, is reduced by dehydrogenases present in the plasma membrane and is combined with the electron acceptor PMS, which causes a change in media colour to yellow (136). These

methods of measuring proliferation may not be reliable in this type of investigation. Insulin is known to affect the metabolic activity of cells. Thus, insulin stimulation may induce changes in the levels of certain metabolites, without affecting proliferation rate (or not affecting it relative to cell number). In this investigation, the crystal violet cell viability assay was used to measure cellular proliferation. This method relies on the detection of biomass of viable cells, not their metabolic activity (137). Hence it is a more reliable way to assess cellular proliferation of insulin treated cells. In addition, many studies use supra-physiological concentrations of insulin, going up to about 2500ng/ml and not below 30ng/ml (101,129,135). Taking into consideration that maximum physiological concentration of insulin is about 10ng/ml, these conditions are very different from those found in humans. In this investigation I used insulin doses ranging from 1ng/ml to 1000ng/ml, which encompass the physiological range.

The adenoma to carcinoma cell line series used in these experiments has been derived from a patient diagnosed with familiar adenomatous poliposis (FAP) (125). Therefore, it may not be entirely representative of sporadic cancers, which constitute 90% of all colorectal cancer incidence (138). However, FAP patients have an APC mutation, which is present in the majority of sporadic colorectal cancers (139). Differences in genetic mutations present in various cell lines may affect tumour phenotype and responsiveness to growth factors. For example, it has been demonstrated that different types of APC mutations in colorectal tumours can influence tumour phenotype and prognosis (138). Therefore, it was important to carry out my analysis in different *in vitro* models.

I used the S/RG adenoma cell line to replicate my findings in the AA/C1 cell line. This cell line is derived from a patient with sporadic cancer and in contrast to AA/C1 it expresses the full length APC (140). The results of proliferation assays performed with the S/RG cell line show similarity to those in the AA/C1 cell line. There was a significant increase in proliferation of S/RG cell line when stimulated with all concentrations of insulin used except 1ng/ml. These results suggest that it is the early stages of colorectal tumourigenesis which are the most sensitive to insulin. However, due to time restrictions this experiment was performed only once. Therefore, more research is needed to confirm these findings.

3.5. Summary

The results presented in this chapter show that cell lines representing the early adenoma stage of colorectal tumour progression are the most sensitive to insulin stimulation. However, this observation may not be true for all colorectal cell lines. As mentioned earlier in this chapter, each cell line has specific mutations and some of them may impact on the effect of insulin. Therefore, in the future, proliferation assays with other cell lines should be performed in order

to confirm these findings. The results of this investigation show that insulin does not increase the proliferation of late stage colorectal tumour cell lines. However, it may promote other properties of cancer cells. In the future, it will be worth exploring the effect of insulin on other phenotypes such as migration, invasion and angiogenesis.

The results of proliferation assays show that it is not possible to entirely inhibit insulin stimulated growth with an Akt inhibitor in early stage cells. This suggests that insulin may promote proliferation of these cells through other pathways as well. In the next chapter, I will describe how insulin may increase proliferation of colorectal tumour cells through metabolic reprogramming.

Chapter 4. The effect of insulin on metabolic reprogramming in colorectal tumour cells

4.1. Introduction

Results described in the previous chapter show that insulin increases proliferation of early adenoma, but not adenocarcinoma cells. Although my results suggest that Akt signalling plays a role, the specific molecular mechanisms, by which insulin promotes proliferation of early adenoma cells remains unclear. In addition, the reasons behind insulin not affecting proliferation of adenocarcinoma cells are also unexplained. In order to proliferate tumour cells must reprogramme their intracellular metabolism to meet the demands of chronic proliferation. Therefore, I hypothesised that insulin might impact cell proliferation in the adenoma cells by promoting changes to cellular metabolism. I hypothesised that insulin may promote changes in the adenoma cells and not in the adenocarcinoma cells. Therefore, the aim of this chapter was to examine the effect of insulin on metabolic reprogramming in colorectal early adenoma and adenocarcinoma cells. In order to address this aim I have used stable isotope tracer analysis (SITA) and investigated my findings further using western blotting analysis and qPCR. The abundance of metabolites and metabolic flux was compared in insulin treated and non-treated early adenoma and adenocarcinoma cells using SITA. Western blotting analysis was performed to examine whether insulin treatment affects the expression of various metabolic proteins and enzymes in early adenoma and adenocarcinoma cells. Data obtained from this experiment helped me determine some aspects of metabolism affected by insulin, such as aerobic glycolysis. Metabolic enzymes participating in glycolysis were further analysed by qPCR.

4.1.1 Stable Isotopomer Tracer Analysis (SITA)

Stable isotopomer tracer analysis (SITA) involves incubating cells with a stably labelled isotopomer (commonly glucose or glutamine) and quantifying the incorporation of the labelled carbon into cellular metabolites using mass spectrometry. Here, I am using uniformly labelled glucose (U-[^{13}C]-glucose) and glutamine (U-[^{13}C]-glutamine). The heavy labelled carbon can be distinguished from the unlabelled, naturally abundant carbon, due to the extra neutron on the ^{13}C. Therefore, uniformly labelled glucose (U-[^{13}C]-glucose), with 6 ^{13}C carbons is 6 mass units heavier than ^{12}C glucose. This is referred to as m+6 glucose and the unlabelled, naturally abundant glucose as m+0 glucose.

Glucose is metabolized down the glycolytic pathway into pyruvate, lactate and alanine. From uniformly labelled glucose (U-[^{13}C]-glucose) fully labelled or m+3 pyruvate, lactate and alanine are produced (Figure 19). Glucose can also be converted from 3PG to generate the amino

acids serine and glycine. From uniformly labelled glucose m+3 serine and m+2 glycine would be produced. Pyruvate is oxidized and decarboxylated to generate m+2 acetyl-CoA and this enters the TCA cycle. Acetyl-CoA m+2 condenses with oxaloacetate to generate citrate, if the OAA is unlabelled as would be expected in the first turn of the TCA cycle it will produce m+2 citrate. Citrate is decarboxylated to form m+2 α-ketoglutarate and the 2 labelled carbons continue around the TCA cycle until again OAA condenses with another m+2 acetyl-CoA to form m+4 citrate in the second turn of the TCA cycle. The cycle continues and the labelling patterns generated are demonstrated in Figure 20.

The key advantage of SITA is that it allows you to assess both the relative abundance of metabolites and metabolic pathway activity by looking at how carbon is incorporated into different pathways. This is done by assessing the heavy labelled carbon labelling patterns of metabolites using mass isotopomer distribution (MID) analysis. This determines how many carbons are labelled from the tracer (in this case either glucose or glutamine). This analysis breaks the whole metabolite pool (equal to 1) down to asses which mass isotopalogues the pool is composed of. For example, for lactate, which has 3 carbons, the pool is composed of either unlabelled lactate (denoted m+0), lactate labelled at one carbon (m+1), lactate labelled at two carbons (m+2) or lactate labelled at three carbons (m+3). As mentioned above, because of how U-[^{13}C]-glucose is metabolised by glycolysis into lactate, the majority of the lactate produced will be the m+3 mass isotopalogues (there will be very little m+1 and m+2 contributing to the MID for lactate). Shifts in the proportions of mass isotopalogues can indicate altered metabolic pathway flux and tell us about what metabolic pathways are engaged or prioritised in different conditions.

Uniformly labelled glutamine (U-[13C]-glutamine) has 5 ^{13}C carbons and is therefore 5 mass units heavier than ^{12}C glutamine. U-[13C]-glutamine is metabolised to m+5 glutamate and it enters the TCA cycle as m+5 α-KG, this process is called glutamine anaplerosis. Once in the TCA cycle, α-KG is metabolised in an either oxidative (clockwise to succinate) or reductive (anticlockwise to citrate) manner. The m+5 mass isotopalogue of citrate is indicative of reductive metabolism (conversion of α-KG to citrate). The m+4 mass isotopalogues of succinate, fumarate, malate and citrate is indicative of oxidative metabolism.

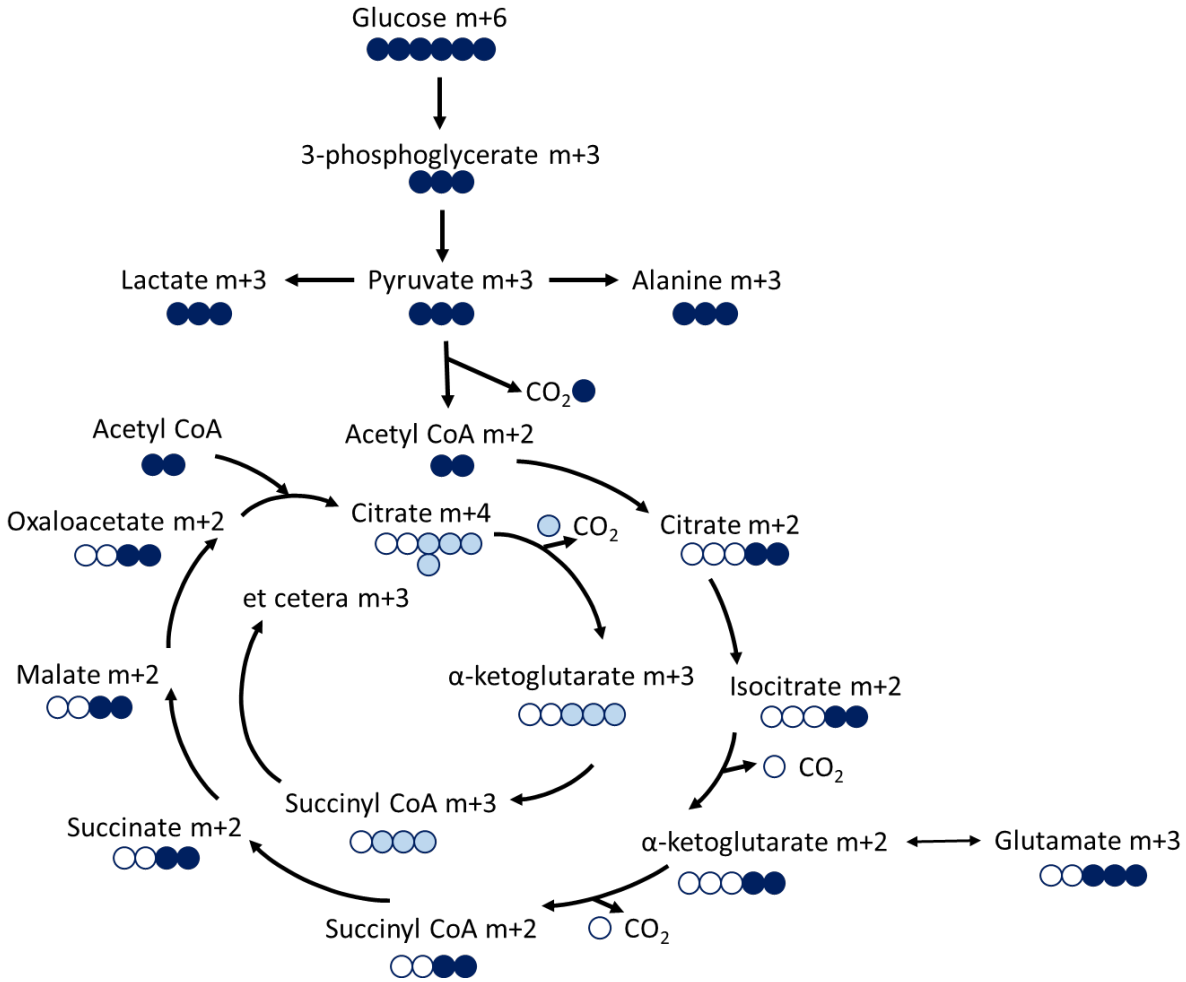

Figure 19. Labelling patterns for glycolysis and TCA cycle metabolites resulting from incubation of cells with uniformly labelled glucose (U-[13C]-glucose). U-[13C]-glucose (m+6) is taken up by cells and is metabolised to m+3 pyruvate, lactate and alanine. Pyruvate is decarboxylated and enters the TCA cycle as m+2 acetyl-CoA. This condenses with m+0 oxaloacetate to give m+2 citrate. The TCA cycle progresses, maintaining the m+2 label until oxaloacetate again condenses with acety-CoA, giving m+4 citrate. This time a labelled CO_2 is lost resulting in m+3 α-KG and the cycle continues. Figure adapted from: (141).

4.2. The impact of insulin on metabolic flux in colorectal adenoma and adenocarcinoma cells.

In order to examine the metabolic changes in colorectal tumour cells stimulated with insulin I performed SITA. In SITA ^{13}C labelled nutrients (glucose or glutamine) are supplied to cells, upon extraction of the metabolites it is possible to measure the abundance and labelling patterns of metabolites (indicative of metabolic pathway usage) using GCMS. These data allow me to determine how the cell use key carbon sources and whether this changes when they are incubated with insulin.

In this investigation SITA was performed using AA/C1 and AA/C1/SB/10C/M cell lines. I decided to compare the model of early adenoma most impacted by insulin incubation (AA/C1) to the most progressed cell line in the series least impacted by insulin (AA/C1/SB/10C/M). I have used SITA to compare the incorporation of carbon from glucose and glutamine into the metabolites of two key cellular metabolic pathways: glycolysis and TCA cycle, in insulin treated and non-treated cells. In addition, the abundance of amino acids was also determined in the presence and absence of insulin treatment.

4.2.1. SITA using uniformly labelled glucose (U-[^{13}C]-glucose)

In the first experiment, uniformly labelled ^{13}C glucose (U-[^{13}C]-glucose) was used as the tracer molecule. The tracer was supplied to cells 2 hours before to extraction. Cells were treated with insulin for the 72 hours before to extraction.

I have grouped the metabolites according to the pathways they are in; glycolysis (Figure 20A), TCA cycle (Figure 20B) and amino acids (Figure 20C). Figure 20 shows the relative abundance of the metabolites in these pathways and indicates (by the black bars) how much labelled carbon from glucose has been incorporated into each metabolite. The results of U-[^{13}C]-glucose SITA showed a significant increase in the abundance of labelled lactate and alanine in the insulin stimulated AA/C1 cell line ($p \leq 0.01$ for alanine, $p \leq 0.05$ for lactate) (Figure 20A). In contrast, there was no change in the amount of labelled lactate and alanine in the AA/C1/SB/10C/M cell line in response to insulin. This suggests insulin might increase glycolytic activity in the AA/C1 cell line but not in the AA/C1/SB/10C/M. In addition, there was also an increase in the amount of unlabelled glycine ($p \leq 0.01$) and serine ($p \leq 0.05$) in the insulin treated AA/C1 cell line compared to control. There is little evidence of incorporation of labelled glucose into either serine or glycine, suggesting that AA/C1 and AA/C1/SB/10C/M do not use glucose to synthesise these amino acids and likely transport then into the cell from the culture media.

Next I assessed the abundance of glucose carbon incorporated into the TCA cycle (Figure 20B). The metabolic changes in response to insulin in the TCA cycle are less consistent. Insulin appears to increase carbon incorporation into some TCA cycle metabolites (malate, fumarate and α-ketoglutarate) upon insulin stimulation in both the AA/C1 and AA/C1/SB/10C/M cell lines.

Next I assessed the relative abundance of amino acids in the cells. Amino acids are essential biosynthetic building blocks for proliferating cells. In several of the amino acids, insulin increased their intracellular abundance in the AA/C1 cells but not in the AA/C1/SB/10C/M cells. This was most obvious in the essential amino acids (isoleucine, leucine, valine, methionine and phenylalanine). This suggests insulin might increase amino acid uptake in the AA/C1 cells

but not in the AA/C1/SB/10C/M cells. This might help support the increase in cellular proliferation in the AA/C1 cells. In addition, the amount of unlabelled amino acids was much higher in AA/C1 cell line than in AA/C1/SB/10C/M cell line regardless of the presence or absence of insulin.

I next further analysed cellular metabolism by considering the labelling patterns of the metabolites or the mass isotopomer distribution (MID). This determines how many carbons are labelled from the tracer (in this case glucose). This analysis breaks the whole metabolite pool (equal to 1) down to asses which mass isotopalogues the pool is composed of. As mentioned above, the majority of the lactate and alanine produced will be the m+3 mass isotopalogues. Figure 21A shows the MID for glycolysis metabolites. Consistent with no incorporation from glucose in serine and glycine (Figure 21A) the MID indicates mainly the m+0 mass isotopalogue for these amino acids. For alanine and lactate there is a decrease in m+0 and an increase in m+3 in response to insulin in both cell lines tested. This suggests insulin increases conversion of glucose into lactate and alanine in both cell lines.

I next assessed the MID of the TCA cycle intermediates. Glucose carbon enters the TCA cycle most commonly as acetyl-CoA. This condenses with OAA to from citrate. See Section 4.1.1 for more detail. Changes to TCA cycle metabolites are again quite inconsistent across cell lines and upon insulin stimulation (Figure 21B). Insulin appears to increase glucose conversion into citrate and α-ketoglutarate upon insulin stimulation in both cell lines (indicated by reduced m+0 in response to insulin). This is not apparent in other TCA cycle intermediates (except fumarate).

4.2.2. SITA using uniformly labelled glutamine (U-[^{13}C]-glutamine)

Next, I performed another SITA in AA/C1 and AA/C1/SB/10C/M cell lines, but this time I used ^{13}C-glutamine (U-[^{13}C]-glutamine) as the tracer molecule.

As expected, I did not observe glutamine carbon in the glycolysis intermediates (Figure 22A). With regards to the total abundances of glycolytic metabolites, I observed the same results as in the glucose tracing SITA (Figure 20A). This demonstrates the reproducibility of this result.

Glutamine SITA indicated that insulin treatment increases the abundance of some of the labelled TCA cycle intermediates (citrate, α-ketoglutarate, fumarate, malate and glutamate) in AA/C1 cell line but not in the AA/C1/SB/10C/M cells (Figure 22B). However, not all the total abundance results are replicated from the glucose experiment, therefore this experiment should be repeated before drawing too many conclusions.

Similarly, to glucose tracing SITA, glutamine tracing SITA indicated an increase in the amount of unlabelled amino acids in insulin treated AA/C1 cell line compared to control. In addition,

there was an increase in the amount of labelled proline in AA/C1 cell line when treated with insulin. These results replicate the results observed in the glucose tracing SITA.

I next further analysed glutamine metabolism by considering the MID of the TCA cycle intermediates (Figure 23). Glutamine is converted to glutamate and enters the TCA cycle as α-KG, this process is known as glutamine analplerosis (see section 4.1.1. for more detail). α-KG is then metabolised in the TCA cycle in an either oxidative (to succinate) or reductive (to citrate) manner. The m+5 mass isotopalogue of citrate is indicative of reductive metabolism (conversion of α-KG to citrate), as this is low in both cell lines and unchanged by insulin stimulation I will focus only on oxidative metabolism here. The m+0 mass isotopalogue is decreased and the m+4 mass isotopalogue increased consistently in all TCA cycle intermediates in the AA/C1 cells in response to insulin. These are unchanged in response to insulin in the AA/C1/SB/10C/M cells. This suggests that the AA/C1 cells are increasing oxidative glutamine anaplerosis in response to insulin.

Figure 20A

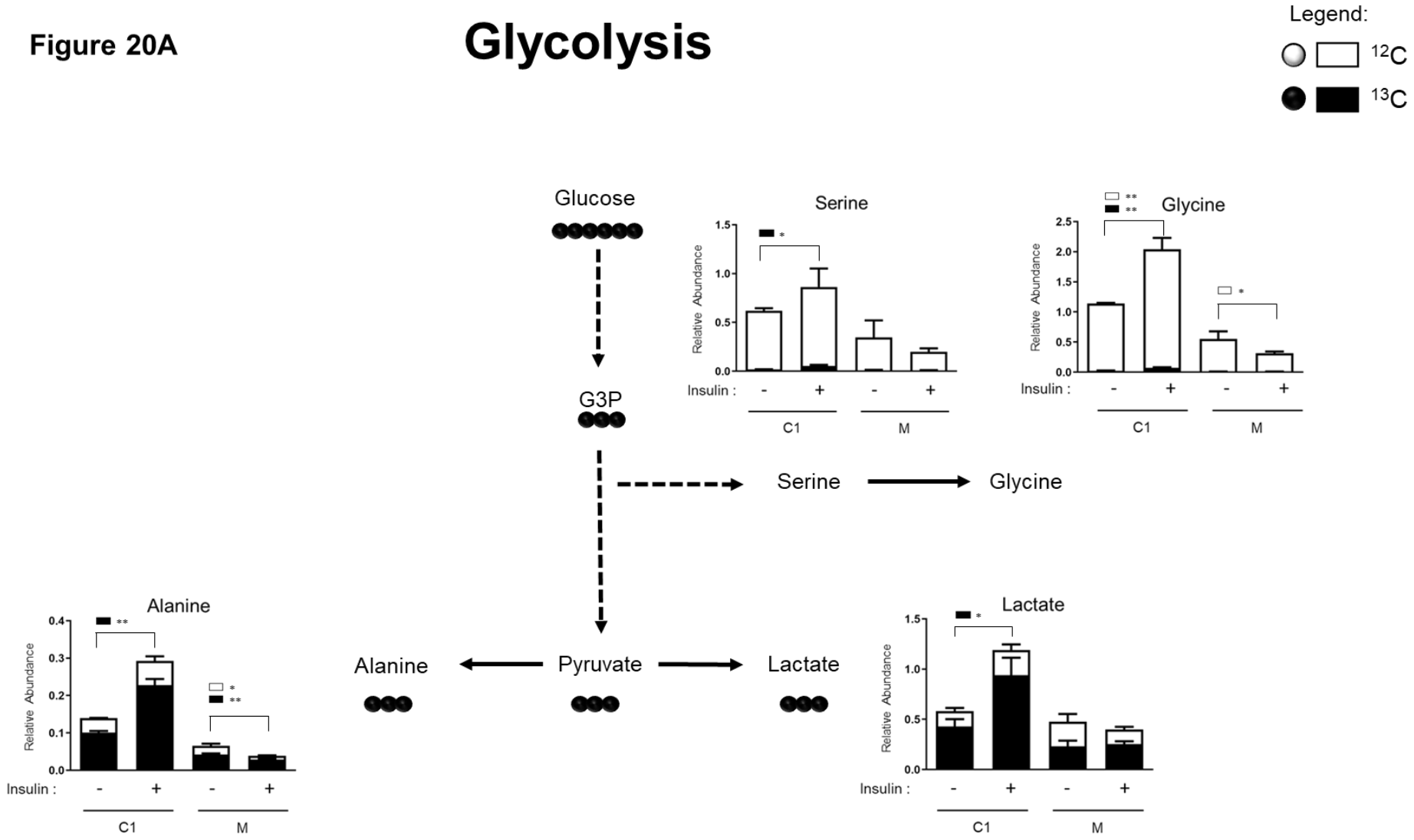
Glycolysis
Legend:
12C
13C
Glucose
G3P
Serine
Glycine
Alanine
Pyruvate
Lactate
Relative Abundance
Insulin :
C1
M

Figure 20B

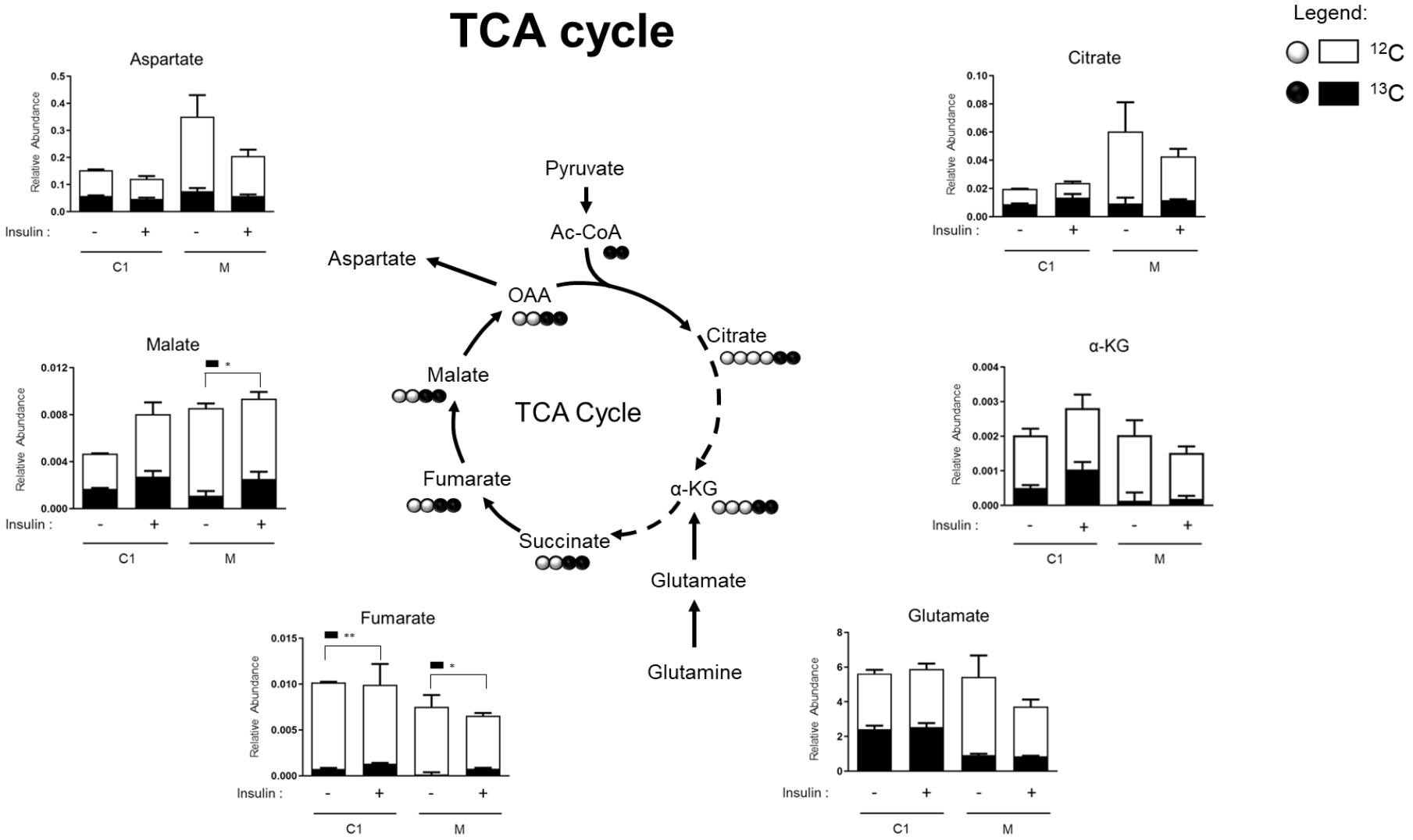
TCA cycle
Legend:
12C
13C
Pyruvate
Ac-CoA
OAA
Citrate
α-KG
Succinate
Fumarate
Malate
Aspartate
Glutamate
Glutamine
TCA Cycle
Aspartate
Citrate
Malate
α-KG
Fumarate
Glutamate
Relative Abundance
Insulin : - + - +
C1
M

Figure 20C

Amino acids

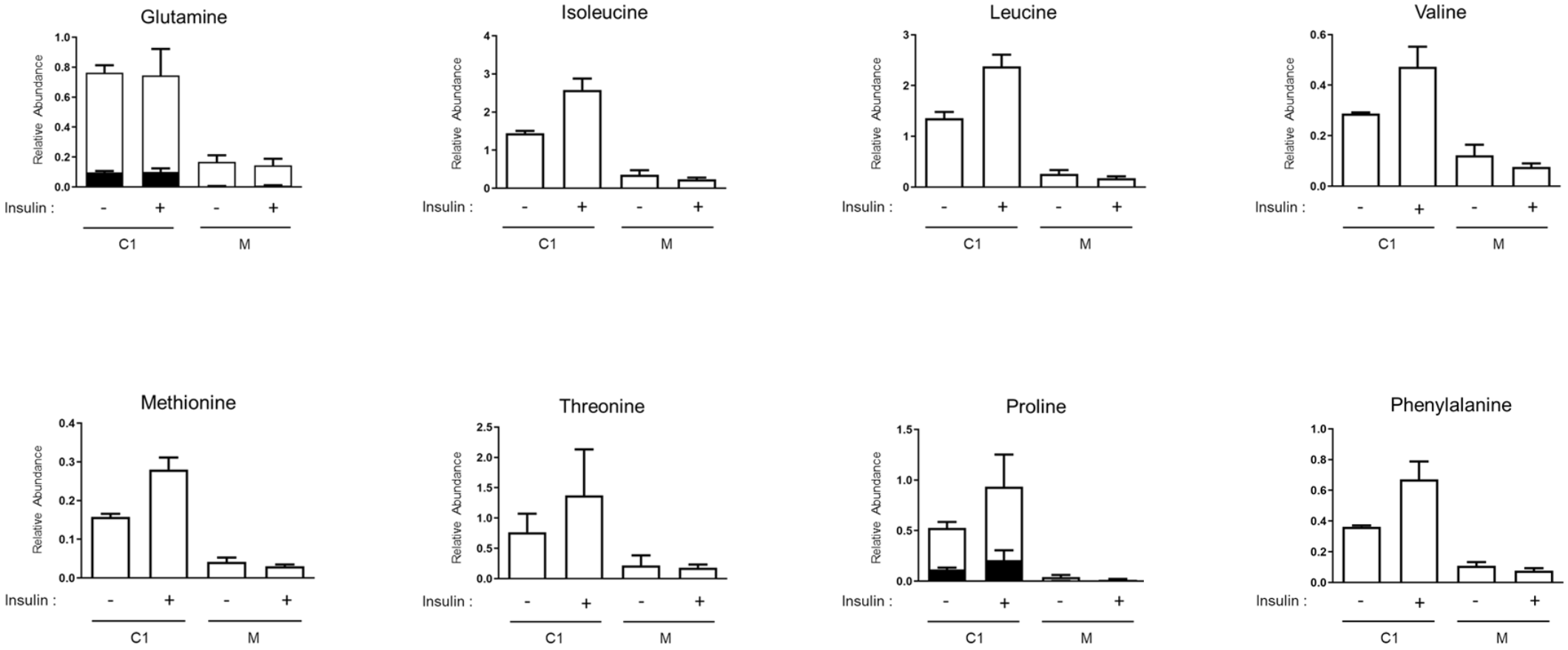

Figure 21A

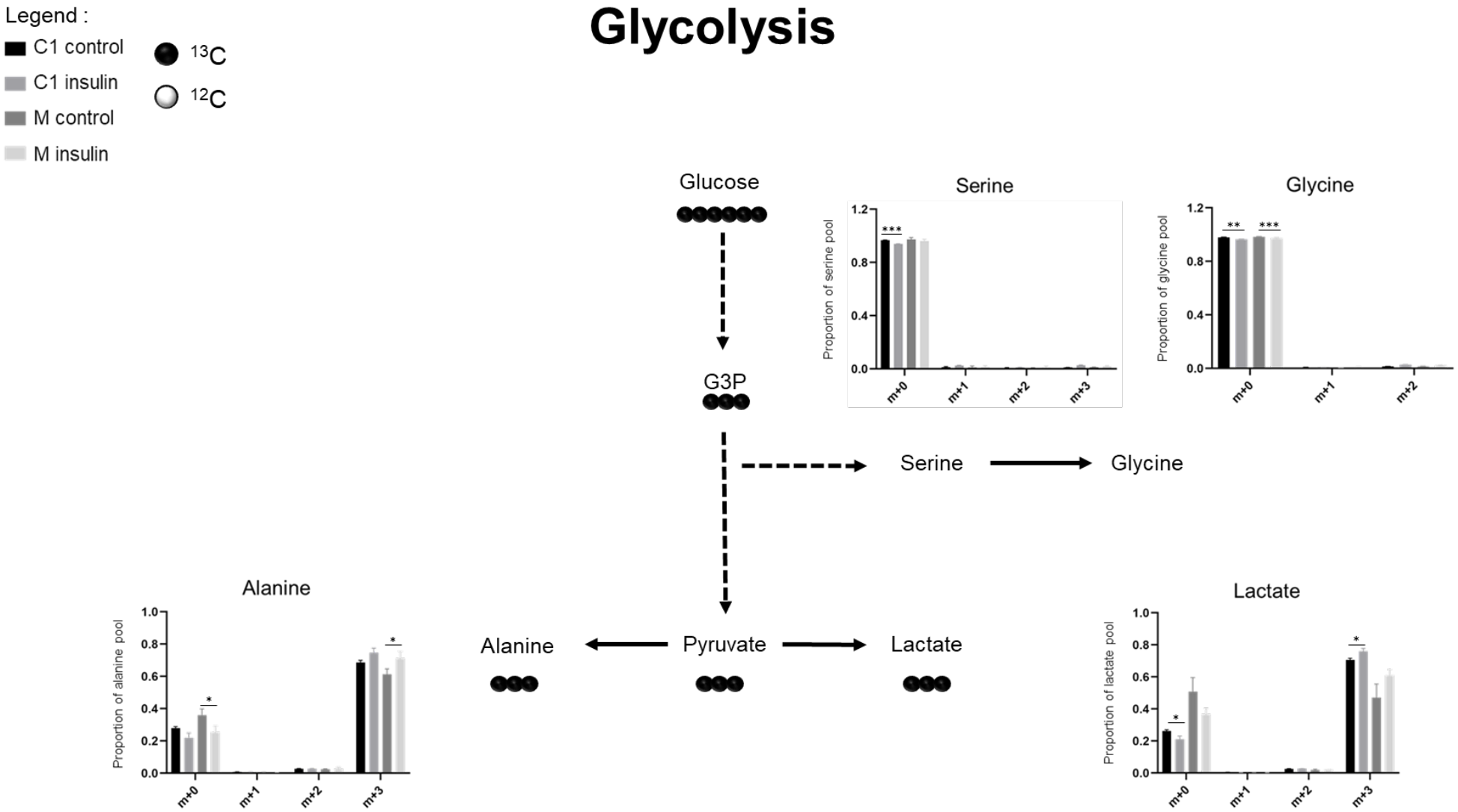
Legend :
C1 control
C1 insulin
M control
M insulin
13C
12C
Glycolysis
Glucose
G3P
Pyruvate
Serine
Glycine
Alanine
Lactate
Proportion of serine pool
Proportion of glycine pool
Proportion of alanine pool
Proportion of lactate pool
m+0
m+1
m+2
m+3

Figure 21B

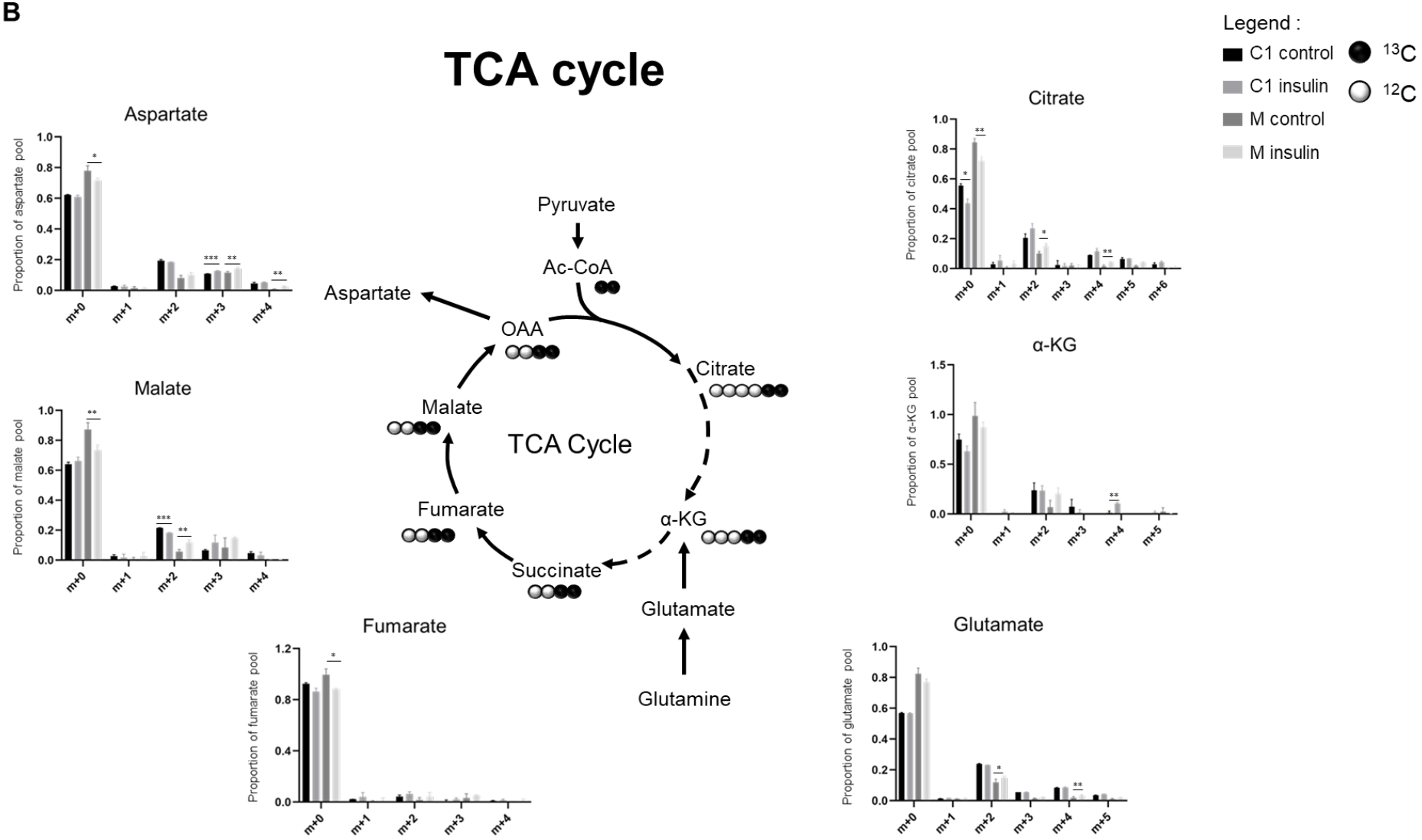
TCA cycle
Legend :
C1 control
C1 insulin
M control
M insulin
^{13}C
^{12}C
Pyruvate
Ac-CoA
OAA
Aspartate
Citrate
α-KG
Succinate
Fumarate
Malate
TCA Cycle
Glutamate
Glutamine
Aspartate
Proportion of aspartate pool
Malate
Proportion of malate pool
Fumarate
Proportion of fumarate pool
Citrate
Proportion of citrate pool
α-KG
Proportion of α-KG pool
Glutamate
Proportion of glutamate pool
m+0
m+1
m+2
m+3
m+4
m+5
m+6

Figure 22A

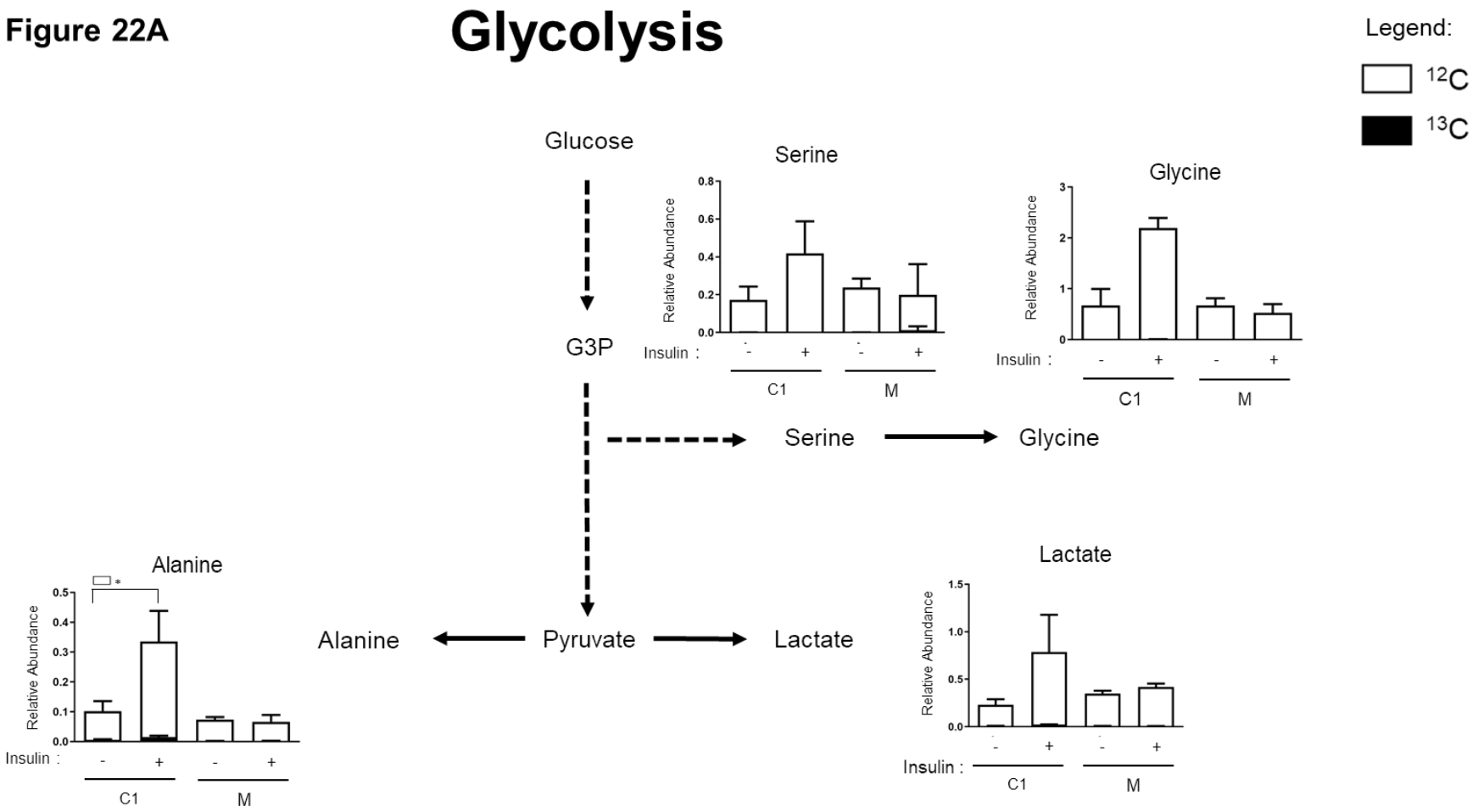
Glycolysis
Legend:
12C
13C
Glucose
G3P
Pyruvate
Serine
Glycine
Alanine
Lactate
Relative Abundance
Insulin :
C1
M

Figure 22B

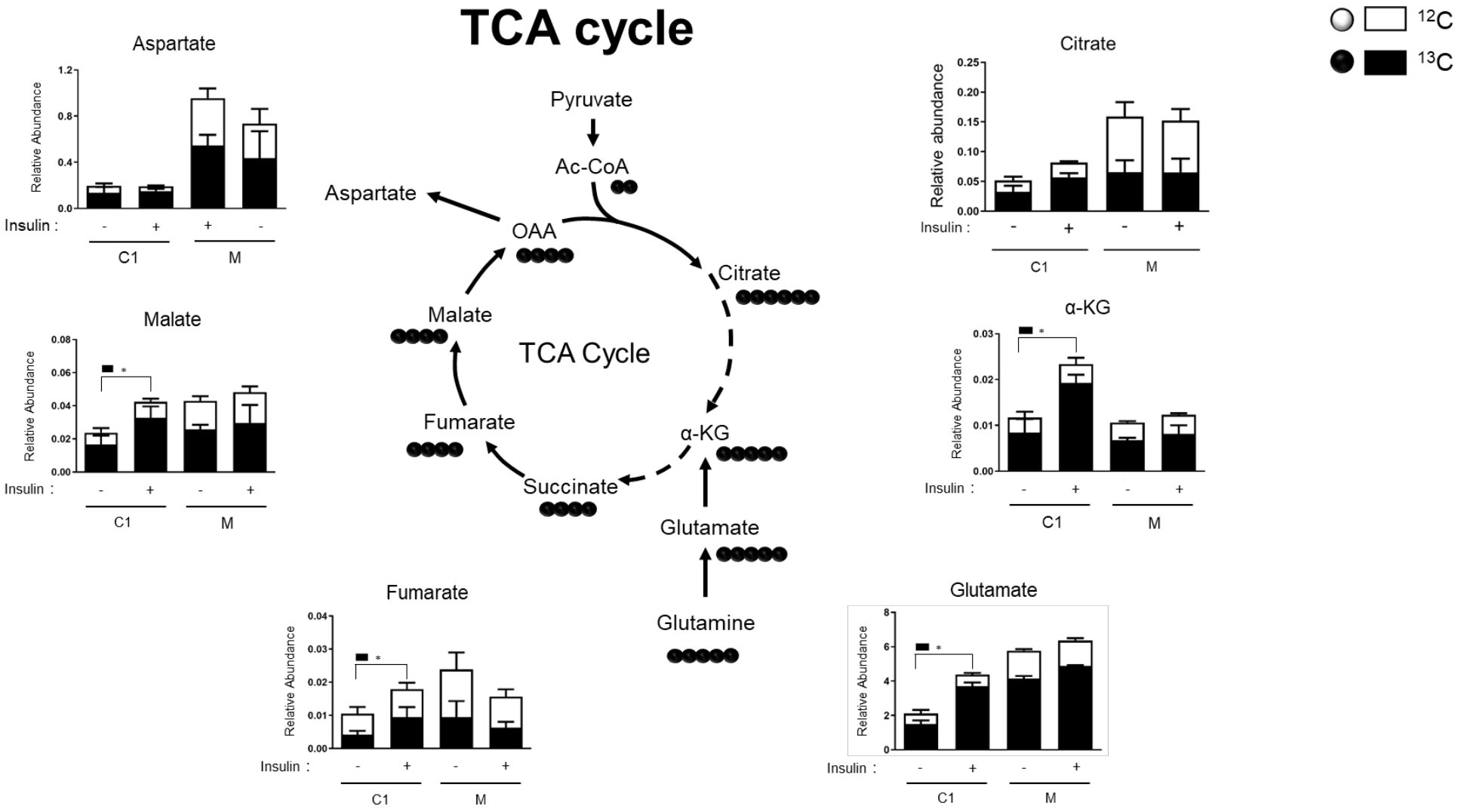
TCA cycle
Legend:
12C
13C
Pyruvate
Ac-CoA
OAA
Citrate
α-KG
Glutamate
Glutamine
Succinate
Fumarate
Malate
Aspartate
TCA Cycle
Aspartate
Relative Abundance
Insulin :
C1
M
Malate
Fumarate
Citrate
Relative abundance
α-KG
Glutamate

Figure 22C

Amino acids

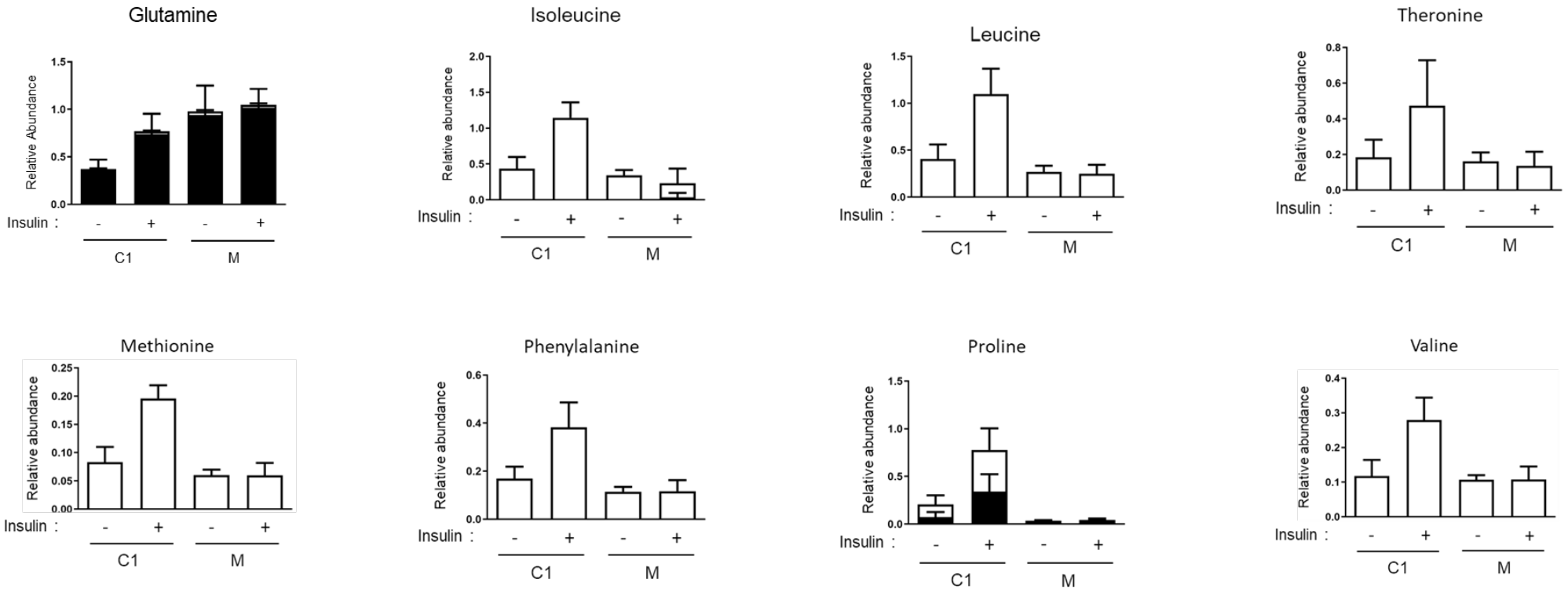

Figure 23

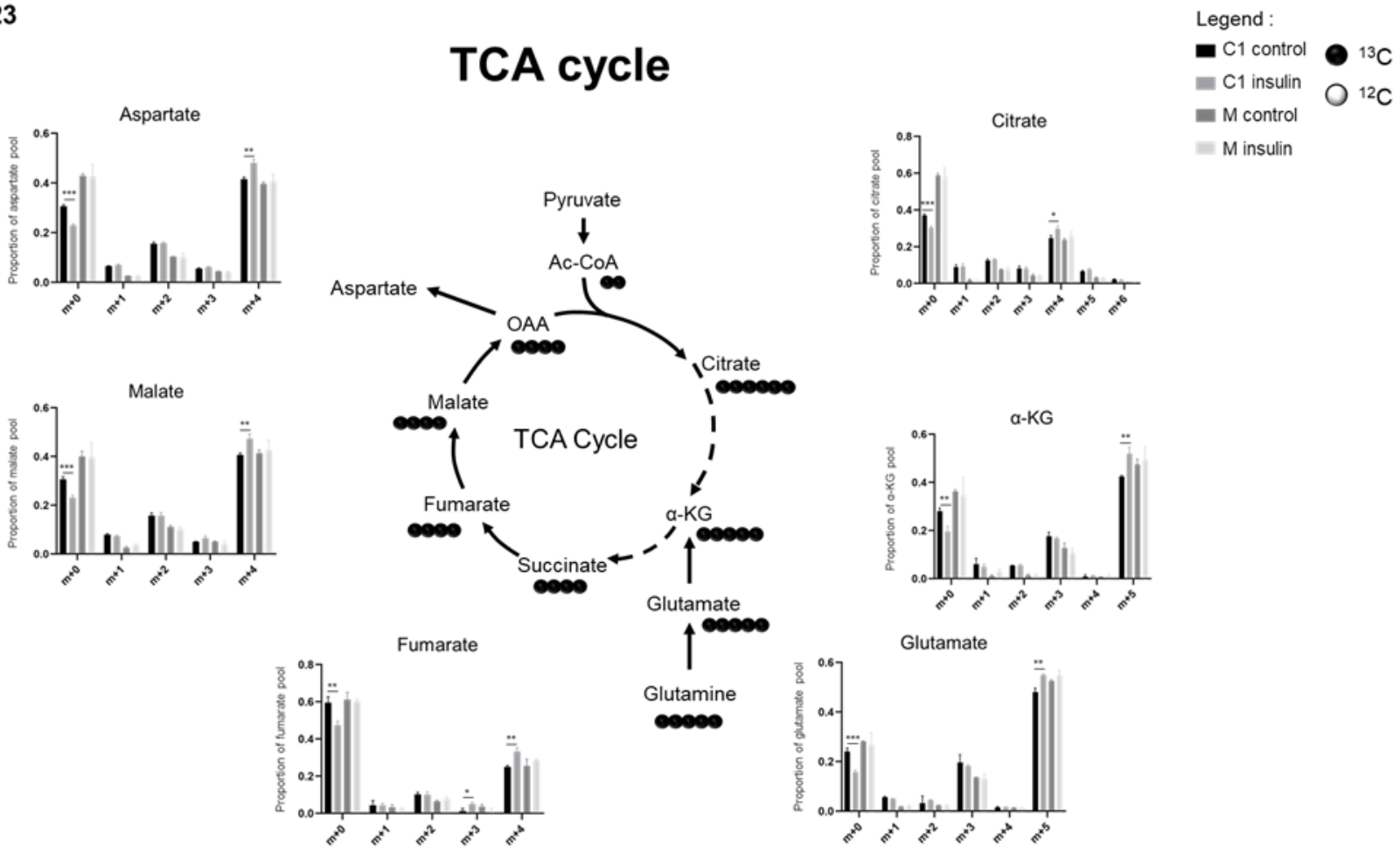
TCA cycle
Legend :
C1 control
C1 insulin
M control
M insulin
13C
12C
Pyruvate
Ac-CoA
OAA
Citrate
α-KG
Glutamate
Glutamine
Succinate
Fumarate
Malate
Aspartate
TCA Cycle
Aspartate
Citrate
Malate
α-KG
Fumarate
Glutamate
Proportion of aspartate pool
Proportion of citrate pool
Proportion of malate pool
Proportion of α-KG pool
Proportion of fumarate pool
Proportion of glutamate pool
m+0
m+1
m+2
m+3
m+4
m+5
m+6

Figure 20. The impact of insulin on intracellular metabolism. Stable isotope tracer analysis (SITA) with uniformly labelled ^{13}C glucose (U-[^{13}C]-glucose) was performed in AA/C1 and AA/C1/SB/10C/M cell lines. Relative abundance of the components of glycolysis (A), TCA cycle (B) and amino acids (C) was measured in insulin treated AA/C1 and AA/C1/SB/10C/M cell lines. Cells were seeded and treated with insulin 72h later. Cells were treated with insulin for 2h. Before extraction cells were incubated with ^{13}C glucose (U-[^{13}C]-glucose) for 2h. Metabolite abundances are relative to myristic acid, the internal standard. The total abundance of each metabolite is shown as the total of ^{12}C (white bars) and ^{13}C (black bars). The schematics demonstrates the labelling of U-[^{13}C]-glucose into the glycolytic (A) and TCA cycle (B) metabolites. Statistically significant values are indicated (using a p value threshold of p = 0.05). Significance indicated in asterisk (*), where: * means $p \leq 0.05$, ** means $p \leq 0.01$, *** means $p \leq 0.001$.

Figure 21. The impact of insulin on intracellular metabolism. Stable isotope tracer analysis (SITA) with uniformly labelled ^{13}C glucose (U-[^{13}C]-glucose) was performed in AA/C1 and AA/C1/SB/10C/M cell lines. A. The Mass isotopomer distribution (MID) pattern for the metabolites is presented for glycolysis (A) and the TCA cycle (B) in insulin treated AA/C1 and AA/C1/SB/10C/M cell lines. Cells were seeded and treated with insulin 72h later. Cells were treated with insulin for 2h. Before extraction cells were incubated with ^{13}C glucose (U-[^{13}C]-glucose) for 2h. The data are presented as a proportion of the total metabolites pool (equal to 1). The schematics demonstrates the labelling of U-[^{13}C]-glucose into the glycolytic (A) and TCA cycle (B) metabolites. Statistically significant values are indicated (using a p value threshold of p = 0.05). Significance indicated in asterisk (*), where: * means $p \leq 0.05$, ** means $p \leq 0.01$, *** means $p \leq 0.001$.

Figure 22. The results of stable isotope tracer analysis (SITA) with uniformly labelled ^{13}C glutamine (U-[^{13}C]-glutamine). A**.** Relative abundance of the components of glycolysis was measured in insulin treated AA/C1 and AA/C1/SB/10C/M cell lines. **B.** Relative abundance of TCA cycle intermediates was measured in insulin treated AA/C1 and AA/C1/SB/10C/M cell lines. Statistically significant values are indicated (using a p value threshold of p = 0.05). Significance indicated in asterisk (*), where: * means $p \leq 0.05$, ** means $p \leq 0.01$, *** means $p \leq 0.001$.

Figure 23. The results of stable isotope tracer analysis (SITA) with uniformly labelled ^{13}C glutamine (U-[^{13}C]-glutamine). Mass isotopomer distribution of the components of glycolysis was measured in insulin treated AA/C1 and AA/C1/SB/10C/M cell lines. **B.** Mass isotopomer distribution of TCA cycle intermediates was measured in insulin treated AA/C1 and AA/C1/SB/10C/M cell lines. Statistically significant values are indicated (using a p value threshold of p = 0.05). Significance indicated in asterisk (*), where: * means $p \leq 0.05$, ** means $p \leq 0.01$, *** means $p \leq 0.001$.

4.3. The impact of insulin on the expression levels of metabolic proteins and enzymes in the early adenoma and adenocarcinoma cells.

After establishing that insulin treatment increases proliferation and changes metabolism in a model of early adenoma, I wanted to understand if insulin altered the expression of metabolic proteins and enzymes to support this. Western blotting analysis was performed to examine the levels of expression of various metabolic proteins and enzymes in AA/C1 cells in response to insulin stimulation (Figure 24). Results obtained from this analysis indicated some changes in metabolic proteins and enzymes following insulin treatment. A decrease in insulin receptor expression after 48 and 72 hours of treatment, indicated that the cells were responding to insulin. Because levels of essential amino acids were elevated in AA/C1 cells after insulin stimulation (Figure 24A) I wanted to test the expression of LAT1 (a branched chain amino acid transporter) in insulin treated cells. Unexpectedly, LAT1 expression decreased after 48 hours of treatment and was unchanged at 72h. Because I found that glutamine anaplerosis was increased in insulin treated AA/C1 cells (Figure 22A), I wanted to assess the expression of a glutamine transporter (ASCT2) and the enzyme that catalyses the first step in glutamine anaplerosis (GLS1). Expression of neither of these enzymes was changed by insulin stimulation. Because there is an increase in glycolysis metabolites in AA/C1 cells I wanted to test the expression of PDK1. Increased expression of PDK1 could lead to an increase in glycolysis, as it phosphorylates and inhibits PDH (see section 1.4.2.5. in introduction). I observed an increase in PDK1 expression in AA/C1 cells after 48 and 72 hours of treatment (Figure 24B).

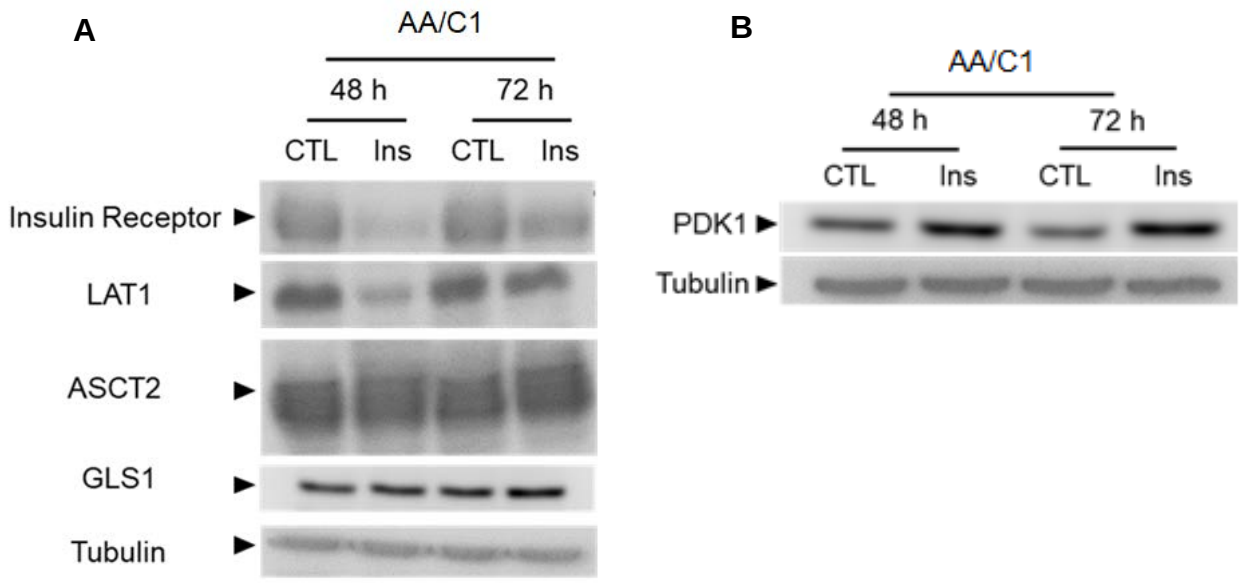

Figure 24. The impact of insulin on the expression levels of metabolic proteins and enzymes. A. Western blotting analysis was performed for insulin receptor (isoform β), LAT1, ASCT2 and GLS1. The experiment was carried out using the AA/C1 cell line. Cells were treated with 100 ng/ml of insulin for 48 and 72 hours. Tubulin was used as a loading control. **B.** Western blotting analysis was performed for pyruvate dehydrogenase kinase 1 (PDK1) in the AA/C1 cell line. Cells were treated with 100 ng/ml insulin for 48 and 72 hours.

The elevated levels of PDK1 expression induced by insulin may provide an explanation for increased proliferation of early adenoma cells. Therefore, western blotting analysis was performed to compare the expression levels of PDK1 in the early adenoma cell line – AA/C1 and adenocarcinoma cell line – AA/C1/SB/10C/M. The results indicated an increase in PDK1 expression in both cell lines after 24 and 72 hours of insulin treatment (Figure 25). This therefore suggests that this metabolic response is not unique to the AA/C1 cells. To further analyse the changes in tumour cell metabolism, that happen particularly during pyruvate entry into TCA cycle, I performed western blotting analysis for MPC1. MPC1 transports pyruvate into the mitochondria for use in the TCA cycle. The levels of expression of MPC1 was analysed and compared in AA/C1 and AA/C1/SB/10C/M cell lines after 72 hours of insulin treatment. The results of this analysis showed that MPC1 expression is the same in insulin treated and non-treated AA/C1 cells. However, there was very little MPC1 expression detectable in both insulin treated and non-treated AA/C1/SB/10C/M cells.

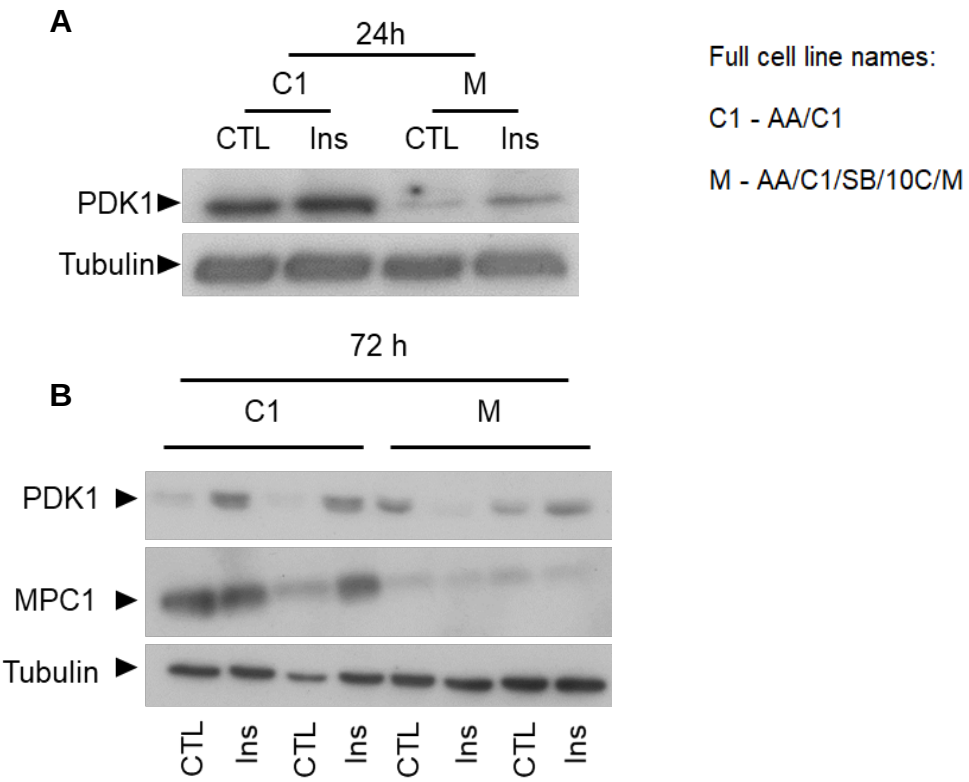

Figure 25. The impact of insulin on the expression levels of PDK1 and MPC1. A. Western blotting analysis was performed to test PDK1 expression in AA/C1 and AA/C1/SB/10C/M cell lines. Both cell lines were treated with 100ng/ml of insulin for 24 hours. Tubulin was used as a loading control. The results indicated an increase in PDK1 expression in both cell lines in response to insulin. **B.** Western blotting analysis was performed to test the expression of PDK1 and MPC1 in C1 and AA/C1/SB/10C/M cell lines. Both cell lines were treated with 50ng/ml of insulin for 72 hours. Tubulin was used as a loading control. The results indicated an increase in PDK1 expression in both cell lines in response to insulin. There was no change in the expression levels of MPC1 in AA/C1 cell line. The expression of MPC1 in AA/C1/SB/10C/M cell line is lost.

4.4. The impact of insulin on the mRNA expression of glycolytic enzymes in colorectal adenoma and adenocarcinoma cells

Western blotting analysis showed an increase in PDK1 expression in response to insulin in both cell lines tested. PDK1 is an important regulator of glycolysis, hence I decided to further

explore this pathway. qPCR was performed to analyse the mRNA expression levels of various enzymes involved in glycolysis, in response to insulin. This experiment was carried out for AA/C1 and AA/C1/SB/10C/M cell lines.

Data obtained from qPCR showed that the mRNA expression levels of multiple enzymes increase when cells are treated with insulin. Insulin up-regulated HIF1α, PDK1, PKM1 and LDH mRNA expression in both cell lines tested. The insulin-induced increase in HIF1α mRNA expression was greater in the AA/C1/SB/10C/M cell line than in the AA/C1 cells. However, the size of error bars indicates high variability in this data. Therefore, this experiment should be repeated before conclusions are drawn.

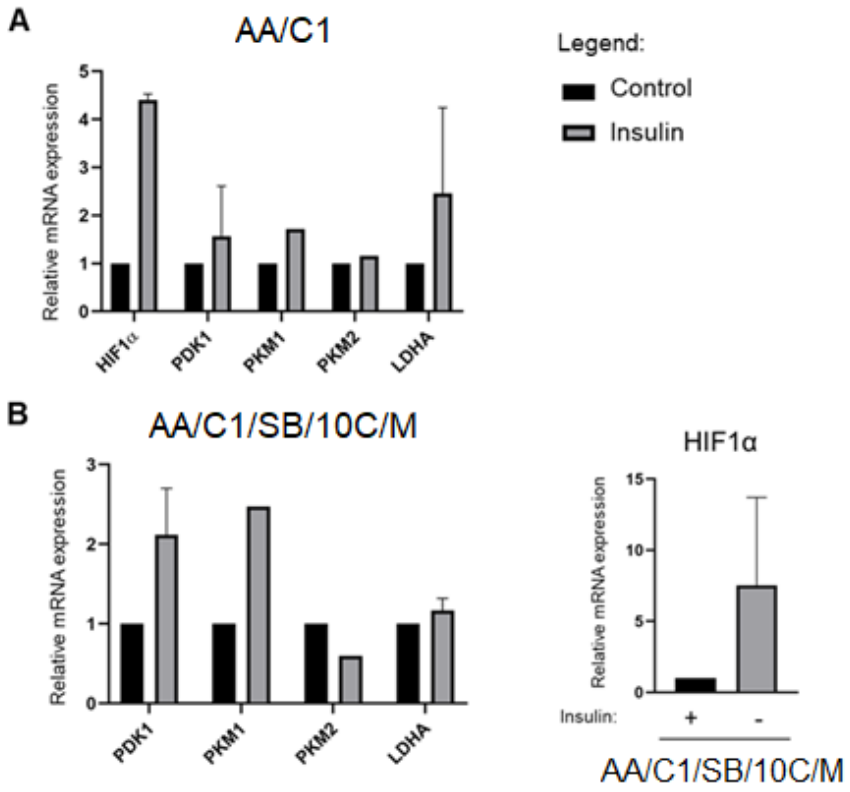

Figure 26. The impact of insulin on the mRNA expression of metabolic enzymes. qPCR was performed to test the mRNA expression levels of different metabolic enzymes: HIF1α, PDK1, PKM1, PKM2, LDHA in the AA/C1 cell line (A) and the AA/C1/SB/10C/M cell line (B). Cells were treated with 50 ng/ml of insulin for 72 hours.

4.5. Discussion

4.5.1. Insulin promotes Warburg effect in colorectal tumour cells

SITA indicates that insulin increases glycolysis in the AA/C1 early adenoma cells. An increase in labelled lactate and alanine were detected in insulin treated early adenoma cells by SITA. The results of glucose MID analysis indicated a decrease in m+0 and an increase in m+3 lactate and alanine in insulin treated AA/C1 and AA/C1/SB/10C/M cell lines. Suggesting both cell lines have an increased conversion rate of glucose to lactate and alanine upon insulin stimulation. Western blotting analysis also revealed that insulin stimulation increased PDK1 expression levels in both early adenoma and adenocarcinoma cells. Due to the fact that PDK1 inhibits pyruvate conversion to acetyl-CoA, elevated levels of this enzyme may promote a glycolytic phenotype in tumour cells. Under the conditions of high PDK1 expression, pyruvate entry to TCA cycle will be reduced, this will lead to elevated levels of lactate and alanine production. In this way insulin may promote Warburg effect in colorectal tumour cells.

qPCR results showed an increase in LDHA and HIF1α mRNA levels upon insulin treatment in both cell lines. Elevated levels of LDHA mRNA may indicate an increase in pyruvate conversion to lactate confirming a shift towards aerobic glycolysis. A rise in HIF1α mRNA expression in insulin treated cells may explain an increase in PDK1 expression. HIF1α is known to regulate PDK1 expression (142) and also to be activated by insulin in some cell lines (108) (109). However, western blotting analysis and siRNA knockdown experiments should be performed in the future to confirm whether PDK1 activation is induced by HIF1α in the AA/C1 and AA/C1/SB/10C/M cell lines used here.

Inhibition of PDK1 may be a possible therapeutic target to counteract the Warburg effect in tumour cells. Some PDK1 inhibitors are already in clinical trials. For example, dichloroacetate (DCA), which was investigated as a possible treatment for type 2 diabetes (143). DCA modulates glucose and fat metabolism and has been investigated for its effects on cancer. It has been shown to increase pyruvate dehydrogenase (PDH) activity and decrease circulating lactate concentration upon oral administration (143). There are two possible mechanisms of DCA action. DCA may increase PDH activity by binding to its pyruvate binding pocket and blocking PDKs binding to its E2 domain. Another possible mechanism is that DCA triggers a conformational change in nucleotide and lipoamine binding sites, what leads to the inhibition of PDKs bindingc(143). However, its effectiveness on cancer and possible side effects on humans are still under investigation.

4.5.2. Insulin may promote other cancer hallmarks in colorectal adenocarcinoma cells through the activation of HIF1α

Elevated levels of glycolysis and the resulting increase in biosynthetic reactions in insulin stimulated colorectal tumour cells may explain the increase in the proliferation of the AA/C1 cell line when treated with the hormone. However, data obtained from western blotting analysis and qPCR suggests that both AA/C1 and AA/C1/SB/10C/M cell lines show very similar metabolic changes when treated with insulin. It may be possible that an activation of the same metabolic pathways promotes different phenotypes in early adenoma than in adenocarcinoma cells. Taking into consideration that there was very little expression of MPC1 protein in insulin treated and non-treated adenocarcinoma cells, it is likely that pyruvate entry to TCA cycle is already reduced at this stage of tumour progression (144,145). This is consistent with studies that have shown reduced expression of MPC1 is advances CRC (53,145). Therefore, the insulin stimulated increase in PDK1 expression may not have much effect on the level of glycolysis in AA/C1/SB/10C/M cell line.

HIF1α activation may be increased by high lactate production in colorectal cells. It has been found by Wei *et.al* that high levels of lactic acid within cells may inhibit degradation of HIF1α under normoxic conditions in endothelial cells (146). This leads to an increase in vascular endothelial growth factor (VEGF) and promotion of angiogenesis (146).

If insulin promotes metabolic reprogramming in colorectal tumour cells via activation of HIF1α, it is possible that multiple hallmarks of cancer cells may be promoted through this pathway simultaneously. The primary role of HIF1α in tumour cells is to provide adaptation to hypoxia (147). Hypoxia is a common event in more advanced solid tumours (148). It occurs when tumours outgrow the oxygen supply provided by the vasculature (148). In the condition of oxygen deprivation, HIF1α drives numerous changes in cellular signalling in order to sustain tumour cell growth and proliferation (147). These adaptations triggered by HIF1α involve evasion of cell death by apoptosis and necrosis, promotion of migratory behaviour, angiogenesis and proliferation (147). As described in Chapter 1, HIF1α can be activated by insulin signalling (108) (109). It may be possible that insulin activated HIF1α provides adaptation to hypoxia in AA/C1/SB/10C/M cell line but does not have proliferation promoting effects in normoxia. This speculation may be examined by performing a proliferation assay in a hypoxic chamber to measure the viable cell number in response to insulin dosing and oxygen deprivation.

HIFα is a potential target for cancer therapy. There are many studies investigating HIF1α inhibitors and their efficacy as anticancer drugs. It has been found that such drugs as digoxin (149) and acriflavine (150) are able to supress tumour growth through inhibiting HIF1α. Elevated levels of HIF1α has been shown to increase resistance to chemotherapy. Therefore,

HIF1α inhibitors have potential to be used as a component of combination anti-cancer therapies in the future (151).

4.5.3. Insulin promotes glutamine anaplerosis in early adenoma cells

Not all the changes to metabolism are happening in both the early, AA/C1 and late stage AA/C1/SB/10C/M cells. An increase in glutamine anaplerosis was observed only in the early adenoma cells. Although tumour cell metabolism is usually shifted towards glycolysis, the levels of the TCA cycle and oxidative phosphorylation are also often increased in tumour cells (152). However, because of the high levels of aerobic glycolysis, there is a limited amount of pyruvate entering mitochondria. Therefore, it is common for tumour cells to increase the usage of glutamine as a carbon source for the TCA cycle (65). This phenomena is known as anaplerosis (65). Data collected by SITA indicated a large increase in the amount of labelled glutamine, glutamate and α-KG in insulin treated AA/C1 cells compared to control. These results indicate that insulin increases anaplerosis in early adenoma cells. When glutamine is used by cells as a carbon source for the TCA cycle, it is first broken down to glutamate by an enzyme called GLS1 in a process called glutaminolysis (119). In the next step glutamate is converted into α-KG, an intermediate of TCA cycle (119). The increase in the flux of these metabolites in AA/C1 upon stimulation with insulin indicates that increased anaplerosis occurs. In contrast, there was no increase in the amounts of labelled glutamine, glutamate and α-KG in insulin stimulated adenocarcinoma cells compared to control. This result indicates that insulin affects glutamine metabolism in early adenoma cells, but not in adenocarcinoma cells. That may, at least partially, explain the increase proliferation of AA/C1 cells in response to insulin treatment. The amounts of TCA cycle intermediates, as well as glutamine and glutamate was generally higher in AA/C1/SB/10C/M cell line than in AA/C1. It is possible that adenocarcinoma cells already have mutations in some components of glutamine metabolism, hence insulin does not affect them as much.

The results of glutamine MID analysis also support this speculation. The increased proportion of labelled carbons in response to insulin in TCA cycle intermediates (m+4 succinate, fumarate, malate and citrate) correlates with the hypothesis that increased anaplerosis in response to insulin occurs in early adenoma and not in adenocarcinoma cells.

The expression levels of some proteins participating in glutamine metabolism were investigated by using western blotting analysis. For example, the levels of expression of glutamine transporter – ASCT2 was analysed in early adenoma and adenocarcinoma cells in response to insulin. The results of this experiment showed no difference in expression of the transporter. In addition, western blotting analysis was carried out to check the expression levels

of GLS1 in insulin treated and non-treated early adenoma cells. Again, there was no difference visible in the expression of this protein in response to insulin stimulation. Nonetheless, there are many more enzymes involved in glutamine metabolism, whose aberrant activation could cause increased anaplerosis in early adenoma cells. For example, there is another glutamine transporter called $ATB^{0,+}$, which mediates glutamine uptake into cells (153). $ATB^{0,+}$ is expressed in tissues at low levels, however, it has been found to be up-regulated in some breast cancers (153). Moreover, mutation in *SLC6A14* – gene encoding $ATB^{0,+}$ are studied for their association with X-linked obesity (154). It may be worth examining whether insulin affects the expression of this transporter. Insulin may also affect the activity of the transporters and enzymes involved in glutamine anaplerosis without affecting their expression.

Another mechanism, which may promote analperosis in colorectal tumour cells is caused by mutations in the *PIK3CA* gene(155). It has been shown in colorectal tumour cells that mutations in this gene increase expression of glutamate pyruvate transaminase 2 (GPT2), one of the enzymes that triggers glutamate conversion to α-KG (155). This results in tumour cells developing glutamine dependency (155). PI3K is a part of the insulin signalling pathway (156), so it is possible that insulin promotes glutamine anaplerosis via this mechanism. Western blotting analysis could be carried out for PI3K and GPT2 in order to test this hypothesis. In addition, qPCR could be performed to examine the mRNA expression levels of various components of glutamine metabolism in insulin treated AA/C1 and AA/C1/SB/10C/M cell lines.

Glutamine metabolism is a potential target for cancer therapy. GLS, GDH and aminotransferase inhibitors are investigated for cancer treatment (66)**.** However, most of the drugs are still in preclinical trials (66). There are many limitations of targeting glutamine metabolism. For example, glutamine anaplerosis can be driven by many different enzymes. Hence, inhibiting one class of enzymes would not prevent glutamine from supplying carbons into TCA cycle (66). A combination of many different inhibitors would be necessary. In addition, a lot of drugs investigated to target glutamine metabolism have been rejected due to high cytotoxicity (66).

4.5.4. Insulin increases amino acids synthesis in early adenoma cells

Data obtained from SITA showed an increase in the amount of various amino acids in insulin stimulated AA/C1 cells compared to control. This may be explained by the fact that insulin signalling activates mTORC1, which triggers amino acid synthesis (156). Interestingly, amino acids levels are less in the adenocarcinoma cells than in early adenoma cells. This may be because amino acid pools are depleted quicker in the more progressed, highly proliferative cells. Further research is needed to explore the reasons for the difference in amino acids abundance in colorectal tumour cells representing different stages of tumour progression.

4.5.4.1. Insulin increases BCAAs uptake in early adenoma cells

Insulin increased the intracellular levels of essential amino acids in the early adenoma cells and not in the late stage cells. The insulin induced changes in the levels of the branched chained amino acids (BCAAs) are of particular interest. Elevated serum levels of BCAAs – leucine, isoleucine and valine have been associated with increased risk of developing T2DM by epidemiological studies (157). BCAAs metabolism is also an important aspect of metabolic reprogramming in cancer cells. They are used as biosynthetic intermediates and to generate ATP (158). They also activate mTORC1, and as a consequence drive protein synthesis, cell growth and survival (158). In addition, when BCAAs are catabolized, acetyl-CoA and succinyl CoA are produced, so additional sources of carbon for the TCA cycle are generated (158). Taking into consideration all of these properties, high levels of circulating BCAAs may support tumour cell proliferation and contribute to cancer development in people with T2DM.

Data obtained from SITA showed an increase in the amount of BCAAs in insulin stimulated AA/C1 cells. Increased BCAA uptake stimulated by insulin may explain why AA/C1 cells proliferate more in response to insulin. BCAA intake is mediated by L-type amino acid transporter 1 (LAT1) (159). Western blotting analysis was performed for LAT1 in AA/C1 cell line stimulated with insulin for 48 and 72h. The results of this experiment indicated a decrease in the levels of LAT1 expression after 48 hours of insulin treatment. This result does not support the data showing an increase in the levels of BCAAs in insulin treated cells. In the future, western blotting analysis could be performed to analyse the expression levels of LAT1 in insulin treated AA/C1 cells at more timepoints. In addition, western blotting could be performed for other components of BCAAs metabolism. For example, branched-chain aminotransferase 1 and 2 (BCAT1 and BCAT2), which catalyse BCAAs catabolism in cytosol and mitochondria respectively (158).

4.5.4.2. Insulin increases proline synthesis

Proline metabolism is an important aspect of metabolic reprogramming in tumour cells. Although only a few studies have explored proline metabolism in colorectal cancer, there is a large body of evidence for its importance obtained from the models of other tumours (160) (161) (162). Proline catabolism has been found to promote breast cancer cells proliferation in 3D cell cultures (162). In addition, proline catabolism has been shown to be increased in metastatic breast cancer cells compared to primary tumour cells (162).

Data obtained from SITA showed an increase in labelled proline in early adenoma cells in response to insulin stimulation. In addition, the results of glutamine MID analysis showed that the largest proportion of proline was the m+5 mass isotopalogue. This suggests that proline is synthesized from glutamine in the cells. Proline can be synthesized from glutamate by a process catalysed by P5C synthase (P5CS) and P5C reductase (PYCR) and mediated by

pyrroline-5-carboxylate (P5C) (163). In addition, proline can be converted back to glutamate by a two-step reaction catalysed by POX/PRODH and P5C dehydrogenase (P5CDH) (163). Proline catabolism is normally triggered by stress factors such as inflammation or nutrient deprivation and results in cell cycle arrest and initiation of apoptosis (163)**.** Due to the fact that the POX/PRODH enzyme catalyses the first step of proline catabolism it acts as a metabolic tumour suppressor. POX/PRODH is expressed at low levels in tumour cells and has been shown to inhibit tumour growth when expressed in a mouse xenograft tumour model (163). It has been found by Lui et.al that mutations in the myc oncogene can affect proline and glutamate interconversion (163). Myc is able to supress the expression of POX/PRODH and in this way promote tumour growth (163).

It is possible that insulin stimulates expression of *myc* in early adenoma cells. As a consequence *myc* inhibits the expression of POX/PRODH and promotes proliferation in early adenoma cells. Adenocarcinoma cells may already harbour a mutation in *myc* so insulin treatment does not affect the amount of proline present in those cells.

4.6. Summary

The results presented in this chapter show that insulin treatment promotes metabolic reprogramming in colorectal tumour cells. First of all, insulin increases Warburg effect in both early and late stage cells. This effect may be explained by insulin increasing PDK1 expression in those cell lines. As mention in chapter 1, PDK1 is a known target of HIF1α, which can be activated by insulin signalling. Therefore, it is possible that insulin promotes Warburg effect via this pathway. Another aspect of metabolism, which is influenced by insulin treatment is glutamine anaplerosis. Interestingly, insulin is increasing glutamine anaplerosis exclusively in early adenoma cell line. Similarly, insulin increases amino acids abundance in only early adenoma cell line. The specific changes to glutamine anaplerosis and amino acid uptake may explain why insulin increased proliferation only in AA/C1 and not in AA/C1/SB/10C/M cells.

Appendix

Appendix to Figure 12. Proliferative response of an adenoma derived cell line series following incubation with insulin.

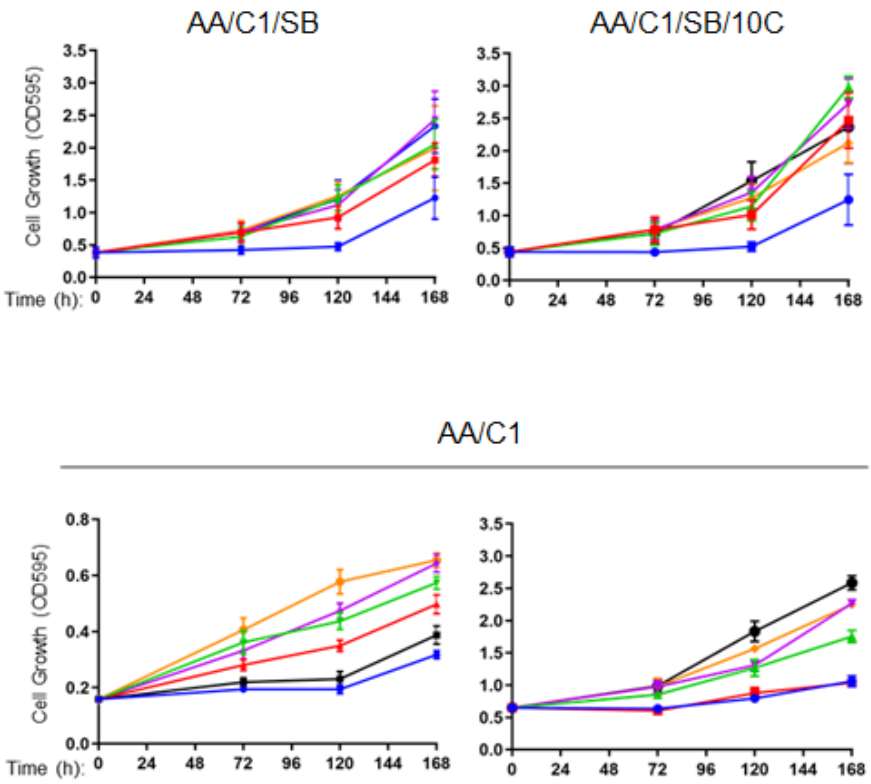

Appendix to Figure 14. The effects of insulin treatment on Akt signalling in colorectal adenoma cell lines.

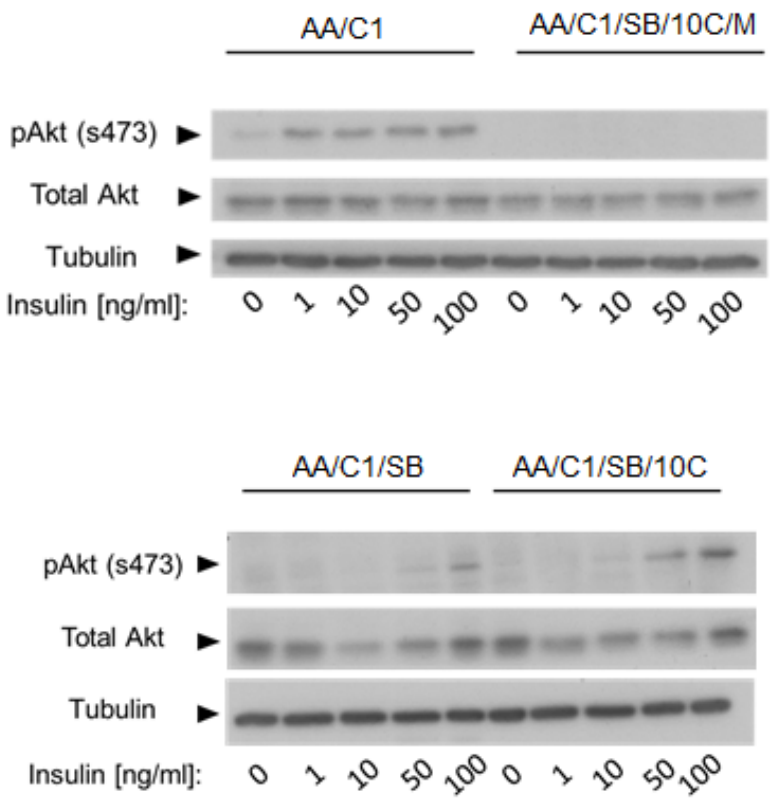

Bibliography

1. Haggar FA, Boushey RP. Colorectal cancer epidemiology: incidence, mortality, survival, and risk factors. Clin Colon Rectal Surg;22(4):191–7. 2009.

2. Kuipers EJ, Grady WM, Lieberman D, Seufferlein T, Sung JJ, Boelens PG, et al. Colorectal cancer. Nat Rev Dis Prim;1:15065. 2015.

3. Colorectal Cancer Survival by Stage. National Cancer Registeration and Analysis Service; Available from: http://www.ncin.org.uk/publications/data_briefings/colorectal_cancer_survival_by_stage

4. Bowel cancer screening: programme overview - GOV.UK. Available from: https://www.gov.uk/guidance/bowel-cancer-screening-programme-overview

5. Bowel cancer incidence statistics | Cancer Research UK. Available from: https://www.cancerresearchuk.org/health-professional/cancer-statistics/statistics-by-cancer-type/bowel-cancer/incidence#heading-Two

6. Li D. Recent advances in colorectal cancer screening. Chronic Dis Transl Med.;4(3):139.2018.

7. Vuik FE, Nieuwenburg SA, Bardou M, Lansdorp-Vogelaar I, Dinis-Ribeiro M, Bento MJ, et al. Increasing incidence of colorectal cancer in young adults in Europe over the last 25 years. Gut. 2019.

8. Young JP, Win AK, Rosty C, Flight I, Roder D, Young GP, et al. Rising incidence of early-onset colorectal cancer in Australia over two decades: Report and review. J Gastroenterol Hepatol ;30(1):6–13.2015.

9. Harriss DJ, Atkinson G, George K, Tim Cable N, Reilly T, Haboubi N, et al. Lifestyle factors and colorectal cancer risk (1): systematic review and meta-analysis of associations with body mass index. Color Dis ;11(6):547–63.2009.

10. Moradi T, Gridley G, Björk J, Dosemeci M, Ji B-T, Berkel HJ, et al. Occupational physical activity and risk for cancer of the colon and rectum in Sweden among men and women by anatomic subsite. Eur J Cancer Prev;17(3):201–8.2008.

11. Friedenreich C, Norat T, Steindorf K, Boutron-Ruault M-C, Pischon T, Mazuir M, et al. Physical Activity and Risk of Colon and Rectal Cancers: The European Prospective Investigation into Cancer and Nutrition. Cancer Epidemiol Biomarkers

Prev;15(12):2398–407.2006.

12. Hu FB, Manson JE, Liu S, Hunter D, Colditz GA, Michels KB, et al. Prospective Study of Adult Onset Diabetes Mellitus (Type 2) and Risk of Colorectal Cancer in Women. JNCI J Natl Cancer Inst;91(6):542–7.1999.

13. Ishida H, Iwama T. Epidemiology of hereditary colorectal cancer. Nihon Rinsho;74(11):1790–5.2016.

14. Castellsagué E, Foulkes WD. Lynch syndrome: five unanswered questions. Clin Genet;87(6):503–6.2015

15. Markowitz SD, Bertagnolli MM. Molecular origins of cancer: Molecular basis of colorectal cancer. N Engl J Med;361(25):2449–60.2009

16. AIMS OF THE SYSCOL PROJECT | SYSCOL Available from: http://syscol-project.eu/about-syscol/

17. Kastrinos F, Stoffel EM. History, genetics, and strategies for cancer prevention in Lynch syndrome. Clin Gastroenterol Hepatol;12(5):715–27.2014.

18. Half E, Bercovich D, Rozen P. Familial adenomatous polyposis. Orphanet J Rare Dis;4:22.2009.

19. Bogaert J, Prenen H. Molecular genetics of colorectal cancer. Ann Gastroenterol;27(1):9.2014

20. Weinberg RA (Robert A. The biology of cancer. 28 p.

21. Kwong Chung C, Brasseit J, Althaus-Steiner E, Rihs S, Mueller C. Mouse Model of Reversible Intestinal Inflammation. BIO-PROTOCOL;7(6).2017

22. Markowitz SD, Bertagnolli MM. Molecular origins of cancer: Molecular basis of colorectal cancer. N Engl J Med;361(25):2449–60.2009.

23. Schatoff EM, Leach BI, Dow LE. Wnt Signaling and Colorectal Cancer. Curr Colorectal Cancer Rep;13(2):101–10.2017

24. Clevers H, Nusse R. Wnt/β-catenin signaling and disease. Cell;149(6):1192–205.2012.

25. Li VSW, Ng SS, Boersema PJ, Low TY, Karthaus WR, Gerlach JP, et al. Wnt Signaling through Inhibition of β-Catenin Degradation in an Intact Axin1 Complex. Cell ;149(6):1245–56.2012.

26. Armaghany T, Wilson JD, Chu Q, Mills G. Genetic alterations in colorectal cancer. Gastrointest Cancer Res;5(1):19–27.2012

27. Wnt Target genes | The Wnt Homepage. Available from: https://web.stanford.edu/group/nusselab/cgi-bin/wnt/target_genes

28. Roock W De, Vriendt V De, Normanno N, Ciardiello F, Tejpar S. KRAS, BRAF, PIK3CA, and PTEN mutations: implications for targeted therapies in metastatic colorectal cancer. Lancet Oncol;12(6):594–603.2011

29. Colorectal Cancer and KRAS/BRAF: Practice Essentials, Overview, Clinical Implications of the Genetic Mutations. Available from: https://emedicine.medscape.com/article/1690010-overview

30. Discovery medicine medicine on the leading edge. Discovery Medicine; Available from: http://www.discoverymedicine.com/Marianne-Berg/2012/09/27/egfr-and-downstream-genetic-alterations-in-krasbraf-and-pi3kakt-pathways-in-colorectal-cancer-implications-for-targeted-therapy/

31. Ward PS, Thompson CB. Metabolic Reprogramming: A Cancer Hallmark Even Warburg Did Not Anticipate. Cancer Cell;21(3):297.2012

32. Yoon M-S. The Role of Mammalian Target of Rapamycin (mTOR) in Insulin Signaling. Nutrients ;9(11).2017

33. Hanahan D, Weinberg RA. The hallmarks of cancer. Cell ;100(1):57–70.2000.

34. Brabletz T, Jung A, Dag S, Hlubek F, Kirchner T. beta-catenin regulates the expression of the matrix metalloproteinase-7 in human colorectal cancer. Am J Pathol;155(4):1033–8.1999.

35. Hanahan D, Weinberg RA. Hallmarks of Cancer: The Next Generation. Cell;144(5):646–74.2011.

36. El-Tanani M, Dakir E-H, Raynor B, Morgan R. Mechanisms of Nuclear Export in Cancer and Resistance to Chemotherapy. Cancers (Basel);8(3):35.2016.

37. DeBerardinis RJ, Thompson CB. Cellular Metabolism and Disease: What Do Metabolic Outliers Teach Us? Cell;148(6):1132–44.2012.

38. Teicher BA, Linehan WM, Helman LJ. Targeting Cancer Metabolism. Clin Cancer Res;18(20):5537–45.2012

39. WARBURG O. On the origin of cancer cells. Science];123(3191):309–14.1965

40. Vander Heiden MG, Cantley LC, Thompson CB. Understanding the Warburg effect: the metabolic requirements of cell proliferation. Science];324(5930):1029–33.2009.

41. Liberti M V, Locasale JW. The Warburg Effect: How Does it Benefit Cancer Cells? Trends Biochem Sci;41(3):211–8.2016.

42. Martin SD, McGee SL. Metabolic reprogramming in type 2 diabetes and the development of breast cancer. J Endocrinol];237(2):R35–46.2018.

43. Deberardinis RJ, Chandel NS. Fundamentals of cancer metabolism INTRODUCTION AND OVERARCHING PRINCIPLES;2(5).2016.

44. Hsu PP, Sabatini DM. Cancer cell metabolism: Warburg and beyond. Cell;134(5):703–7.2008.

45. Zhu A, Lee D, Shim H. Metabolic positron emission tomography imaging in cancer detection and therapy response. Semin Oncol;38(1):55–69.2011.

46. Uguccioni M, Allavena P, Alves-Filho JC, Br; J, Pålsson-Mcdermott EM. Pyruvate Kinase M2: A Potential Target for Regulating inflammation;7:1.2016.

47. Feng Y, Xiong Y, Qiao T, Li X, Jia L, Han Y. Lactate dehydrogenase A: A key player in carcinogenesis and potential target in cancer therapy. Cancer Med];7(12):6124–36.2018.

48. Fantin VR, St-Pierre J, Leder P. Attenuation of LDH-A expression uncovers a link between glycolysis, mitochondrial physiology, and tumor maintenance. Cancer Cell;9(6):425–34.2006.

49. Koukourakis MI, Giatromanolaki A, Sivridis E, Gatter KC, Harris AL, Tumour Angiogenesis Research Group. Lactate Dehydrogenase 5 Expression in Operable Colorectal Cancer: Strong Association With Survival and Activated Vascular Endothelial Growth Factor Pathway—A Report of the Tumour Angiogenesis Research Group. J Clin Oncol;24(26):4301–8.2006.

50. Wang J, Ye C, Chen C, Xiong H, Xie B, Zhou J, et al. Glucose transporter GLUT1 expression and clinical outcome in solid tumors: a systematic review and meta-analysis. Oncotarget;8(10):16875–86.2017.

51. Feng W, Cui G, Tang C, Zhang X, Dai C, Xu Y, et al. Role of glucose metabolism related gene GLUT1 in the occurrence and prognosis of colorectal cancer. Oncotarget;8(34):56850–7.2017.

52. Rauckhorst AJ, Taylor EB. Mitochondrial pyruvate carrier function and cancer

metabolism. Curr Opin Genet Dev;38:102–9.2016.

53. Schell JC, Olson KA, Jiang L, Hawkins AJ, Van Vranken JG, Xie J, et al. A Role for the Mitochondrial Pyruvate Carrier as a Repressor of the Warburg Effect and Colon Cancer Cell Growth. Mol Cell ;56(3):400–13.2014.

54. Liu T, Yin H. PDK1 promotes tumor cell proliferation and migration by enhancing the Warburg effect in non-small cell lung cancer. Oncol Rep;37(1):193–200.2017.

55. Liu T, Yin H. PDK1 promotes tumor cell proliferation and migration by enhancing the Warburg effect in non-small cell lung cancer. Oncol Rep];37(1):193–200.2017.

56. Nam SO, Yotsumoto F, Miyata K, Fukagawa S, Yamada H, Kuroki M, et al. Warburg effect regulated by amphiregulin in the development of colorectal cancer. Cancer Med;4(4):575–87.2015.

57. Pate KT, Stringari C, Sprowl-Tanio S, Wang K, TeSlaa T, Hoverter NP, et al. Wnt signaling directs a metabolic program of glycolysis and angiogenesis in colon cancer. EMBO J;33(13):1454–73.2014.

58. Kuiper C, Dachs GU, Munn D, Currie MJ, Robinson BA, Pearson JF, et al. Increased Tumor Ascorbate is Associated with Extended Disease-Free Survival and Decreased Hypoxia-Inducible Factor-1 Activation in Human Colorectal Cancer. Front Oncol;4:10.2014.

59. Sreedhar A, Zhao Y. Dysregulated metabolic enzymes and metabolic reprogramming in cancer cells (Review). Biomed Reports];8(1):3–10.2017.

60. de Carvalho C, Caramujo M. The Various Roles of Fatty Acids. Molecules;23(10):2583.2018.

61. Bröer S, Bröer A. Amino acid homeostasis and signalling in mammalian cells and organisms. Biochem J;474(12):1935–63.2017.

62. Sajnani K, Islam F, Smith RA, Gopalan V, Lam AK-Y. Genetic alterations in Krebs cycle and its impact on cancer pathogenesis. Biochimie;135:164–72.2017.

63. Yang M, Soga T, Pollard PJ, Adam J. The emerging role of fumarate as an oncometabolite. Front Oncol;2:85.2012.

64. Iommarini L, Porcelli AM, Gasparre G, Kurelac I. Non-Canonical Mechanisms Regulating Hypoxia-Inducible Factor 1 Alpha in Cancer. Front Oncol;7:286.2017.

65. Altman BJ, Stine ZE, Dang C V. From Krebs to clinic: glutamine metabolism to cancer

therapy. Nat Rev Cancer;16(10):619–34.2016.

66. Jin L, Alesi GN, Kang S. Glutaminolysis as a target for cancer therapy. Oncogene];35(28):3619–25.2016..

67. IDF diabetes atlas - 2017 Atlas.Available from: https://diabetesatlas.org/resources/2017-atlas.html

68. GBD 2013 Mortality and Causes of Death Collaborators. Global, regional, and national age–sex specific all-cause and cause-specific mortality for 240 causes of death, 1990–2013: a systematic analysis for the Global Burden of Disease Study 2013. Lancet:117–71.2015.

69. Ndisang JF, Vannacci A, Rastogi S. Insulin Resistance, Type 1 and Type 2 Diabetes, and Related Complications 2017. J Diabetes Res;2017:1478294.2017.

70. Holman N, Young B, Gadsby R. Current prevalence of Type 1 and Type 2 diabetes in adults and children in the UK. Diabet Med;32(9):1119–20.2015.

71. Fuchsberger C, Flannick J, Teslovich TM, Mahajan A, Agarwala V, Gaulton KJ, et al. The genetic architecture of type 2 diabetes. Nature;536(7614):41–7.2016.

72. Chatterjee S, Khunti K, Davies MJ. Type 2 diabetes. Lancet;389(10085):2239–51.2017.

73. DeFronzo RA. From the Triumvirate to the Ominous Octet: A New Paradigm for the Treatment of Type 2 Diabetes Mellitus. Diabetes;58(4):773–95.2009.

74. Stumvoll M, Goldstein BJ, van Haeften TW. Type 2 diabetes: principles of pathogenesis and therapy. Lancet;365(9467):1333–46.2005.

75. Giovannucci E, Harlan DM, Archer MC, Bergenstal RM, Gapstur SM, Habel LA, et al. Diabetes and Cancer: A consensus report. Diabetes Care;33(7):1674–85.2010.

76. Barone BB, Yeh H-C, Snyder CF, Peairs KS, Stein KB, Derr RL, et al. Long-term All-Cause Mortality in Cancer Patients With Preexisting Diabetes Mellitus;300(23):2754.2008.

77. Lipscombe LL, Goodwin PJ, Zinman B, McLaughlin JR, Hux JE. The impact of diabetes on survival following breast cancer. Breast Cancer Res Treat;109(2):389–95.2008.

78. Mills KT, Bellows CF, Hoffman AE, Kelly TN, Gagliardi G. Diabetes mellitus and colorectal cancer prognosis: a meta-analysis. Dis Colon Rectum;56(11):1304–

19.2013.

79. Campbell PT, Newton CC, Patel A V., Jacobs EJ, Gapstur SM. Diabetes and Cause-Specific Mortality in a Prospective Cohort of One Million U.S. Adults. Diabetes Care;35(9):1835–44.2012.

80. Coughlin SS, Calle EE, Teras LR, Petrelli J, Thun MJ. Diabetes Mellitus as a Predictor of Cancer Mortality in a Large Cohort of US Adults. Am J Epidemiol;159(12):1160–7.2004.

81. Doronzo G, Russo I, Mattiello L, Riganti C, Anfossi G, Trovati M. Insulin activates hypoxia-inducible factor-1α in human and rat vascular smooth muscle cells via phosphatidylinositol-3 kinase and mitogen-activated protein kinase pathways: impairment in insulin resistance owing to defects in insulin signalling. Diabetologia;49(5):1049–63.2006.

82. Pandey V, Chaube B, Bhat MK. Hyperglycemia regulates MDR-1, drug accumulation and ROS levels causing increased toxicity of carboplatin and 5-fluorouracil in MCF-7 cells. J Cell Biochem;112(10):2942–52.2011.

83. Alenzi EO, Kelley GA. The association of hyperglycemia and diabetes mellitus and the risk of chemotherapy-induced neutropenia among cancer patients: A systematic review with meta-analysis. J Diabetes Complications;31(1):267–72.2017.

84. Crawford J, Dale DC, Lyman GH. Chemotherapy-induced neutropenia. Cancer;100(2):228–37.2004.

85. Kruijsdijk RCM van, Wall E van der, Visseren FLJ. Obesity and Cancer: The Role of Dysfunctional Adipose Tissue. Cancer Epidemiol Prev Biomarkers;18(10):2569–78.2009.

86. Varfolomeev EE, Ashkenazi A. Tumor necrosis factor: an apoptosis JuNKie? Cell 116(4):491–7.2004.

87. Yang G, Li C, Gong Y, Fang F, Tian H, Li J, et al. Assessment of Insulin Resistance in Subjects with Normal Glucose Tolerance, Hyperinsulinemia with Normal Blood Glucose Tolerance, Impaired Glucose Tolerance, and Newly Diagnosed Type 2 Diabetes (Prediabetes Insulin Resistance Research). J Diabetes Res ;2016:9270768.2016.

88. Bevan P. Insulin signalling. J Cell Sci. 2001;114(8).2001.

89. Heuson JC, Legros N, Heimann R. Influence of insulin administration on growth of the

7,12-dimethylbenz(a)anthracene-induced mammary carcinoma in intact, oophorectomized, and hypophysectomized rats. Cancer Res;32(2):233–8.1972.

90. Schoen RE, Tangen CM, Kuller LH, Burke GL, Cushman M, Tracy RP, et al. Increased Blood Glucose and Insulin, Body Size, and Incident Colorectal Cancer. JNCI J Natl Cancer Inst;91(13):1147–54.1999.

91. Gunter MJ, Hoover DR, Yu H, Wassertheil-Smoller S, Manson JE, Li J, et al. A Prospective Evaluation of Insulin and Insulin-like Growth Factor-I as Risk Factors for Endometrial Cancer. Cancer Epidemiol Biomarkers Prev;17(4):921–9.2008.

92. Gunter MJ, Hoover DR, Yu H, Wassertheil-Smoller S, Rohan TE, Manson JE, et al. Insulin, Insulin-Like Growth Factor-I, and Risk of Breast Cancer in Postmenopausal Women. JNCI J Natl Cancer Inst;101(1):48–60.2009.

93. Onitilo AA, Engel JM, Glurich I, Stankowski R V, Williams GM, Doi SA. Diabetes and cancer I: risk, survival, and implications for screening. Cancer Causes Control ;23(6):967–81.2012.

94. Garg SK, Maurer H, Reed K, Selagamsetty R. Diabetes and cancer: two diseases with obesity as a common risk factor. Diabetes Obes Metab;16(2):97–110.2014.

95. Rena G, Hardie DG, Pearson ER. The mechanisms of action of metformin. Diabetologia;60(9):1577–85.2017.

96. Yang J, Nishihara R, Zhang X, Ogino S, Qian ZR. Energy sensing pathways: Bridging type 2 diabetes and colorectal cancer? J Diabetes Complications;31(7):1228–36.2017.

97. American Diabetes Association. 3. Foundations of Care and Comprehensive Medical Evaluation. Diabetes Care;S23–35.2016.

98. Sharma A, Ng H, Kumar A, Teli K, Randhawa J, Record J, et al. Colorectal Cancer: Histopathologic Differences in Tumor Characteristics Between Patients With and Without Diabetes. Clin Colorectal Cancer;13(1):54–61.2014.

99. Tran TT, Naigamwalla D, Oprescu AI, Lam L, McKeown-Eyssen G, Bruce WR, et al. Hyperinsulinemia, But Not Other Factors Associated with Insulin Resistance, Acutely Enhances Colorectal Epithelial Proliferation *in Vivo*. Endocrinology;147(4):1830–7.2006.

100. Corpet DE, Jacquinet C, Peiffer G, Taché S. Insulin injections promote the growth of aberrant crypt foci in the colon of rats. Nutr Cancer;27(3):316–20.1997.

101. Lu C-C, Chu P-Y, Hsia S-M, Wu C-H, Tung Y-T, Yen G-C. Insulin induction instigates

cell proliferation and metastasis in human colorectal cancer cells. Int J Oncol ;50(2):736–44.2017.

102. Liu JJ, Druta M, Shibata D, Coppola D, Boler I, Elahi A, et al. Metabolic syndrome and colorectal cancer: is hyperinsulinemia/insulin receptor-mediated angiogenesis a critical process? J Geriatr Oncol ;5(1):40–8.2014.

103. Keku TO, Lund PK, Galanko J, Simmons JG, Woosley JT, Sandler RS. Cancer Epidemiology Biomarkers & Prevention. Cancer Epidemiol Biomarkers Prev;11(11):1361–8.2005.

104. Ortiz AP, Thompson CL, Chak A, Berger NA, Li L. Insulin resistance, central obesity, and risk of colorectal adenomas. Cancer];118(7):1774–81.2012.

105. Poloz Y, Stambolic V. Obesity and cancer, a case for insulin signaling. Cell Death Dis 6(12):e2037.2015.

106. Wang Q, Somwar R, Bilan PJ, Liu Z, Jin J, Woodgett JR, et al. Protein kinase B/Akt participates in GLUT4 translocation by insulin in L6 myoblasts. Mol Cell Biol;19(6):4008–18.1999.

107. McManus EJ, Sakamoto K, Armit LJ, Ronaldson L, Shpiro N, Marquez R, et al. Role that phosphorylation of GSK3 plays in insulin and Wnt signalling defined by knockin analysis. EMBO J;24(8):1571–83.2005.

108. Wang F, Li SS, Segersvärd R, Strömmer L, Sundqvist K-G, Holgersson J, et al. Hypoxia Inducible Factor-1 Mediates Effects of Insulin on Pancreatic Cancer Cells and Disturbs Host Energy Homeostasis. Am J Pathol 170(2):469–77.2007.

109. Wang L, Fan J, Yan C, Ling R, Yun J. Activation of hypoxia-inducible factor-1α by prolonged in vivo hyperinsulinemia treatment potentiates cancerous progression in estrogen receptor-positive breast cancer cells. Biochem Biophys Res Commun;491(2):545–51.2017.

110. Wang L, Zhou W, Gou S, Wang T, Liu T, Wang C. Insulin promotes proliferative vitality and invasive capability of pancreatic cancer cells via hypoxia-inducible factor 1α pathway. J Huazhong Univ Sci Technol Medical Sci;30(3):349–53.2010.

111. Kim J, Tchernyshyov I, Semenza GL, Dang C V. HIF-1-mediated expression of pyruvate dehydrogenase kinase: A metabolic switch required for cellular adaptation to hypoxia. Cell Metab;3(3):177–85.2006.

112. Firth JD, Ebert BL, Ratcliffe PJ. Hypoxic Regulation of Lactate Dehydrogenase A. J

Biol Chem 270(36):21021–7.1995.

113. Denko NC. Hypoxia, HIF1 and glucose metabolism in the solid tumour. Nat Rev Cancer;8(9):705–13.2008.

114. Iqbal M, Siddiqui F, Gupta V, Chattopadhyay S, Gopinath P, Kumar B, et al. Insulin enhances metabolic capacities of cancer cells by dual regulation of glycolytic enzyme pyruvate kinase M2. Mol Cancer;12(1):72.2013.

115. Wagle A, Jivraj S, Garlock GL, Stapleton SR. Insulin regulation of glucose-6-phosphate dehydrogenase gene expression is rapamycin-sensitive and requires phosphatidylinositol 3-kinase. J Biol Chem;273(24):14968–74.1998.

116. Cho ES, Cha YH, Kim HS, Kim NH, Yook JI. The Pentose Phosphate Pathway as a Potential Target for Cancer Therapy. Biomol Ther (Seoul);26(1):29–38.2018.

117. Palmada M, Speil A, Jeyaraj S, Böhmer C, Lang F. The serine/threonine kinases SGK1, 3 and PKB stimulate the amino acid transporter ASCT2. Biochem Biophys Res Commun;331(1):272–7.2005.

118. Scalise M, Pochini L, Console L, Losso MA, Indiveri C. The Human SLC1A5 (ASCT2) Amino Acid Transporter: From Function to Structure and Role in Cell Biology. Front cell Dev Biol;6:96.2018.

119. Choi YK, Park KG. Targeting glutamine metabolism for cancer treatment. Vol. 26, Biomolecules and Therapeutics. Korean Society of Applied Pharmacology; p. 19–28.2018.

120. Fogh J. Human tumor cells in vitro. Springer Science+Business Media; p557.1975.

121. Ilyas M, Tomlinson IP, Rowan A, Pignatelli M, Bodmer WF. Beta-catenin mutations in cell lines established from human colorectal cancers. Proc Natl Acad Sci U S A;94(19):10330–4.1997.

122. Berg KCG, Eide PW, Eilertsen IA, Johannessen B, Bruun J, Danielsen SA, et al. Multi-omics of 34 colorectal cancer cell lines - a resource for biomedical studies. Mol Cancer;16(1):116.2017.

123. Leibovitz A, Stinson JC, McCombs WB, McCoy CE, Mazur KC, Mabry ND. Classification of human colorectal adenocarcinoma cell lines. Cancer Res;36(12):4562–9.1976.

124. Williams AC, Harper SJ, Paraskeva C. Neoplastic transformation of a human colonic epithelial cell line: in vitro evidence for the adenoma to carcinoma sequence. Cancer

Res;50(15):4724–30.1990.

125. Williams AC, Harper SJ, Paraskeva C. Neoplastic transformation of a human colonic epithelial cell line: in vitro evidence for the adenoma to carcinoma sequence. Cancer Res;50(15):4724–30.1990.

126. Paraskeva C, Finerty S, Mountford RA, Powell SC. Specific cytogenetic abnormalities in two new human colorectal adenoma-derived epithelial cell lines. Cancer Res;49(5):1282–6.1989.

127. McGuirk S, Gravel S-P, Deblois G, Papadopoli DJ, Faubert B, Wegner A, et al. PGC-1α supports glutamine metabolism in breast cancer. Cancer Metab;1(1):22.2013.

128. Nanchen A, Fuhrer T, Sauer U. Determination of Metabolic Flux Ratios From 13C-Experiments and Gas Chromatography-Mass Spectrometry Data. In: Methods in molecular biology. p. 177–97.2007.

129. Zhang D, Fei Q, Li J, Zhang C, Sun Y, Zhu C, et al. 2-Deoxyglucose Reverses the Promoting Effect of Insulin on Colorectal Cancer Cells In Vitro. PLoS One;11(3):e0151115.2016.

130. Teng J-A, Wu S-G, Chen J-X, Li Q, Peng F, Zhu Z, et al. The Activation of ERK1/2 and JNK MAPK Signaling by Insulin/IGF-1 Is Responsible for the Development of Colon Cancer with Type 2 Diabetes Mellitus. Ahmad A, editor. PLoS One;11(2):e0149822.2016.

131. Vincent EE, Elder DJE, Thomas EC, Phillips L, Morgan C, Pawade J, et al. Akt phosphorylation on Thr308 but not on Ser473 correlates with Akt protein kinase activity in human non-small cell lung cancer. Br J Cancer ;104(11):1755–61.2011.

132. Vasudevan KM, Barbie DA, Davies MA, Rabinovsky R, McNear CJ, Kim JJ, et al. AKT-Independent Signaling Downstream of Oncogenic PIK3CA Mutations in Human Cancer. Cancer Cell;16(1):21–32.2009.

133. Saha M, Kumar S, Bukhari S, Balaji SA, Kumar P, Hindupur SK, et al. AMPK–Akt Double-Negative Feedback Loop in Breast Cancer Cells Regulates Their Adaptation to Matrix Deprivation. Cancer Res;78(6):1497–510.2018.

134. Chen X, Liang H, Song Q, Xu X, Cao D. Insulin promotes progression of colon cancer by upregulation of ACAT1. Lipids Health Dis;17(1):122.2018.

135. Ayiomamitis GD, Notas G, Zaravinos A, Drygiannakis I, Georgiadou M, Sfakianaki O, et al. Effects of octreotide and insulin on colon cancer cellular proliferation and

correlation with hTERT activity. Oncoscience;1(6):457–67.2014.

136. Riss TL, Moravec RA, Niles AL, Duellman S, Benink HA, Worzella TJ, et al. Cell Viability Assays [Internet]. Assay Guidance Manual. Eli Lilly & Company and the National Center for Advancing Translational Sciences; 2004.

137. Crystal violet Assay Kit (ab232855) | Abcam. Available from: https://www.abcam.com/crystal-violet-assay-kit-cell-viability-ab232855.html

138. Hereditary Colorectal Cancer | ASCRS. Available from: https://www.fascrs.org/patients/disease-condition/hereditary-colorectal-cancer-0

139. Young M, Ordonez L, Clarke AR. What are the best routes to effectively model human colorectal cancer? Mol Oncol;7(2):178–89.2013.

140. Cellosaurus cell line S/RG (CVCL_8756). Available from: https://web.expasy.org/cellosaurus/CVCL_8756

141. Courtney KD, Bezwada D, Mashimo T, Pichumani K, Vemireddy V, Funk AM, et al. Isotope Tracing of Human Clear Cell Renal Cell Carcinomas Demonstrates Suppressed Glucose Oxidation In Vivo. Cell Metab];28(5):793-800.e2.2018.

142. Kim J, Tchernyshyov I, Semenza GL, Dang C V. HIF-1-mediated expression of pyruvate dehydrogenase kinase: A metabolic switch required for cellular adaptation to hypoxia. Cell Metab;3(3):177–85.2006.

143. Stacpoole PW. Therapeutic Targeting of the Pyruvate Dehydrogenase Complex/Pyruvate Dehydrogenase Kinase (PDC/PDK) Axis in Cancer. JNCI J Natl Cancer Inst;109(11).2017.

144. Schell JC, Olson KA, Jiang L, Hawkins AJ, Van Vranken JG, Xie J, et al. A role for the mitochondrial pyruvate carrier as a repressor of the Warburg effect and colon cancer cell growth. Mol Cell;56(3):400–13.2014.

145. Tai Y, Cao F, Li M, Li P, Xu T, Wang X, et al. Enhanced mitochondrial pyruvate transport elicits a robust ROS production to sensitize the antitumor efficacy of interferon-γ in colon cancer. Redox Biol;20:451–7.2019.

146. Wei Y, Xu H, Dai J, Peng J, Wang W, Xia L, et al. Prognostic Significance of Serum Lactic Acid, Lactate Dehydrogenase, and Albumin Levels in Patients with Metastatic Colorectal Cancer. Biomed Res Int. 2018.

147. Ioannou M, Paraskeva E, Baxevanidou K, Simos G, Papamichali R, Papacharalambous C, et al. HIF-1α in colorectal carcinoma: review of the literature

;20(3):680-9.2015.

148. Muz B, de la Puente P, Azab F, Azab AK. The role of hypoxia in cancer progression, angiogenesis, metastasis, and resistance to therapy. Hypoxia;83.2015.

149. Zhang H, Qian DZ, Tan YS, Lee KA, Gao P, Ren YR, et al. Digoxin and other cardiac glycosides inhibit HIF-1α synthesis and block tumor growth. Proc Natl Acad Sci U S A.;105(50):19579–86.2008.

150. Lee K, Zhang H, Qian DZ, Rey S, Liu JO, Semenza GL. Acriflavine inhibits HIF-1 dimerization, tumor growth, and vascularization. Proc Natl Acad Sci U S A;106(42):17910–5.2009.

151. Semenza GL. Targeting HIF-1 for cancer therapy. Vol. 3, Nature Reviews Cancer. European Association for Cardio-Thoracic Surgery; p. 721–32.2003.

152. Anderson NM, Mucka P, Kern JG, Feng H. The emerging role and targetability of the TCA cycle in cancer metabolism. Protein Cell ;9(2):216–37.2018.

153. Karunakaran S, Ramachandran S, Coothankandaswamy V, Elangovan S, Babu E, Periyasamy-Thandavan S, et al. SLC6A14 (ATB0,+) protein, a highly concentrative and broad specific amino acid transporter, is a novel and effective drug target for treatment of estrogen receptor-positive breast cancer. J Biol Chem;286(36):31830–8.2011.

154. Suviolahti E, Oksanen LJ, Öhman M, Cantor RM, Ridderstråle M, Tuomi T, et al. The SLC6A14 gene shows evidence of association with obesity. J Clin Invest;112(11):1762–72.2003.

155. Hao Y, Samuels Y, Li Q, Krokowski D, Guan BJ, Wang C, et al. Oncogenic PIK3CA mutations reprogram glutamine metabolism in colorectal cancer. Nat Commun ;7.2016.

156. Boucher J, Kleinridders A, Ronald Kahn C. Insulin receptor signaling in normal and insulin-resistant states. Cold Spring Harb Perspect Biol;6(1).2014.

157. KARUSHEVA Y, VAN GEMERT T, SIMON M-C, MARKGRAF DF, STRASSBURGER K, SCHMOLL D, et al. Effect of Reduced Intake of Branched-Chain Amino Acids (BCAA) on Insulin Secretion and Sensitivity in Type 2 Diabetes. Diabetes;67(Supplement 1):773-P. 2018.

158. Ananieva EA, Wilkinson AC. Branched-chain amino acid metabolism in cancer. Vol. 21, Current Opinion in Clinical Nutrition and Metabolic Care. Lippincott Williams and

Wilkins; p. 64–70.2018.

159. Hodson N, Brown T, Joanisse S, Aguirre N, West DWD, Moore DR, et al. Characterisation of L-type amino acid transporter 1 (LAT1) expression in human skeletal muscle by immunofluorescent microscopy. Nutrients;10(1).2018.

160. Loayza-Puch F, Agami R. Monitoring amino acid deficiencies in cancer. Cell Cycle;15(17):2229–30.2016.

161. Loayza-Puch F, Rooijers K, Buil LCM, Zijlstra J, Oude Vrielink JF, Lopes R, et al. Tumour-specific proline vulnerability uncovered by differential ribosome codon reading. Nature;530(7591):490–4.2016.

162. Elia I, Broekaert D, Christen S, Boon R, Radaelli E, Orth MF, et al. Proline metabolism supports metastasis formation and could be inhibited to selectively target metastasizing cancer cells. Nat Commun;8.2017.

163. Liu W, Le A, Hancock C, Lane AN, Dang C V., Fan TWM, et al. Reprogramming of proline and glutamine metabolism contributes to the proliferative and metabolic responses regulated by oncogenic transcription factor c-MYC. Proc Natl Acad Sci U S A;109(23):8983–8.2012.